DOE/MC/26031 -- 5038
(DE96000560)

Field Verification of CO_2 Foam

Final Report

F. David Martin
John P. Heller
William W. Weiss
Jim Stevens
Ken Harpole
Terry Siemers
Matt Gerard
Laura Sugg
Irwan Hidajat
Ahmad Moradi-Araghi
David Zornes
Reid Grigg
Eric Chang
Jyun-Syung Tsau
Ahmed Ouenes
Junaid Sultan
John Killough
Don Kuehne

June 1995

Work Performed Under Contract No.: DE-FG21-89MC26031

For
U.S. Department of Energy
Office of Fossil Energy
Morgantown Energy Technology Center
Morgantown, West Virginia

By
New Mexico Petroleum Recovery Research Center
Socorro, New Mexico

DISCLAIMER

DOE/MC/26031 -- 5038
(DE96000560)
Distribution Category UC-122

Field Verification of CO_2 Foam

Final Report

F. David Martin
John P. Heller
William W. Weiss
Jim Stevens
Ken Harpole
Terry Siemers
Matt Gerard
Laura Sugg
Irwan Hidajat
Ahmad Moradi-Araghi
David Zornes
Reid Grigg
Eric Chang
Jyun-Syung Tsau
Ahmed Ouenes
Junaid Sultan
John Killough
Don Kuehne

Work Performed Under Contract No.: DE-FG21-89MC26031

For
U.S. Department of Energy
Office of Fossil Energy
Morgantown Energy Technology Center
P.O. Box 880
Morgantown, West Virginia 26507-0880

By
New Mexico Petroleum Recovery Research Center
New Mexico Institute of Mining and Technology
Kelly Building
Socorro, New Mexico 87801

June 1995

TABLE OF CONTENTS

LIST OF TABLES

LIST OF FIGURES

ABSTRACT

The East Vacuum Grayburg/San Andres Unit (EVGSAU), operated by Phillips Petroleum Company, was the site selected for a comprehensive evaluation of the use of foam for improving the effectiveness of a CO_2 flood. This project, entitled "Field Verification of CO_2-Foam," was jointly funded by the EVGSAU working interest owners, the U.S. Department of Energy (DOE), and the State of New Mexico. The DOE provided $2 million or approximately 34% of the total project costs, the EVGSAU provided $2.46 million, the State of New Mexico contributed approximately $1.2 million, and about $103,000 of other industrial funds were used. The Petroleum Recovery Research Center (PRRC), a division of the New Mexico Institute of Mining and Technology, provided laboratory and research support for the project. A joint project advisory team composed of technical representatives from several major oil companies provided input, review, and guidance for the project. The project, which began in 1989, had a scheduled duration of four years, but the DOE granted a no-cost extension to the end of March 1995 for the purpose of continued project evaluation.

A field test of the CO_2-foam has been successfully conducted, and preliminary results are promising. Response in the foam injection well has been as anticipated, and an offset producing well experienced a positive oil response as a result of the foam test. Based on the favorable results observed in the foam injection test, a second foam test was conducted.

The monitoring program included analysis of injectivity data, pressure falloff tests, observation well logs, interwell tracer response, production logs, history of production rates, and changes in gas-oil ratio. This report presents an overview of the project and provides results of the laboratory work, simulation studies, and field tests.

EXECUTIVE SUMMARY

In September 1989, the Petroleum Recovery Research Center (PRRC), a division of New Mexico Institute of Mining and Technology, received a grant from the U.S. Department of Energy (DOE) for a project entitled "Field Verification of CO_2-Foam." The grant provided for an extension of the PRRC laboratory work to a field testing stage to be performed in collaboration with an oil producer actively conducting a CO_2 flood. The objectives of this project were to: 1) conduct reservoir studies, laboratory tests, simulation runs, and field tests to evaluate the use of foam for mobility control or fluid diversion in a New Mexico CO_2 flood, and 2) evaluate the concept of CO_2-foam in the field by using a reservoir where CO_2 flooding is ongoing, characterizing the reservoir, modeling the process, and monitoring performance of the field test. Seven tasks were identified for the successful completion of the project: 1) evaluate and select a field site, 2) develop an initial site-specific plan, 3) conduct laboratory CO_2-foam mobility tests, 4) perform reservoir simulations, 5) design the foam slug, 6) implement a field test, and 7) evaluate results.

By evaluating information from candidate CO_2 floods, a suitable field site in New Mexico, the East Vacuum Grayburg/San Andres Unit (EVGSAU), operated by Phillips Petroleum Company (PPCo), was identified by PRRC as appropriate for the proposed work. The four-year project is jointly funded by the EVGSAU Working Interest Owners (WIO), the U.S. Department of Energy (DOE), and the State of New Mexico. The PRRC provided laboratory and research support for the project. A Joint Project Advisory Team (JPAT) composed of technical representatives from several WIO companies provides input, review, and guidance for the project.

The EVGSAU is located about 15 miles northwest of Hobbs, New Mexico in the Vacuum Field. The primary productive interval is a dolomitized carbonate sequence in the upper 300 feet of the San Andres formation at a depth of approximately 4500 feet. The San Andres has been described as a very layered series of fining-upward, carbonate sequences with varying degrees of permeability. Some layers in certain parts of the field have permeabilities in the range of 200 to 600 millidarcies. These scattered layers of high permeability have led to premature breakthrough of CO_2 in certain producers. The goal of the field trial was to investigate foam for conformance control to aid in suppressing this rapid CO_2 breakthrough. Specifically the prime directive of our trial was to prove that a foam could be generated and that it could change the mobility of CO_2 in the reservoir. Proving or even determining economics or optimizing the size of the foam slug, while important, was not our original goal.

A suitable pattern in the EVGSAU was selected, based on the criterion that the production there be typical of other patterns without a distinctly better or worse record of CO_2 breakthrough than in the rest of the field. An observation well was drilled in the pattern approximately 150 ft from the pattern injection well. The observation well was cored and logged to improve reservoir characterization in the pattern area, as well as to provide reservoir cores for laboratory tests with suitable foam-generating surfactants. In order to use the borehole as a logging monitor well, the bottom 800 ft was cased with fiberglass.

A geological characterization of the pilot area and surrounding patterns was assembled for the history matching and reservoir simulation studies. The foam-flood mechanistic model developed at the PRRC was incorporated into a field-scale reservoir simulator.

During the course of the project, several reports[1-5] and technical papers[6-15] related to the EVGSAU project were prepared and presented at conferences. The technical papers prepared in the latter stages of the project document the results that were obtained.

The first and second annual reports[1,2] summarized the project plans, the baseline field testing, and the laboratory test results that pertain to surfactant selection. A commercial surfactant was approved for the field test by the JPAT representatives. Following the baseline testing, surfactant injection began in the first quarter of 1992. Following three months of a pre-foam surfactant pad to satisfy the adsorption of the reservoir, a rapid cycle of surfactant alternated with CO_2 was injected to generate an 80% quality foam. The third and fourth annual reports[3,4] provided details of the project results and interpretations of the foam test. Based on the favorable response of the field test, a second foam test was proposed. The DOE granted no-cost extensions to allow continued project evaluation. The fifth annual report[5] provided an update on the project.

Foam may improve injection conformance in two directions: 1) in a horizontal direction by increasing sweep efficiency and 2) in a vertical direction by diverting fluids to other, under-injected zones. The foam pilot pattern (an inverted 9-spot with the injection well in the center) was selected because a high permeability channel existed between one of the eight producers and the injection well. This producer produced over 80% of the CO_2 injected into that pattern. This well, EVGSAU 3332-032, henceforth called the "offending well", had consistently flowed very strongly after each period of CO_2 injection. This made operation of the offending well difficult and eventually the well was shut down. For purposes of the foam test, the offending well was allowed to produce during the baseline period and it averaged only 5 BOPD and up to 2 MMSCFPD of CO_2.

Having chosen the pilot pattern, an observation well was drilled and sponge core taken as part of a detailed geologic study across the pattern area. The geologic study identified nine major layers designated A through I and identified a portion of the C layer designated C_2 and C_3 as the layers that were channeling to the offending well. Production and injection logs were run in the injector and offending well which confirmed the channel.

The tracer program was performed to determine if the injector and offending well were connected via a fracture. This was due to a concern in the JPAT that the foam may not be propagated in a fracture since it is designed for a porous media. However, the tracers did not transit the reservoir quickly and therefore indicated that the two wells were connected by a high permeability streak instead of a fracture.

The JPAT designed the method and timing of surfactant injection. An operating plan was developed that encompassed the foam slug design as well as the extensive data gathering program and contingency plans. Daily injection rate and pressure data, multiple injection profiles, falloff tests and a tracer program were developed for the injection well. Fluid sampling and monthly (sometimes weekly) production tests were performed in the producing wells in the pattern, and a series of observation well logging runs were made to document saturation changes occurring in the foam pattern away from the channel.

Reduced injectivity, as evidenced by surface injection pressure and rate data, provided an immediate indication that the in-situ foam generation and mobility reduction had been achieved. This reduced injectivity persisted for over three months. The presence of a large negative skin and significant linear flow behavior in pressure falloff tests does not necessarily rule out the use of foam for mobility control. The apparent in-situ mobility of CO_2 after foam generation was approximately one-third of that observed during the baseline CO_2 injection. In-situ mobilities calculated using Hall plots were comparable to falloff test results.

Injection profile surveys indicated that the foam did achieve a noticeable diversion of injected fluid away from the high permeability zone and into lower permeability zones that had not been taking desired quantities of CO_2 prior to the foam treatment. Time lapse monitor logging in the observation well indicated that foam generation was effective in slowing the rapid movement of CO_2 through a high permeability interval. More frequent logging during the project would have helped reduce the uncertainties in interpreting the monitor logging results. Positive response to foam injection was evidenced by changes in the CO_2 production and oil rate performance at the "offending" production well in the foam pilot pattern.

Seven flow units or zones are laterally continuous across the foam pilot area, and injection profile tests in Well 3332-001 indicate that the high permeability flow unit (Zone C) is the major flow unit. Prior to the foam test, approximately 60% of the injected water was entering Zone C. An average of ten profiles obtained during the SAG foam test suggested that fluids continued to enter the high permeability zones, although a 10-15% decrease was observed in Zone C. The results suggested that the bulk of the foam was probably generated in the high permeability Zone C, but a slight improvement in the injection profile was observed. Injection profiles obtained with CO_2 after the first foam test suggest that the fluid distribution from the wellbore returned to the distribution observed prior to the foam test. Thus, the effect near the wellbore was not a permanent profile modification. However, the pressure/rate data suggest that foam was still present away from the wellbore.

The CO_2-foam field trial performed at EVGSAU proved that a strong foam could be formed in situ and that the foam reduced the mobility of CO_2 by one-third. Incremental oil was produced in three of the eight producers in the pattern, and gas cycling was dramatically reduced in the offending well as a direct result of surfactant injection. In light of the fact that a large amount of surfactant was injected, the revenue and savings produced from the foam injection shows promise of being an economical method for conformance control. Control of gas breakthrough in the offending well during a second CO_2 injection period was achieved with a much smaller amount of surfactant.

INTRODUCTION

BACKGROUND

The use of CO_2 as a displacement fluid during enhanced recovery processes has increased in recent years, and work involving the selection and development of mobility control additives for use in CO_2 flooding has gained importance. Several organizations have been working on processes to improve the efficiency of CO_2 displacements that consist of the injection of a mixture of dense CO_2 with an aqueous solution of a suitable surfactant. This mixture generates lamellae (bubble films) in the pore space of the rock, which allows the mixture to move through the rock with a mobility that is significantly lower than that of CO_2 alone. The CO_2-foam that is generated can also reduce the nonuniformities of the displacement front that are otherwise induced by flow through the heterogeneities of the rock. Thus, the use of CO_2-foam as a displacement fluid can give two benefits over the use of CO_2 alone: it can reduce or suppress the formation of fingers caused by the instability of the displacement front, and it can reduce the severity of channels or preferential flow that would otherwise occur because of heterogeneity of the reservoir rock.

For several years, laboratory work has been conducted at the Petroleum Recovery Research Center (PRRC), a division of New Mexico Institute of Mining and Technology (NMIMT), on the use of

surfactants to generate foam for increasing the efficiency of CO_2 floods. This work has been supported by the U.S. Department of Energy (DOE), the New Mexico Research and Development Institute (NMRDI), and a consortium of oil companies. The DOE expressed interest for a continuation of the research program and provided a grant to the NMIMT in September 1989 to take the laboratory work to a field-testing stage. The grant provides for an extension of the PRRC laboratory work to a field-verification stage to be conducted by the PRRC in collaboration with an oil producer actively involved in CO_2 flooding.

OBJECTIVES

This project is a cooperative industry-university-government effort to transfer laboratory research technology to a field demonstration test. The primary objectives of the project are to conduct reservoir studies, laboratory tests, and simulation runs necessary to design the field test, and to evaluate the use of foam for mobility control and fluid diversion in a field-scale CO_2 flood. Seven tasks were identified for the successful completion of this project: 1) evaluate and select a field site, 2) develop an initial site-specific plan, 3) conduct laboratory CO_2-foam mobility tests, 4) perform reservoir simulations, 5) design the foam slug, 6) implement a field test, and 7) evaluate results.

SITE SELECTION

During the first year of the project, the PRRC identified the East Vacuum Grayburg/San Andres Unit (EVGSAU) operated by PPCo as appropriate for the proposed work. Representatives from the PRRC and PPCo prepared an initial site-specific plan for the proposed work at the EVGSAU which was approved by the EVGSAU Working Interest Owners (WIO) in June 1990. A Joint Project Advisory Team (JPAT), representing several of the EVGSAU WIO companies, served as a technical steering committee that acted in an advisory capacity.

DISCUSSION

EVGSAU GEOLOGIC SETTING

The Vacuum Field, located about 15 miles northwest of Hobbs in Lea County, New Mexico, is comprised of several large Units and leases. The East Vacuum Grayburg-San Andres Unit (EVGSAU) covers more than 7000 acres on the eastern side of the Vacuum Field. The primary productive interval at EVGSAU is comprised of the dolomitized carbonate sequences in the upper few hundred feet of the San Andres Formation, at a depth of approximately 4500 feet. The San Andres structure is an east-west trending anticline with more than 400 feet of closure above the original oil/water contact. The reservoir section is informally subdivided into a "lower" San Andres section and an "upper" San Andres section, separated by the more siliciclastic Lovington Sandstone Member.

FIELD DEVELOPMENT HISTORY

The Vacuum Field was discovered in 1929, however significant development did not begin until 1938 due to the lack of transportation facilities and a low demand for crude oil. The initial field development, which included the drilling of about 330 wells, was substantially completed by 1941. Waterflood development began in 1958 and gradually spread across the field. The EVGSAU was one of the last areas to be unitized within the Vacuum Field.

The EVGSAU was formed in December, 1978. At that time the Unit was comprised of 169 producing wells drilled on 40-acre spacing. Total Unit production was about 4000 STB/D at unitization. Beginning in 1979, the Unit was infill drilled to 20-acre spacing. Water injection began in 1980, with the Unit being converted to an 80-acre inverted ninespot pattern waterflood development by 1982. The EVGSAU became the site of the first full-scale miscible carbon dioxide injection project in the state of New Mexico when CO_2 injection began at EVGSAU in September, 1985. The same 80-acre inverted ninespot pattern development was used, and the CO_2 project was operated using a 2:1 WAG ratio with each of three WAG injection areas in the Unit receiving four months of CO_2 injection followed by eight months of water injection. CO_2 injection into each pattern represents approximately 2 percent HCPV per WAG cycle. Unit oil production rate at the end of 1993 was about 8500 STB/D. Field development and initial results of the CO_2 flood at the EVGSAU have been described previously.[16] Reservoir and fluid properties for the EVGSAU, included in Table 1, are similar to other San Andres reservoirs in the vicinity.

TABLE 1
EVGSAU RESERVOIR PARAMETERS[16]

Reservoir and Fluid Characteristics		
Type Formation		dolomite
Depth (ft)		4400
Reservoir Temperature (°F)		101
Original Reservoir Pressure (psig)		1613
Current Average Reservoir Pressure (psig)		2100
Average Net Pay (ft)		71
Average Porosity (%)		11.7
Average Permeability (md)		11.0
Unit Area (acres)		7025
CO_2 Project Area (acres)		5000
Oil Gravity (°API)		38
OOIP (MMSTBO)		297
Forecasted Recoveries	MMSTBO	% OOIP
Primary	78.0	25
Secondary	40.8	15
Tertiary	20.7	8*

*of CO_2 project area

While the overall project performance has been very encouraging, certain wells/patterns have shown anomalously high CO_2 production. This has resulted in isolated cases of poor pattern sweep efficiency, inefficient CO_2 utilization, and increased recycling costs and compression requirements. Since the start-up of CO_2 injection, a number operational problems have arisen including early breakthrough and channeling of injected CO_2 into some producing wells, excessive accumulation of asphaltenes and paraffins in wells where CO_2 breakthrough has occurred, and increased calcium-sulfate scale formation in a number of wells in those areas of the field experiencing early CO_2 breakthrough. It was suspected early on[16] that these problems resulted from channeling of injected fluids through high permeability zones, most likely exacerbated by dissolution of anhydrite in these high permeability channels. PPCo began investigative work in the late 1980's to identify effective mobility control methods for mitigating the channeling problems, and laboratory investigations were conducted to identify crosslinked polymer gel systems and/or CO_2-foams suitable for in-depth mobility control applications in this project. The CO_2-foam field verification pilot test was designed to evaluate the application of foam mobility control technology for controlling the excessive CO_2 production problems in a field-scale CO_2 flood project.

SITE DESCRIPTION

A pattern in the EVGSAU CO_2 flood was selected to test the efficacy of using surfactant-generated foam to reduce CO_2 mobility. The location of the pattern selected for the foam pilot test is shown in Fig. 1. This pattern was selected for the field trial based on the following criteria:

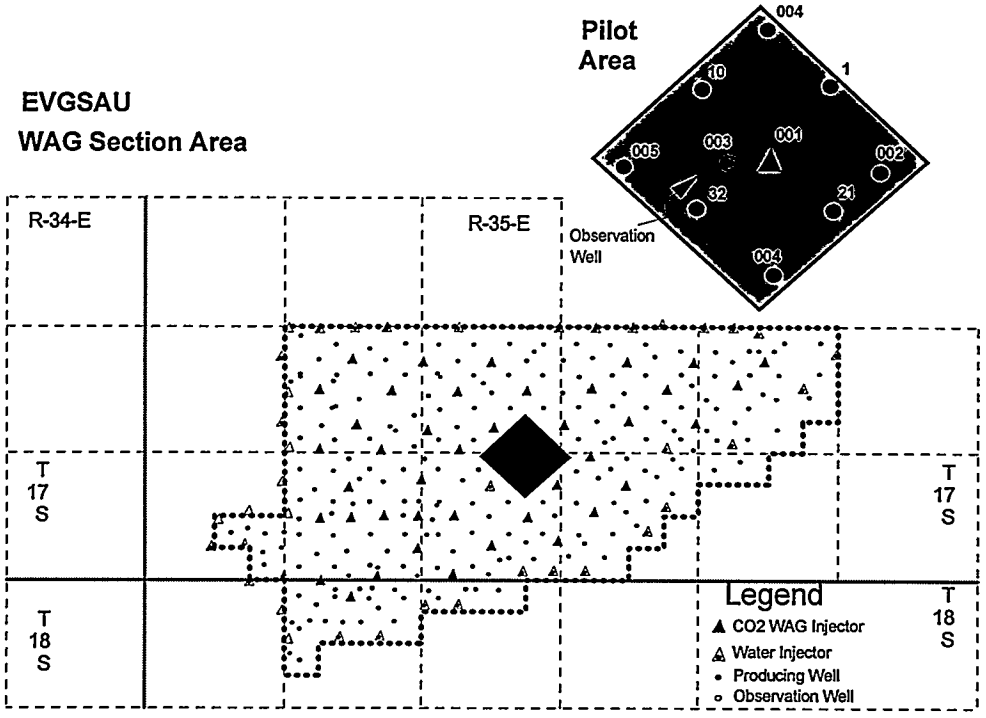

Fig. 1. Location of the EVGSAU Foam Pilot Area

1) The pattern has shown excessive CO_2 breakthrough in one of the production wells (3332-032); the remainder of the wells in the pattern have shown more typical CO_2 response.

2) The reservoir geology in the pattern area is representative of most of the EVGSAU reservoir to allow results from the pilot to be scaled up to the entire Unit;

3) The injection well in the pattern (3332-001) has sufficient injectivity to reduce the chance of the well becoming pressure-limited during foam injection.

An observation well was drilled to improve reservoir characterization in the pattern area, to serve as an observation well, and to provide core material for laboratory tests. The location of the observation well (3332-003) in the pilot pattern, about 150 feet from the WAG injector, is shown in Fig. 1. This well was sponge cored to provide current oil saturation information, as well as additional details on the reservoir geology in the pattern area. Openhole logs (compensated neutron/density log, induction log, sonic log, dual laterolog, and repeat formation tester) and cased hole logs (compensated neutron log, cement evaluation log, induction log, and pulsed neutron capture log) were obtained at the time the well was completed.

A geological characterization of the pilot area and surrounding patterns was assembled for the history matching and reservoir simulation studies. The EVGSAU produces primarily from the San Andres Formation. At EVGSAU, the San Andres can be divided into upper and lower sections by the Lovington sandstone/siltstone. The San Andres sections consist of a series of shallowing-upward carbonate sequences, each typically 20 to 30 feet thick, which have been extensively dolomitized. Total gross reservoir thickness ranges from 200 to 300 feet. A geologic study of the EVGSAU reservoir identified 12 zones, which are laterally continuous across the foam pilot area (Fig. 2). Zone C (shown subdivided into C1, C2, and C3 on the type log in Fig. 2) is the major flow unit within the pilot area. Zones D and E show good porosity development and high oil saturation, but they are less permeable and take only a small fraction of the fluid injected into this pattern. The A and B zones show little or no reservoir potential in this area; the zones below the Lovington have good porosity and permeability but have high water saturation in the pilot area. Falloff tests from most of the EVGSAU injection wells show an extended period of linear flow behavior, which is interpreted as fracture flow in the reservoir. However, the excessive CO_2 breakthrough problems do not appear to be simply the result of direct fracture communication between injectors and producers.

The production history for the foam injection pilot pattern is shown in Fig. 3. Note that the pattern gas production increased sharply in early 1987 when Well 3332-032, a side producer in the nine-spot pattern (shown in Fig. 1, located to the southwest of the injection well), began to flow spontaneously in response to CO_2 injection. This producer had previously been open to production; however, it was not being pumped because of excessive WOR during the pre-CO_2 waterflood period. Since 1987, the 3332-032 well has been capable of flowing following each CO_2 injection cycle. Although this well has not received any special monitoring during the CO_2 flood prior to initiating the foam project, production records indicate the apparent time lag between the beginning of the CO_2 injection half-cycle and the increase in gas-oil ratio (GOR) in Well 3332-032 has varied from about 6 to 14 weeks. CO_2 production rates from Well 3332-032 at the end of the past two CO_2 injection half-cycles have been 25-30% of the average CO_2 injection rate into the pattern injector (Well 3332-001). Favorable changes in the CO_2 production response characteristics in Well 3332-032 were expected to become an important indicator of successful foam treatment in this pattern.

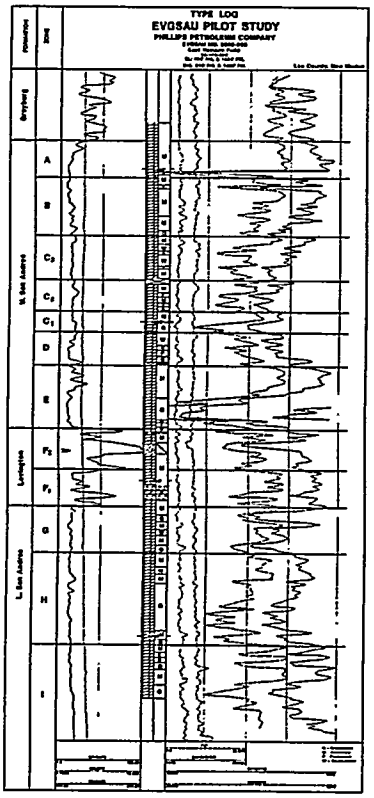

Fig. 2. Type Log from the Pilot Area

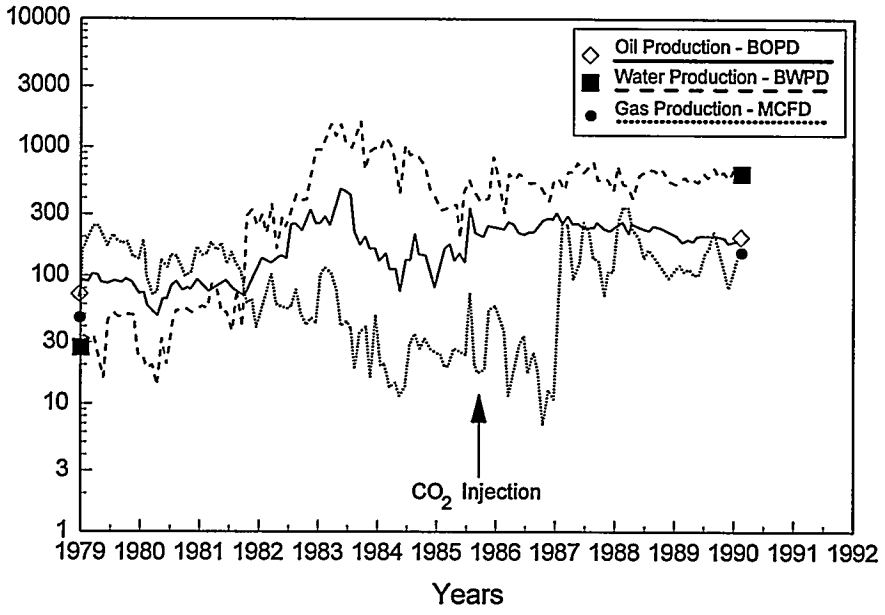

Fig. 3. EVGSAU Foam Pattern Production

GEOLOGICAL STUDY

The purpose of the geological reservoir characterization study[17] was to provide a geologic framework in which to study and evaluate potential solutions to poor CO_2 sweep efficiency at EVGSAU, and most importantly, to evaluate the effectiveness of CO_2-foam minimizing CO_2 breakthrough. The study provided information regarding the stratigraphic, sedimentologic, and diagenetic character of the field and a detailed lithologic characterization of individual flow units, their lateral continuity, and the nature of the pore system that controls the flow properties within these flow units.

The EVGSAU occurs on the Artesia-Lovington uplift, along the northern limit of the Delaware Basin. The San Andres structure is an east-west trending anticline with more than 400 feet of closure above the original oil/water contact of about 700 feet. The unitized interval includes the Grayburg and San Andres formations. The San Andres Formation, the major producer, is subdivided into nine major, correlatable flow units (shown in Fig. 2), in which the properties affecting fluid flow are internally consistent and predictable. Four of these occur above and three occur below the Lovington Sand Member (Layer F). The best reservoir quality within the section occurs in two flow units, Reservoir Layers C and E, both of which lie above the Lovington Sand.

The geological study of the San Andres Formation in the EVGSAU centered around the examination of core material and core samples from two wells (3332-003 and 2913-011) within the field and the analysis of 58 well logs from wells fairly evenly distributed throughout the field. The following conclusions were drawn from this study.

Stratigraphy and Lithofacies

The San Andres reservoir section comprises series of repeated, anhydritic, dolomitized, fining-upward, carbonate sequences composed of grain-rich dolostones that grade upward into mud-rich dolostones. The section is informally subdivided into the "lower" and "upper" San Andres by the Lovington Sandstone. Primary depositional facies recognized within the San Andres reservoir section include: a) skeletal/pelletoidal grain-rich facies, b) oolitic grain-rich facies, c) dolomudstone facies, and d) siliciclastic facies. The fining-upward sequences were deposited as shallowing-upward parasequences on a shallow marine shelf. Skeletal/pelletoidal and oolitic grain-rich facies were deposited under subtidal/shoal paleoenvironmental conditions; dolomudstones were deposited under intertidal and occasionally supratidal conditions; the siliciclastic facies of the Lovington Sandstone was deposited as tidal flat sediments associated with a major sea-level low-stand.

Within the foam pilot pattern area, the zones designated as C2 and C3 (Fig. 2) contain intervals with very high permeability. For example, a 5-foot interval in Zone C2 from the observation well core averages almost 250 millidarcies. Oil saturations obtained from the sponge core in this interval were consistently less than 5% PV, indicating they had probably been contacted by a large volume of CO_2. Injection profiles taken in the WAG injector show almost two-thirds of the injected fluids entering Zone C2 and the lower portion of Zone C3. In contrast, Zone E, which shows high porosity and good oil saturation, is indicated to be taking less than 5% of the injected fluid. One of the primary objectives of the foam injection is to divert a larger percentage of the injected CO_2 into these lower permeability zones that are not being efficiently processed in the current WAG operation.

Porosity averages about 7.0 percent (range = 0.7 to 32.8%) within the reservoir section. Commonly occurring pore types include: a) primary intergranular porosity, b) intercrystalline porosity as a result of dolomitization, c) grain-moldic porosity as a result of the dissolution of partially dolomitized framework grains, and d) vugular and fenestral porosity. The best quality reservoir rock is associated with the subtidal grain-rich lithofacies. Skeletal/pelletoidal grain-rich rocks are dominated by intercrystalline and intergranular pore types with less abundant grain-moldic and vugular pore types. The oolitic grain-rich facies contain mostly intergranular and grain-moldic pores. Permeability does not correlate well with porosity in the oolitic facies because of a high grain-moldic porosity content. The dolomudstone and siliciclastic lithofacies are typically nonreservoir-quality rocks that exhibit vuggy pores and isolated, patchy intercrystalline and intergranular pores. The reservoir is very weakly fractured; fracturing does not appear to have a significant impact on reservoir quality in the study cores.

As noted above, nine major reservoir zones, designated as Zones A through I in Fig. 4 (with Zone

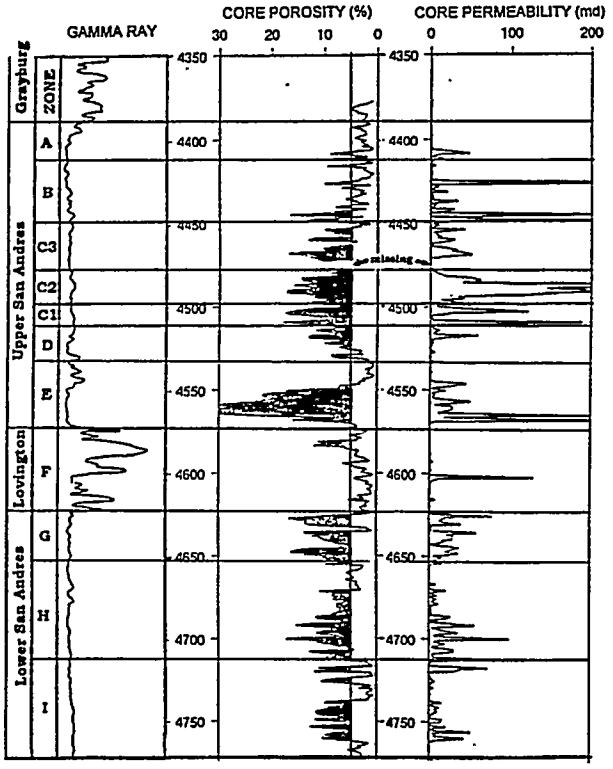

Fig. 4. Geological Zones in the EVGSAU Foam Pilot Area

C divided into three subzones in the foam pattern area), have been correlated and mapped across the Unit. Five of these occur above and three occur below the Lovington Sand. Zones A and B, predominant in the northern area of the field, are the only zones that are not continuous throughout the field. Logs, injection profiles, and production logs indicate that Zones C, D, and E are continuous and exhibit good reservoir quality throughout the field. The best reservoir quality generally occurs in Zones C and E, both of which lie above the Lovington Sand. The three zones below the Lovington (designated as G, H, and I) lie below the oil/water contact in all but the structurally highest areas of the Unit. Porosity within the San Andres reservoir section at EVGSAU ranges from 0.7 to 32.8 percent, and averages 7.0 percent. A porosity cutoff of 5% (based on 100% dolomite matrix) is used to define effective reservoir-quality rock. The reservoir-quality flow units in Zones A through D are composed primarily of skeletal/pelletoidal grain-rich lithofacies. The flow units in Zone E are composed of an oolitic grain-rich facies. Zone F (the Lovington Sandstone) is dominated by the siliciclastic and dolomudstone lithofacies, and generally represents nonreservoir rock. The reservoir-quality flow units in Zones G through I are again composed primarily of skeletal/pelletoidal grain-rich lithofacies.

Diagenesis and Oil Emplacement

The major diagenetic events which enhanced reservoir porosity were dolomitization and dissolution. The primary porosity-destructive diagenetic events were anhydrite cementation and early emplacement of a now immobile, dead oil. Dissolution within the reservoir is represented by the removal of anhydrite cement early in the diagenetic history of the reservoir and by anhydrite-plugged, solution collapse breccias. The collapse breccias likely result from meteoric leaching during the low sea-level stand associated with deposition of the Lovington Sandstone. They are restricted primarily to the "lower" San Andres.

Intercrystalline porosity is estimated to contribute roughly 4 to 5 percent to the total pore system, and the increased porosity as well as the nature of the crystals significantly improved permeability of the reservoir rock. Anhydrite diagenesis (cementation/dissolution patterns), although a major control on reservoir quality, remains a poorly understood phenomena and merits further study. Waterflood-induced dissolution strongly overprints the "natural" diagenetic character of the reservoir and is a major factor in reservoir porosity and permeability. "Thief" zones within the reservoir developed as a result of a lack of uniformity in the depositional and "natural" diagenetic processes through the San Andres section as well as the leaching of anhydrite and dolomite during water injection. The best example occurs in reservoir Layer C2 within the interval from 4465 ft to 4504 ft in EVGSAU Well 3332-003.

The immobile dead oil that occurs in the reservoir is not genetically related to the produced oil (paraffinic). Dead oil represents a water-washed or biodegraded oil that migrated into the reservoir prior to migration of the currently produced oil. Where dead oil occurs in the reservoir, it occupies roughly 65 percent (range = 28 to 89 percent) of the available pore space; within a flow unit, dead oil may plug as much as 20 percent of the available pore space. The presence of the dead oil may affect wettability and the fluid displacement characteristics within a flow unit, a matter that merits further investigation.

Oil migrated up dip from basinal source rocks in the Delaware Basin into the laterally equivalent shelf carbonates of the San Andres Formation. Apparently, two episodes of oil migrations occurred into the San Andres at East Vacuum Field. The first, more terrigenous-sourced oil, only partially filled the capacity of the reservoir and was subsequently degraded into the black, immobile, pore-plugging, dead oil by either water-washing or biodegradation processes. A second, more marine-sourced oil later migrated into the reservoir and constitutes the oil presently produced from the field. The dead oil is a major

component of the reservoir section at East Vacuum Field. This immobile material plugs, or partially plugs, the pore system in the lowermost portion of the grain-rich facies of most depositional cycles.

A geochemical study of both the produced reservoir oil and the dead oil was conducted to compare the geochemical signatures of the two materials. The results indicate that the produced reservoir oil is dominated by paraffinic materials. Analysis of the dead oil shows it is dominated by aromatic compounds. The high aromatic content of the dead oil is indicative of source rocks that are of a more terrigenous nature, whereas, the more paraffinic nature of the produced reservoir oil is indicative of source materials that are more marine in character. The dead oil, therefore, is not genetically related to the produced reservoir oil.

FOAM PATTERN RESERVOIR CHARACTERIZATION

Once a candidate pattern for the CO_2-Foam field trial had been identified, a detailed geologic study of the pattern was conducted to provide information about the stratigraphic, sedimentologic, and diagenetic character of the reservoir in the area selected for the field trial. One of the primary objectives of this study was to identify potential high permeability channels in this pattern which might act as CO_2 thief zones. The geologic model developed in this work provided a framework for understanding fluid flow patterns in the pilot area, interpreting production data, and for subsequent design work and interpretation of the foam project performance. The reservoir characterization effort required integration of injection/production performance, falloff testing, injection and production profile surveys, and interwell tracer studies into the geologic model.

Excessive CO_2 production was observed from one side production well (3332-032) in the inverted ninespot pattern (the "offending" production well in Fig. 1). An observation well (3332-003) was drilled 150 feet from 3332-001, the CO_2 WAG injection well in the foam pattern. This well was cored for geologic study and fiberglass cased to provide a logging observation well during foam pilot operations. The geologic study conducted on the foam pattern emphasized detailed lithologic characterization of individual flow units, their lateral continuity, and the characteristics of the pore system that control fluid flow within these flow units. The study was focused on providing a framework in which to understand and address the problems of CO_2 channeling into the problem well (3332-032).

Core material examined in this study included 422 feet of nearly continuous core from the 3332-003 foam pattern observation well and 118 feet of continuous core from another well located approximately one mile west of the foam pattern. The study also included a reconnaissance examination of scattered pieces of core material from the northernmost producing well in the foam pattern and from a fourth well located approximately one-half mile to the south of the foam pattern. Conventional core analysis measurements of foot-by-foot porosity and permeability were available on all cores. X-ray diffraction analysis of selected reservoir lithologies from the 3332-003 well was performed to identify bulk mineralogy and clay mineral content. Sixty-seven samples were selected for thin-section preparation and study. The thin sections were stained and examined using both transmitted light and ultraviolet fluorescence petrographic techniques to determine mineralogic, textural, and diagenetic character. The thin sections were also evaluated using digital petrographic image analysis to provide detailed, quantitative information regarding reservoir pore geometries and the diagenetic character of the reservoir, particularly with respect to the occurrence of anhydrite, gypsum, and dead oil within reservoir flow units.

Facies Descriptions & Interpretive Sedimentology

The general character of the cored San Andres interval in the vicinity of the foam pattern is typical of most of the EVGSAU reservoir section. The reservoir section is comprised of a series of repeated dolomitized, fining-upward, carbonate depositional sequences in which basal grain-rich dolostones are overlain or capped by dolomudstones. The section contains variable amounts of both nodular/massive and pore-filling anhydrite. The dolostones are generally massive in that they seldom exhibit any recognizable primary internal structure. The reservoir section is dominated by four major lithofacies, each of which displays a fairly similar, recurring suite of sedimentary structures, depositional textures, and framework components. The facies identified include: (1) a skeletal/pelletoidal grain-rich (dolograinstones and dolopackstones) facies, (2) an oolitic grain-rich (dolograinstone) facies, (3) a dolomudstone facies, and (4) a siliciclastic facies.

The "lower" San Andres section (Zones G-H-I) in the 3332-003 core exhibits evidence of major karsting in the form of anhydrite-sealed, solution-collapse breccias, and probable anhydrite-filled solution cavities and solution channels. Above the Lovington Sandstone there is only minor evidence of karsting, which occurs in the form of occasional solution channels and thin, solution-collapse breccias typically linked spatially with the dolomudstone facies. The Lovington Sandstone (Zone F), which separates the "upper" and "lower" San Andres, is composed of dolomitic siltstones and sandstones, silty to sandy dolomudstones and occasional dolomudstones. The "upper" San Andres section is 197 feet thick. The lowermost fining-upward sequence in the "upper" San Andres (Zone E) consists of 17 to 25 feet of oolitic grain-rich facies, capped by 16 to 19 feet of dolomudstone facies. The overlying fining-upward sequence (Zone D) is composed of about 12 feet of skeletal/pelletoidal grain-rich facies, capped by 7 to 15 feet of dolomudstone facies. In the uppermost 113 feet of the "upper" San Andres section (comprising Zones A-B-C), the same skeletal/pelletoidal grain-rich lithotypes and cyclical character can be recognized, but they are interlayered on a finer scale, and sequences tend toward incompleteness. The lower portion of the grain-rich members of these sequences are often partially filled with immobile, pore-plugging dead oil. The occurrence of dead oil appears to be somewhat sporadic and the thickness of the intervals filled with dead oil are variable.

Oolitic packstones and grainstones are a major component of the sedimentary sequence that comprises Zone E. The oolites are typically leached and preserved as partial grains composed of subequant, fine to medium crystalline dolomite. Porosity in the oolitic grain-rich lithofacies averages 18.8 percent, ranging from 4.1 percent to 32.8 percent, depending mostly on the amount of leaching of the framework material that has occurred. Porosity is high because of the well-developed grain moldic pore system; however, because of the isolated character of the molds, permeability can be very low. A porosity vs. permeability plot for the oolitic grainstones (Fig. 5) indicates no consistent relationship between porosity and permeability within this lithofacies. Petrographic Image Analysis (PIA) data indicate that grain-moldic pores constitute roughly 45 to 50 percent of the porosity within this facies. In the lower part of the oolitic grain-rich facies, permeability is also limited by the presence of immobile, dead oil in the pore spaces. Thus, although the oolitic grain-rich facies may exhibit some of the highest porosities that occur within the San Andres reservoir section, this facies is not necessarily the best quality reservoir rock within the section.

The average porosity of the skeletal/pelletal grain-rich facies is 8.9 percent, ranging from 2 to 17.1 percent, depending on the amount of dissolution and anhydrite cementation that has occurred. The predominant pore types within this facies include primary intergranular porosity and intercrystalline porosity resulting from dolomitization. Grain-moldic pores, typically leached skeletal grains and occasionally leached pelletoids, constitute only a small proportion of the porosity in the skeletal/pelletoidal facies. All pore types

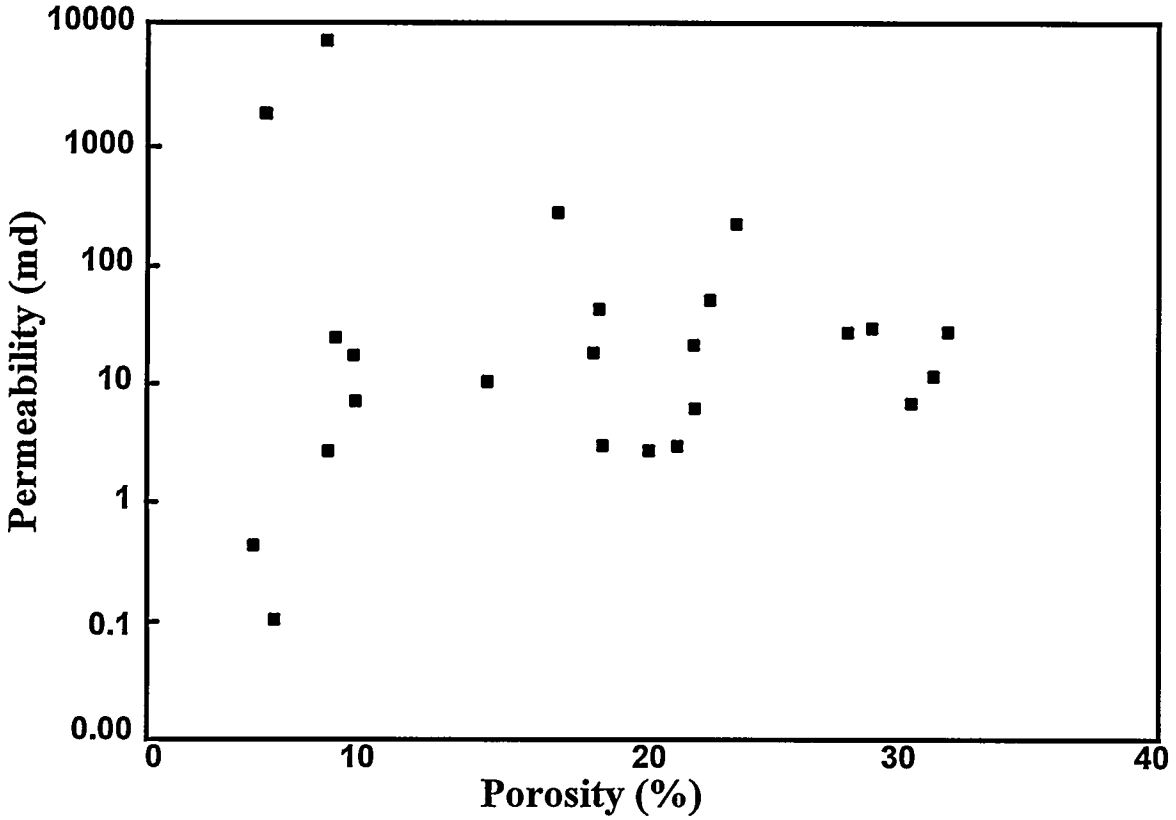

Fig. 5. Porosity vs Permeability in the Oolitic Facies in the EVGSAU 3332-003 Core

show varying degrees of solution enhancement. The average porosity in this facies is less than one-half of the value measured for the oolitic facies, however there is a good correlation between porosity and permeability within this lithofacies (Fig. 6). PIA pore typing shows that within the skeletal/pelletal facies, 42 percent of the pore system is composed of well-interconnected, irregular- and rough-shaped, intermediate-sized pores. Petrographic observation indicates that these occur as a well-developed intercrystalline and intergranular pore network which promotes good permeability. Therefore, although the oolitic facies exhibits the highest porosities, the best quality reservoir rock within the San Andres reservoir section is associated with the somewhat lower porosity, skeletal/pelletal grain-rich facies.

Both the dolomudstone and siliciclastic facies are predominantly low permeability, nonreservoir rock because of (1) the poorly developed nature of their intergranular and intercrystalline pore systems and (2) the isolated character of any vugs and molds that typically constitute the remainder of the pore system. Rocks in the dolomudstone and siliciclastic lithofacies are characterized by low porosity (3-5%) and poor permeability.

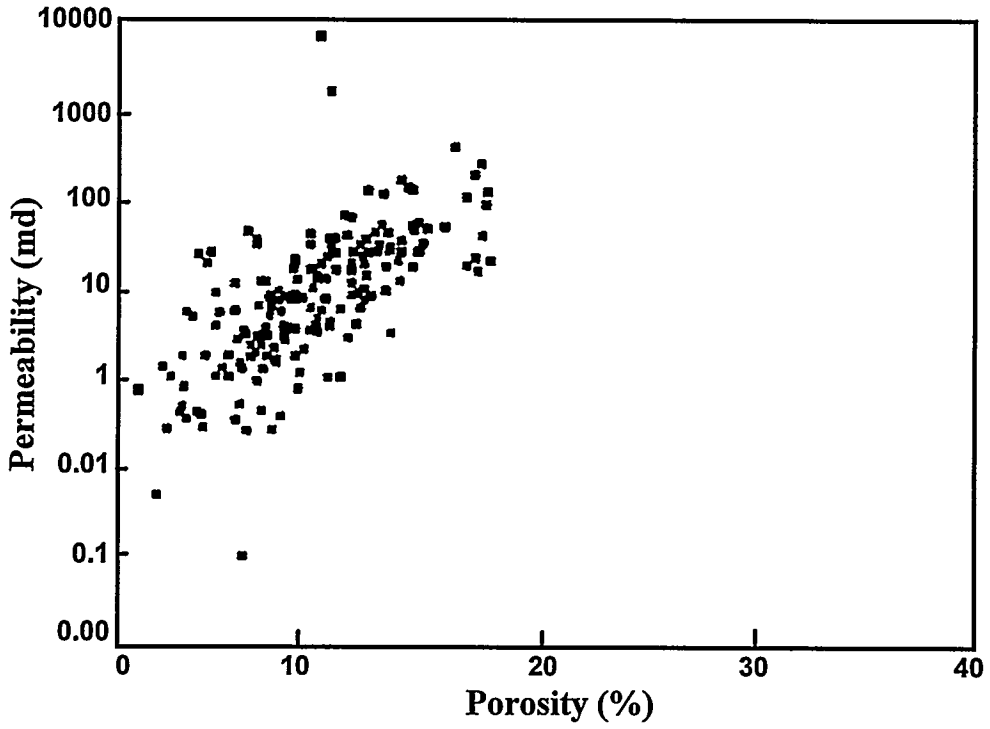

Fig. 6. Porosity vs Permeability in the Skeletal/Pelletal Facies in the EVGSAU 3332-003 Core

Diagenetic Events

The diagenetic events determined to have had a major influence on porosity at East Vacuum include: (1) dolomitization, (2) emplacement of anhydrite, (3) dissolution, and (4) the formation and occurrence of dead oil. The reservoir is only very weakly fractured and fractures are thought to contribute very little to reservoir permeability. Calcium sulfate occurs as both anhydrite and gypsum within the cored intervals. Anhydrite is a primary factor in determining reservoir quality because of the abundant, yet uneven or heterogeneous distribution of the mineral at every scale within the reservoir. The two most commonly occurring forms of the mineral within the field are as pore-filling cement and as void-filling material in solution-controlled collapse breccias and cavities associated with karsting. The most intense anhydrite cementation is commonly associated with the grainstones; some grainstone beds being completely plugged by the mineral. Much of the gypsum occurs as intergranular and intercrystalline pore-filling material in a thick, intensely leached, skeletal/pelletoidal grain-rich section in the uppermost part of the San Andres.

Enhancement of the pore system by dissolution has had a major impact on porosity and permeability within the San Andres reservoir section at East Vacuum. Secondary porosity in the San Andres is caused by the dissolution of calcium carbonate, dolomite, and calcium sulfate. Dissolution is evident from grain-moldic and crystal-moldic pores, irregular framework grain boundaries, ragged-edged anhydrite and dolomite crystals, and over-sized pores. Solution enhancement of the pore system is

particularly strong in the uppermost San Andres section. It is apparent that much of the solution enhancement of the pore system may be a product of waterflooding. Irregular framework grain boundaries and over-sized pores are thought to be good evidence of waterflood-related dissolution. No doubt, considerable anhydrite has been removed by natural leaching. However, high porosity and permeability in association with an anhydrite content that is low, with the remaining anhydrite being ragged-edged and partially altered or replaced by gypsum, provides good evidence of waterflood-related leaching of anhydrite.

Identifying The High Permeability Channels

Macroscopic and thin-section study of the 3332-003 core showed that the reservoir interval from 4,465 to 4,504 feet within reservoir Zone C in this well has undergone extreme leaching. Within this zone, (1) nearly all of the anhydrite has been removed, (2) any remnant anhydrite is ragged-edged and partially replaced by gypsum, (3) dolomitized framework grains are corroded and partially dissolved with no control by rock fabric of the dissolution, (4) channel porosity is commonly observed, and (5) matrix porosity and fractures exhibit strong solution enhancement. Porosity increases somewhat over this interval, however permeability is exceptionally high. It should also be noted that the interval is only very weakly fractured and that the large increase in permeability is controlled primarily by solution enhancement of the matrix pore system. Within the high permeability interval, gypsum is predominant over anhydrite and textural relationships indicate that in some cases the gypsum replaces anhydrite. The potential exists for a considerable amount of fluid to pass through this thin interval within the San Andres reservoir section.

The most extreme dissolution in the 3332-003 core is observed in two intervals (see Fig. 4): (1) a section of rubble and missing core from 4471 to 4478 feet, and (2) a high permeability interval in Subzone C2 from 4486 to 4492 feet. The latter six-foot interval averages 200 millidarcies permeability and 14.3% porosity, whereas the surrounding reservoir rock in Zone C exhibits an average permeability of about 23 millidarcies and an average porosity of 11.1 % (these are arithmetic averages over an interval extending fifteen feet above and below the high permeability section at 4486-4492 feet).

The cored intervals discussed above were part of a sponge core cut in this observation well located 150 feet away from the WAG injector after five cycles of CO_2 injection. The sponge core oil saturations in the interval from 4486 to 4492 feet averaged 3.3%. This compares with oil saturations averaging 8 to 13% in the surrounding rock. The sponge core data also show isolated, lower permeability intervals in the section with oil saturations of 25% to 35% (closer to the waterflood residual oil saturation). These data indicate that, while CO_2 flooding has apparently reduced residual oil saturations below waterflood residual over most of Zone C at the observation well location, a disproportionately large volume of CO_2 may have passed through the high permeability intervals in this core.

High permeability intervals, such as the intervals described in the 3332-003 core, probably developed initially as a result of the primary depositional character and diagenetic history; however there is substantial evidence that these high permeability channels were significantly enhanced by waterflood-related dissolution of anhydrite. Localized regions of high and low permeability developed within the reservoir as a result of the depositional and diagenetic history. During water injection, fluid flow would have been higher through these more permeable beds, resulting in enhanced leaching of the more soluble materials from these beds by the undersaturated injection fluids. Because the high-permeability pathways

are depositionally and diagenetically controlled, they are possibly regional in scale. Thus, based on geologic evidence, Zone C should be considered a potential "thief" zone throughout the area.

LABORATORY TESTING FOR SURFACTANT SELECTION

Three criteria were used in our surfactant selection process: 1) the lowering of mobility due to the presence of surfactant in the brine injected with the CO_2, 2) the amount of adsorption of the surfactant onto the reservoir, and 3) the ability of the surfactant to stabilize aqueous-phase bubble films or foam lamellae in dense CO_2 at reservoir-conditions. The principal goal of this work was to select the surfactant and the concentration of that surfactant to be used in the field tests. In all the laboratory experiments, a synthetic brine with the composition shown in Table 2 was used to simulate the EVGSAU reservoir brine.

TABLE 2
COMPOSITION OF EVGSAU SYNTHETIC RESERVOIR BRINE

Component	gm/1000 gm solution
NaCl	30.628
KCl	0.290
$CaCl_2 \cdot H_2O$	4.769
$MgCl_2 \cdot 6H_2O$	2.594
Na_2SO_4	2.957
H_2O	958.72

Foam Mobility

Cores from EVGSAU were used to assess the extent of mobility reduction provided by foaming agents of CO_2 at reservoir conditions. From the injection flow rate (q), the cross-sectional area of the core (A), and the pressure drop (Δp) across the core length (L), the mobility (λ) can be calculated in Darcies per cp, from

$$\lambda = \frac{(q/A)}{(\Delta p/L)} \qquad (1)$$

The typical effect is decreasing CO_2-foam mobility with increasing surfactant concentration. At higher surfactant concentrations, the increased population and durability of the lamellae (bubble films) retard the movement of CO_2 through porous media. Actual propagation of the foam will be discussed later. At extremely low or zero surfactant concentration, the mobility is indicative of the combined mobilities of dense

CO_2 and brine without surfactant, at the gas-liquid ratio used in the experiment.

Mobility reduction with CO_2-foams will depend on the volumetric flow-rate ratio of the two phases, conventionally given as the flowing fraction of the bulk dispersion that is dense CO_2. This ratio can be expressed as either the CO_2 fraction or foam quality (as a percentage), or as a gas-liquid volumetric ratio (q_g/q_l). For example, if the gas-liquid volumetric ratio is four, the foam quality is 80%. When steady-state conditions are achieved, a mobility reduction factor (MRF) at a given gas fraction can be calculated

$$MRF = \frac{\lambda_{g1}}{\lambda_{g2}} \qquad (2)$$

where λ_{g1} is the gas phase mobility when no surfactant is present in the brine and λ_{g2} is the gas phase mobility when surfactant is present, and where both mobilities are determined at the same gas-liquid volumetric ratios and at the same flow velocities. The MRF can represent the pressure drop attributed to the presence of foam, provided λ_{g1} and λ_{g2} are determined at the same gas fraction and flow velocity. If foam is not generated, MRF would be unity. If foam is generated, the MRF values quantify the effect of the presence of foam.

The mobility of foam is lower than it is for the combined flow of CO_2 and surfactant-free brine, because of the presence of fairly stable bubble films or lamellae spanning some of the pores. These prevent the CO_2 from flowing through the rock freely, constrained only by its own low viscosity. Consequently, the MRF depends on the population of these lamellae, and can be expected to vary with the overall flow rate, the flowing fraction of the two phases, and the rock permeability —as well as with the surfactant type and concentration.

Foam flow in porous media can exhibit a moderate shear-thinning behavior. This behavior is consistent with the notion that higher flow rates will decrease the stability of lamellae (bubble films). While the effect is moderate, this behavior is desirable from a field injectivity standpoint in that the apparent viscosity of the foam can be lower near the vicinity of the wellbore than farther into the reservoir, provided that radial flow conditions exist. However, a recent study[18] found that shear-thinning behavior was apparent at flow velocities above about 1 ft/D, but shear-thickening behavior was observed below that rate.

In experiments described by Lee *et al.*,[19] the mobility did not exhibit the same proportionality to rock permeability as that shown by a simple fluid that follows Darcy's law. In fact, over a range of rock permeability from 4 to 200 md, the mobility did not increase appreciably. Above and below that range of permeability, the expected proportionality was gradually attained. This behavior is very desirable from the viewpoint that the foam is more effective in reducing mobility in higher permeability media and can mitigate some of the inherent reservoir heterogeneities. The effect of rock permeability on foam mobility can depend on the hydrophilic nature of the surfactant and on the stability of the foam.[18] Depending on hydrophilicity, some surfactants yielded a favorable dependence on permeability while others did not.

For foam to be continuously generated in situ, a critical gas velocity or critical pressure gradient must be exceeded.[20] Thus, a minimum pressure gradient may be required to initiate and sustain foam flow. This latter concept is controversial, and further laboratory tests are needed to fully assess the importance of this mechanism. When the foam mobility and propagation tests are done with an oil phase present in cores, the observed behavior can be very complicated and will depend on whether the foam is stable or unstable,

on whether viscous emulsions are formed, and also on the foam-bubble coalescence-time relative to bubble snap-off time.[18] Unstable foams that break and reform may be desirable so that the foam can be propagated through a reservoir at a satisfactory rate.[18]

A commonly used expression to assess the magnitude of mobility reduction is the "resistance factor." The resistance factor, when only CO_2 is flowing through a core, is the CO_2 mobility before foam flow divided by CO_2 mobility after foam. The resistance factor during foam flow is the mobility of the CO_2/brine mixture divided by the mobility of the CO_2/surfactant solution where both measurements are conducted at the same gas-liquid volumetric ratio. Because of the dependence of velocity on foam mobility, resistance factors are calculated at a constant velocity.

Surfactant Selection Criteria

Several significant issues arose during the initial project design discussions. The first was whether the objective of the foam project should be directed toward near-well fluid diversion or more in-depth mobility control throughout the pattern. Preliminary laboratory data indicated surfactant adsorption would be in the range of 600 to 1800 lbs of active surfactant adsorbed per acre-foot of bulk formation volume contacted. Based on economic considerations, it was decided to design the project primarily for near-well fluid diversion using a smaller (approximately 1% HCPV), higher surfactant concentration foam slug rather than attempt to control mobility throughout the pattern using a larger volume slug with a lower surfactant concentration.

Three criteria were used in our surfactant selection process: 1) the effectiveness of the surfactant in reducing CO_2 mobility in coreflood experiments, 2) the amount of surfactant lost to adsorption onto the reservoir rock, and 3) the ability of the surfactant to stabilize aqueous-phase bubble films or foam lamellae in dense CO_2 at reservoir conditions. The principal goal of this work is to select the surfactant and the concentration of that surfactant to be used in the field tests.

Mobility Measurements

To assess the extent of mobility reduction by flowing aqueous foaming agents with CO_2, and to simulate the foam flow behavior, mobility measurements were conducted at reservoir temperature and pressure. In the PRRC experiments, the pregenerated foam from a foam generator (a short piece of core) was injected into the core sample; whereas, in the work of PPCo and Chevron, the foam flowing through the core sample was generated in situ. The reservoir samples were preserved plugs cut from the core recovered from a new observation well. At reservoir conditions of 101 °F and 2100 psig, simultaneous injection of CO_2 and brine at a volumetric flow ratio of 4 to 1 (or quality of 80%) was performed to attain the baseline data. Then, the same ratio of CO_2 and surfactant solution was coinjected into the core at different surfactant concentrations to simulate foam flow through the reservoir. The pressure drop across the core sample was measured at steady state, which normally was attained after multiple pore volumes of injection.

Table 3 shows some of the results obtained from different laboratory experiments. The mobilities were estimated as the ratio of the Darcy velocity (that is, total flow rate divided by the core's cross-sectional area) to the pressure gradient along the core sample. Under similar circumstances, the mobility data are generally lower in PRRC experiments than in those of the other two laboratories. Since different foam generation procedures were applied in each laboratory, the lower mobility of pregenerated foam suggests that the pregenerated foam is more resistant to flow through the core sample compared to the in

TABLE 3
SUMMARY OF MOBILITY MEASURMENTS OF SURFACTANT CD-1045

Laboratory	Permeability (md)	Darcy Velocity (ft/day)	Core Size (ID x Length)	Mobility (md/cp)			
				Surfactant Conc. (ppm)			
				0	500	1000	2500
PRRC	640	10	0.5"x1.0"	95.3	13.5	2.24	
	640	4		75.9	9.29	1.38	
	277	4		49.8	1.11		0.81
	42	4		4.8	0.2		0.15
PPCo	254	6.5	1"x3.0"		14.3	9.3	
Chevron	210	10	1"x1.8"	174	7.5	5.3	4.2
	210	4		124	4.6	3.1	2.5

situ generated foam. Another typical effect is the decreasing CO_2-foam mobility with increasing surfactant concentration, shown in Fig. 7. The mobility shows a much lower dependence on surfactant concentration above the critical micelle concentration (CMC), (which is 600-700 ppm at test conditions for Chevron's CHASER™ CD1045). The lower mobility of foam compared to the baseline mobility of CO_2 and surfactant-free brine is attributed to the presence of surfactant which stabilizes the bubble films or lamellae that span some of the pores. As a result, the movement of CO_2 is retarded and the mobility is decreased. As the surfactant concentration is increased, the foam mobility decreases further because of the increased population and stability of the lamellae. The rate of decreasing mobility decreases at higher concentrations. In the absence of other considerations, the benefit of using higher surfactant concentrations to further reduce the mobility would be difficult to justify in field applications.

The effect of rock permeability on the foam mobility for CD1045 was studied using preserved core samples with a broader range of rock permeabilities in PRRC experiments. Fig. 8 shows some of the mobility results as a function of rock permeability. The mobilities were measured at a Darcy velocity of 4 ft/day. On a log-log scale, the mobility of CO_2 and surfactant-free brine, designated by open square symbols, shows a linear proportionality to the rock permeability. On the log-log plot, these points more or less fall on a unit slope line, suggesting that the simultaneous flow of CO_2 and surfactant-free brine is like that of ordinary fluid flow, whose mobility is proportional to the effective permeability of porous media. By adding a very small amount of surfactant (for example, 150 ppm) to the brine, a very weak foam is observed, accounting for a slight decrease of mobility (as designated by the diamonds). However, the mobility dependence to rock permeability of this weak foam is similar to that of CO_2 and surfactant-free brine. By adding more surfactant into the brine, the mobilities are reduced further (as shown in open

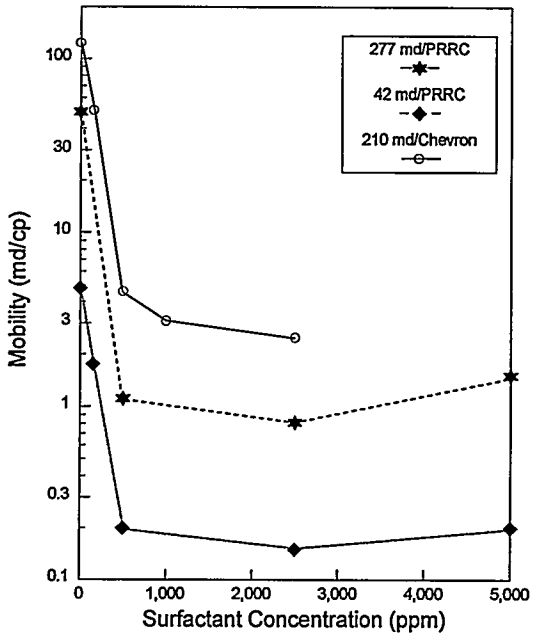

Fig. 7. Effect of Surfactant Concentration on Foam Mobility at 101° F and 2100 psig

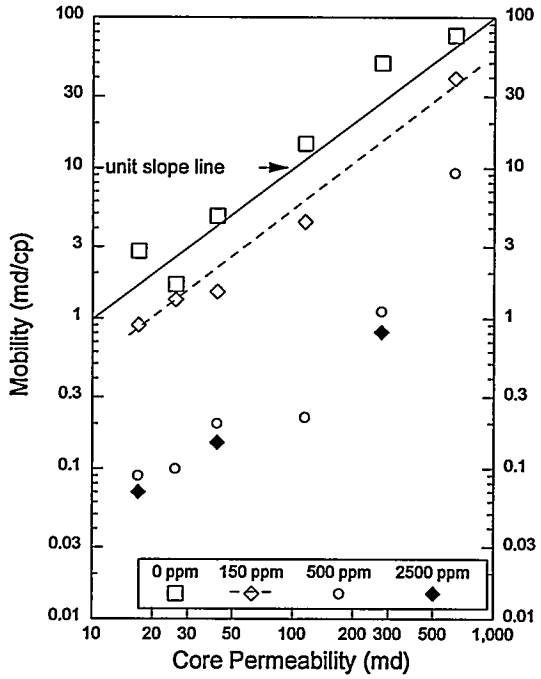

Fig. 8. Foam Mobility of Surfactant CD 1045 in Preserved Cores at 101°F and 2100 psig

circles and solid diamonds). For this surfactant, the mobility dependence on rock permeability is not significantly affected by increasing the surfactant concentration. Only a slightly more favorable slope is observed for rock permeabilities between 20 and 120 md. Unlike the other reported surfactants showing selective mobility reduction (SMR) over a broader range of rock permeabilities,[7,18,19] surfactant CD1045 shows only a slightly favorable dependence on rock permeability of dolomite reservoir cores.

To study the effect of residual oil on the performance of surfactant in CO_2-foam, further mobility measurements were conducted at both the PRRC and Chevron laboratories. At PRRC, preserved core samples were treated by three methods to remove the residual oil in core samples. The first group of samples was cleaned by using the Dean-Stark extraction method. Each core sample was cleaned for 48 hours using toluene as a solvent. A second group of rock samples was oven dried at 60°C for two weeks. Rock samples in the third group were subjected to a previous series of CO_2-foam displacement, cleaned by distilled water, followed by the synthetic brine, and reused. Prior to the mobility measurements, all of these cores were preflushed with at least another 100 pore volumes of synthetic brine. At the Chevron laboratory, a core sample that had been subjected to a previous series of CO_2-foam displacement was cleaned by sequential injection of 1% NaCl, isopropanol, and methanol to remove all surfactant. Following the cleaning, the core was saturated with EVGSAU stock tank oil, flooded with brine and CO_2, and retested with residual oil present.

A summary of the mobility data at a Darcy velocity of 4 ft/day from the PRRC experiments is given in Table 4. Within a similar range of core permeability, the mobility data for three groups of treated core samples are generally similar at the same surfactant concentration. The mobility, however, is higher with treated core samples than with untreated, preserved core samples. To show graphically the effect of core condition on mobility, some data from Table 4 are presented in Fig. 9. The open symbols represent

TABLE 4
EFFECT OF CORE CONDITIONS ON MOBILITY

Initial Condition		Mobility (md/cp)			
		CO_2/Brine	CO_2/Surfactant		
Rock Condition	Brine Perm. (md)	0 ppm	150 ppm	500 ppm	2500 ppm
Preserved (untreated)	640	75.98	39.40	9.29	
	277	49.8		1.11	0.81
	115	14.52	4.38	0.22	
	42	4.8	1.5	0.2	0.15
	26	1.68	1.33	0.1	
	17	2.8	0.9	0.09	0.07
Extracted (treated)	285	61.38		2.34	1.5
	24	5.88	4.48	0.33	
	21	11.4	3.81	0.35	0.11
Oven-Dried (treated)	209	72.2	48.3	4.0	1.8
	115	34.4	19.6	0.93	0.3
	25	5.14	1.55	0.51	0.18
Reused (treated)	296	79	63.7	2.73	1.97
	120	19.03	6.35	1.19	0.83
	91	13.02	2.91	0.89	
	22	7.18	3.55	0.7	0.43

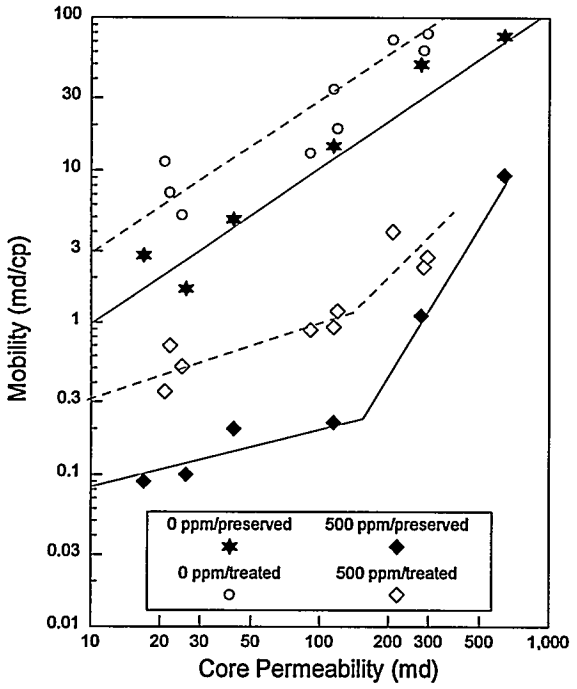

Fig. 9. Effect of Rock Conditions on Mobility at 101 °F and 2100 psig.

mobility data obtained from treated core samples, whereas the solid symbols represent mobility data obtained from preserved core samples. A slightly higher mobility trend observed in treated core samples suggests that mobility is affected by the initial rock conditions. This is probably due to relative permeability effects since the oil saturation was likely low in those cores cleaned by different means. A similar behavior is also observed from the Chevron data. As shown in Fig. 10, the initial CO_2/brine and weak foam mobilities are higher for the series run with no oil injected into the core. However, mobilities at the end of both series of experiments, with and without added oil, were nearly the same indicating that the foam was very effective in displacing residual oil. This is a benefit of foam that is frequently overlooked since emphasis is usually on sweep improvement aspects.

The initial condition of preserved dolomite rock was unknown. But it is likely to be oil-wet as some research has reported.[21-24] Cleaning the core with either toluene or CO_2 extraction tends to make the core more oil-wet[21-24] and foam will become less effective in reducing the mobility of CO_2.[25] Since we did not measure the rock wettability, it is uncertain whether the wettability effect also accounts for changes of mobilities in cleaned core samples during the foam displacement. Further work needs to be done to clarify this effect.

Surfactant Adsorption Measurements

CD1045 is a multicomponent formulation that requires a special analytical procedure to measure concentration. The analytical methods suggested by the manufacturer include a two-phase Hyamine

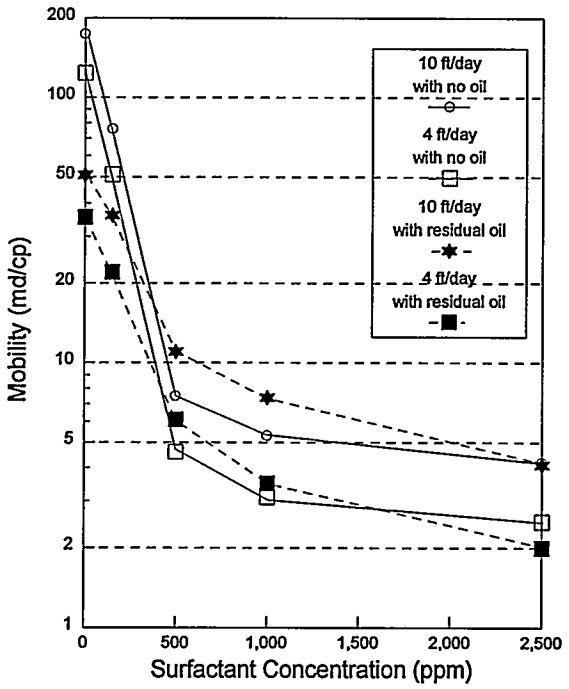

Fig. 10. Mobilities of CO_2-foam in EVGSAU core at different surfactant concentrations

titration method, a colorimetric method, and a refractometric method. The Hyamine titration method can accurately determine surfactant concentrations, working best for concentrations in the range of 100 to 5000 ppm. The colorimetric method works for surfactant concentration as low as 10 ppm. However, this method is time-consuming, and the accuracy of the measurement depends on the background interferences and is degraded by the nonlinearity of the calibration curve. On the other hand, the refractometric method provides a rapid and reliable measurement, provided that the salinity remains constant. As the calibration curve is linear for surfactants in the range of 0 to 2500 ppm, the accuracy of measurements primarily depends on the sensitivity of the refractometer. However, due to the possible interference of impurities in the test sample, quality control of the sample prior to the analysis is very important.

In more recent experiments at PRRC, the refractometric method was used to analyze the surfactant concentration, while the recirculation method was used to estimate the surfactant adsorption at various equilibrium concentrations. The recirculation experimental apparatus consists of a closed system and its schematic is shown in Fig. 11. An LC pump is used to displace the surfactant-free solution (which can be either distilled water or synthetic brine) and surfactant through the core sample or a bypass teflon tube. The effluent from the core sample is directed to a 2.0 micron filter, then through the sample cell of the refractometer (while the reference cell contains the surfactant-free solution), from which it flows back to the effluent flask. The core sample, 0.5 inch in diameter and 1.0 inch in length, is epoxied into a brass cylinder and mounted in a core holder.

A Waters 410 Differential Refractometer was used to measure the concentration of surfactant in the system. This refractometer has a sensitivity of 4.88×10^{-6} RIU at 1% of full scale when set to its most sensitive range. The high sensitivity of the refractometer in this instrument is attained because it is

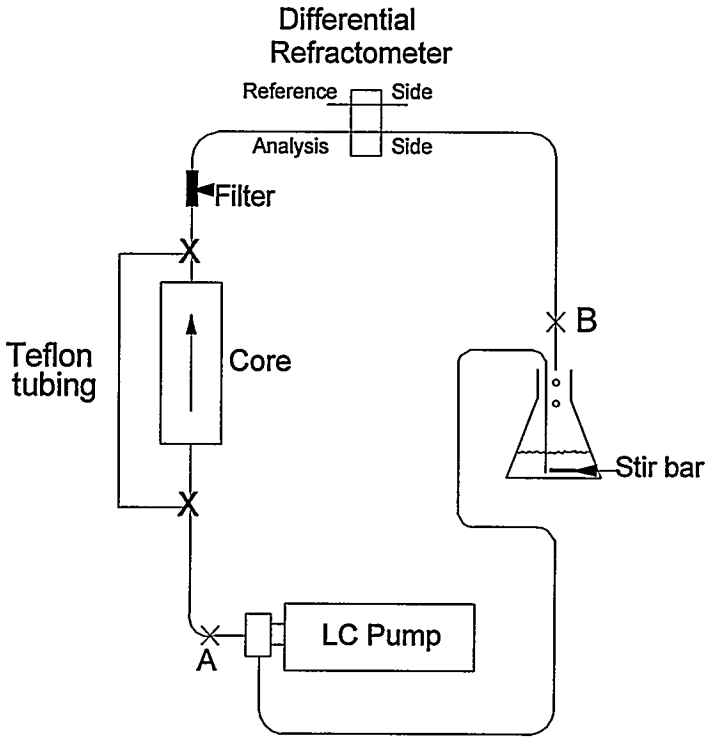

Fig. 11. Adsorption Measurement Apparatus

equipped with a countercurrent heat exchanger to minimize temperature fluctuations in the sample stream during operation.

All adsorption measurements were conducted at room temperature and atmospheric conditions. The internal oven temperature of the refractometer was set at 32°C as suggested by the operator's manual. A sensitivity of 64 and scale factor of 5 were used to obtain refractometer readings.

At the beginning of each measurement, surfactant-free solution was first circulated through the core sample and then through the teflon tubing to double check the baseline reading. When a constant baseline reading was obtained, a known volume of surfactant-free solution was removed from the system and replaced with the same volume of a known concentration of surfactant. The new solution was recirculated through the teflon tubing at 40 cc/hr until the reading stabilized. At this point, the refractometric reading represents the initial surfactant concentration in the system without occurrence of adsorption. To simulate the adsorption process, the solution was directed through the core sample and recirculated until another stabilized reading was reached. Finally, the solution was directed back to the teflon tubing to obtain a final surfactant concentration in the system. If there is no adsorption occurring when surfactant solution is recirculated through the core sample, subsequent readings obtained during two tubing flow cycles should be the same. A difference between the two readings indicates the occurrence of adsorption and the amount of adsorption can be determined. To complete an adsorption isotherm, the cycle of sampling and adding was repeated and the same procedures for recirculating the solution through core and tubing were followed until no additional surfactant was adsorbed.

The possible interference of the measurements using the refractometric method was realized when blank tests were first conducted using distilled water and oil-free Baker dolomite. It was found that the baseline readings were not stabilized until the surfactant-free solution was recirculated for eight hours. The interference was attributed to the dissolution of core sample. To minimize this effect, special care was taken to buffer the sample solution. Normally, about 2000 cc of the surfactant-free solution was precirculated through the candidate core sample for two days. Once the core sample and surfactant-free solution were equilibrated, the same batch of surfactant-free solution was used to prepare the surfactant solution.

The adsorption results using oil-free Baker dolomite are summarized in Table 5. Typical adsorption

TABLE 5
SUMMARY OF ADSORPTION DATA ON BAKER DOLOMITE

Aqueous Medium	Porosity (%)	Adsorption Data										
Distilled Water	18.6	Equilibrium conc. (ppm)	44	129	276	474	696	933	1178	1426	1676	1928	2180
		Adsorption (lb/acre-ft)	8	277	979	1477	1947	2292	2591	2850	3038	3179	3200
Distilled Water	20.6	Equilibrium conc. (ppm)	44	130	282	472	693	931	1178	1430	1682	1934	2184
		Adsorption (lb/acre-ft)	9	234	701	1416	1945	2326	2553	2656	2710	2755	2809
4% Brine	21.8	Equilibrium conc. (ppm)	103	252	445	682	929	1177	1430	1683	1935	2184	
		Adsorption (lb/acre-ft)	290	1371	2501	2892	3134	3359	3412	3427	3454	3460	
4% Brine	19.0	Equilibrium conc. (ppm)	103	256	457	690	933	1179	1432	1684	1935	2186	
		Adsorption (lb/acre-ft)	421	1548	2424	2868	3153	3447	3509	3528	3559	3577	

isotherms for this rock are also presented in Fig. 12. The data reasonably indicate Langmuir-type isotherms. The slope of the adsorption curve and the adsorption values in the plateau region are found to be higher when 4% brine is used as an aqueous medium. The increase of adsorption resulting from the increase of salinity in the aqueous phase is a characteristic of anionic surfactants. Adding multivalent cations to an aqueous medium shifts the surface charge of calcite towards less negative or even positive values.[26] As a result, any anionic component in the surfactant will likely adsorb more onto the rock surface

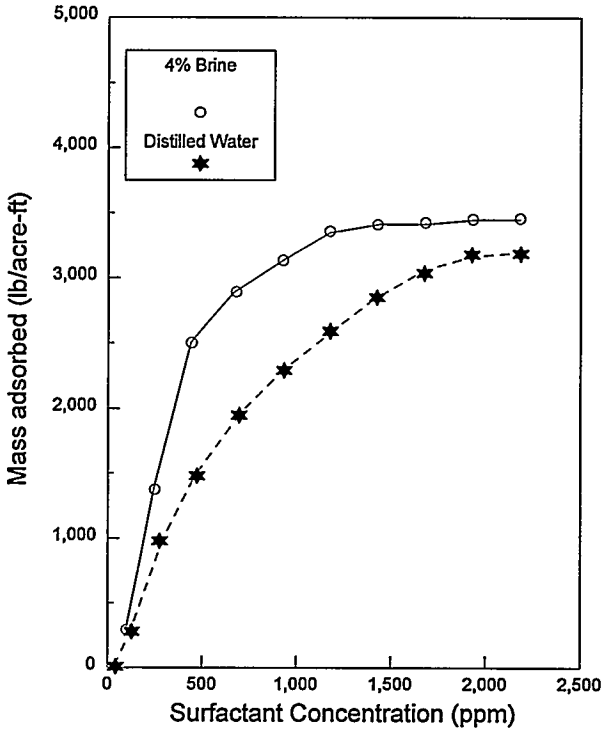

Fig. 12. Adsorption Isotherms of CD1045 with Baker Dolomite

as the salinity of the aqueous medium increases. The adsorption isotherms for preserved EVGSAU core samples are shown in Fig. 13. The rate of adsorption is found to be higher, at concentrations lower than the CMC, when brine is used as an aqueous medium. Adsorption on the preserved cores, however, is found to be lower than that on oil-free Baker dolomite.

Adsorption of CD1045 on an EVGSAU core was also measured at the Chevron laboratory using the recirculation method at 101°F. Adsorption test procedures were similar to those discussed in the PRRC experimental procedures. However, surfactant diluted with 4% synthetic brine was recirculated at 30 cc/hr for at least 24 hours at each concentration. Surfactant concentration was measured with an in-line differential refractometer. Steady state was usually achieved within a few hours. Since there was a tendency for the refractometer to drift, small samples were withdrawn from the system and titrated to determine the surfactant concentration. The data in Fig. 14 also exhibit Langmuir-type behavior with an adsorption value in the plateau region of 3500 lb/acre-ft. These results are higher than those reported in Fig. 13 for EVGSAU cores and similar to those reported in Fig. 12 for Baker dolomite. Adsorption rates can be expected to vary considerably, even for cores from the same reservoir, as a result of differences in rock lithology, surface area and wettability. The presence of an immobile oil phase may also affect adsorption. Furthermore, the error bars in Fig. 14 show how the uncertainty in the adsorption values increases at the higher concentrations using the Hyamine titration method. Small differences in the measured

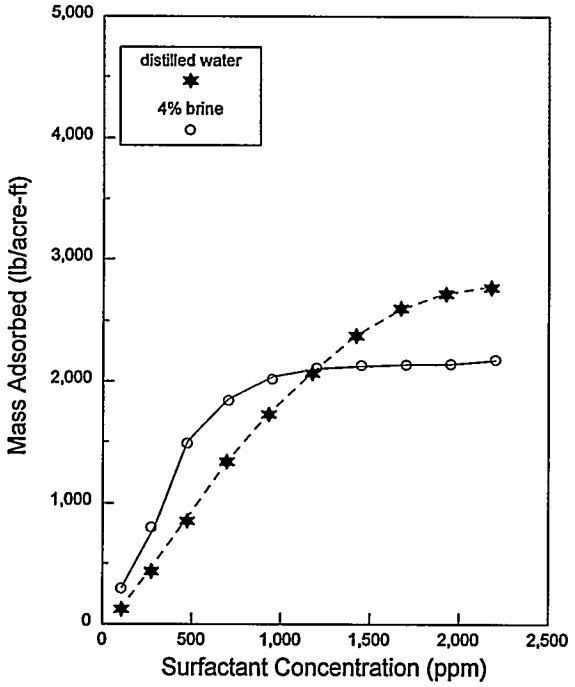

Fig. 13. Adsorption Isotherms of CD1045 with EVGSAU Rock Samples

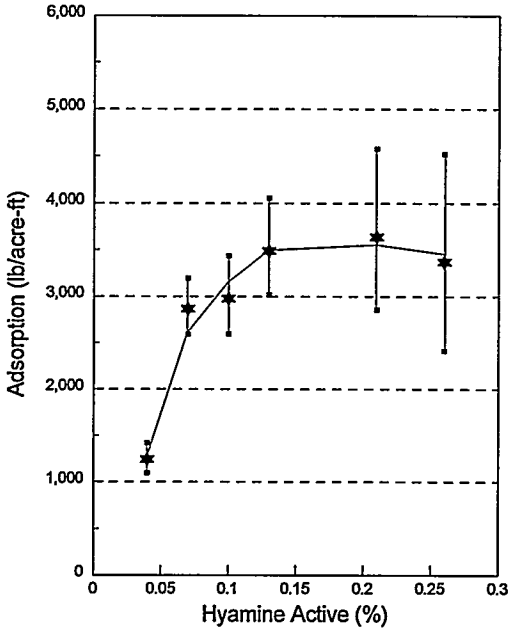

Fig. 14. Adsorption of CD1045 on East Vacuum Core Using Hyamine Titration Method

system volume or in the surfactant concentration can have a large effect on the results. Direct comparison of adsorption results from previous dynamic displacement methods[6,7,25] and current recirculation methods fails to show a good agreement in adsorption values on EVGSAU cores. However, the results reported here are generally higher than those obtained previously by the dynamic displacement method. Further work is needed to understand the differences.

Surfactant Selection

During the second year of the project, sufficient laboratory data were collected to enable the selection of a commercial surfactant for the field test.[2,7,25,27] From an evaluation of all the results collected for this project, surfactant cost data, and other factors, a consensus of the JPAT representatives favored the selection of CD1045 for the field test at EVGSAU. While there was some difference of opinion regarding optimum surfactant concentration, the JPAT representatives agreed that 2500 ppm CD1045 should be used for both a pre-foam pad to satisfy surfactant adsorption in the reservoir as well as for the surfactant solution used during a surfactant-alternating-gas (SAG) cycle of the field test.

OPERATING PLAN

A formal project schedule and detailed operating procedures were developed in a series of open discussions at JPAT project meetings. The final operating plan is necessarily a compromise between the desire to conduct a controlled experiment in the field and the need to mesh the foam project operations into the ongoing WAG operations of a full-field CO_2 flood project at EVGSAU. The resulting project schedule is shown in Fig. 15.

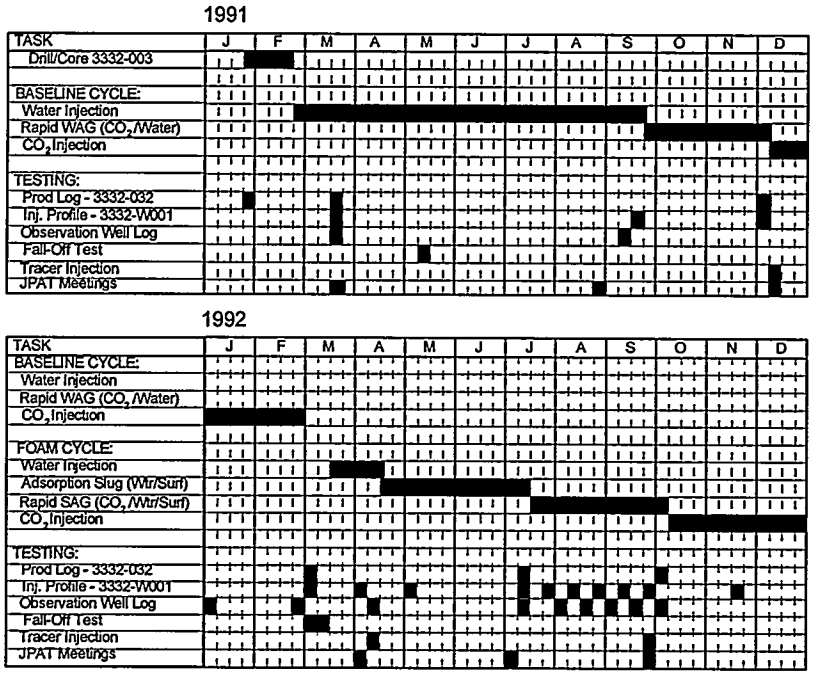

Fig. 15. EVGSAU CO_2 Foam Project Schedule

The project schedule could be characterized in three phases: 1) an extensive pre-foam pattern conditioning and data gathering period, 2) the foam injection period, and 3) a production monitoring period.

PROJECT DESIGN

The CO_2-foam field verification pilot project was designed to achieve in-depth diversion of injected CO_2 by means of in-situ generation of low mobility CO_2-foam within the high permeability channels identified in the pilot pattern area. The Joint Project Advisory Team (JPAT) selected a rapid SAG (surfactant-alternating-gas) injection process to achieve in-situ foam generation. The foam generation period was designed to consist of five rapid SAG injection cycles, with each SAG cycle consisting of 3000 RB of surfactant (2500 ppm of CD1045 in injection brine) followed by 12,000 RB of CO_2. This was designed to generate an 80% quality flowing foam in the reservoir. A large (77,000 RB; approximately 1% pattern pore volume) sacrificial slug of surfactant (also 2500 ppm of CD1045) was to be injected at the end of the water half-cycle immediately preceding the five rapid SAG foam generation cycles to satisfy the surfactant adsorption requirement. The project was designed with a baseline period (consisting of five rapid WAG injection cycles, followed by two months of CO_2 injection, followed by four months of water injection) prior to the foam generation period. All field operations during the baseline period were designed to mimic operations during the foam generation period, except that no surfactant was injected. The objectives of the baseline period were to reduce the chance that changes in pattern performance due to the rapid WAG or other operational variables would be confused with foam response, and also to provide a baseline data collection period for comparison with the foam generation period.

SURFACTANT INJECTION

Baseline Period

Because it was planned to inject the surfactant via a rapid SAG (surfactant alternating gas) schedule of 3 days of surfactant and water followed by 12 days of CO_2 injection, a baseline period of rapid WAG (water alternating gas) was performed in September to December 1991 in order to reduce any concern that injection changes occurring were solely due to the rapid schedule. This rapid WAG was performed to establish a baseline for comparison of the surfactant injection as well as to evaluate whether the rapid schedule and increased CO_2 fraction would affect production rates. Following the rapid WAG, CO_2 was injected for 3 months followed by water for 3 months.

Surfactant Schedule

After the rapid WAG period, the well was put on water injection for 3 months. To satisfy the adsorption requirements of the rock, surfactant injection at the rate of 2500 ppm was begun in the second month of water injection and continued for 3 months until the start of the rapid SAG. Surfactant injection was monitored each morning and adjusted as necessary to obtain 2500 ppm (about 6 bbls/day). Wellhead samples were also taken and a laboratory analysis performed to confirm the surfactant concentration. A total of 105,000 lbs of active surfactant was injected. Approximately 85% (90,000 lbs.) was injected during the adsorption slug and only 15% (15,000 lbs.) was used during the SAG injection.

The size of the foam slug was designed to equal 1% of the pattern pore volume and to be injected in a rapid SAG method. The timing of the rapid SAG was constrained to the shortest SAG cycle that the

field personnel could maintain over a long period of time. This resulted in 3 days of surfactant solution at 1000 bbls/day (3000 res bbls) followed by 12 days of CO_2 (12,000 res bbls) The goal was to inject the same amount of CO_2 in each SAG cycle as was injected in the rapid WAG. Therefore realizing that injectivity would be reduced if a strong foam was formed, the CO_2 volume was monitored during the SAG and the injection period was allowed to fluctuate to match the goal of 12,000 res. bbls of CO_2 per cycle. If the rate had fallen below 250 bbls/day, and it had been agreed that the well would have been returned to water injection to insure that we did not lose all injectivity.

INJECTION WELL RESPONSE TO FOAM INJECTION

Injection Well Pressure and Rate Data

Fig. 16 shows the performance history of Injection Well 3332-001 during and after the foam test,

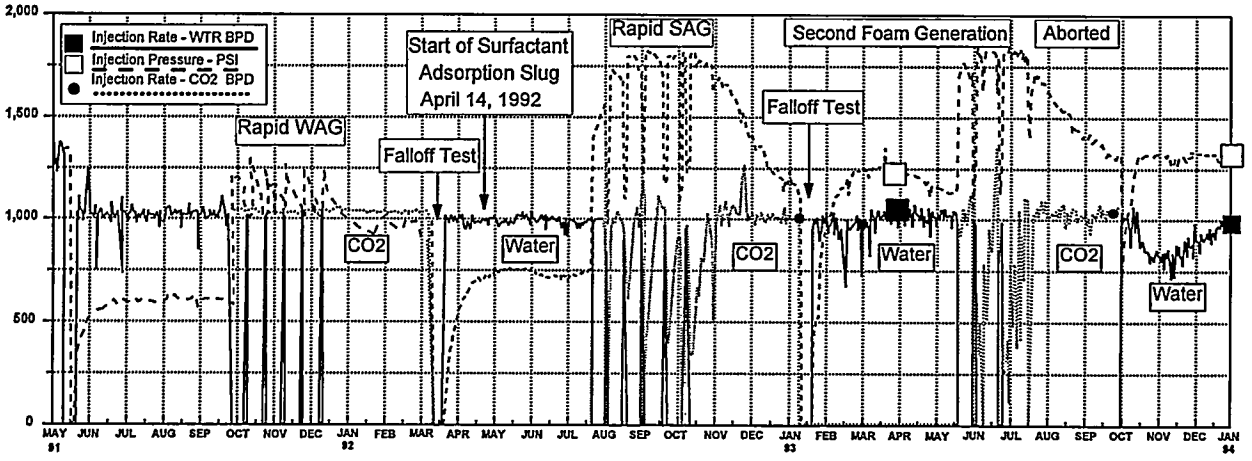

Fig. 16. Complete Pressure and Rate History for Well 3332-001

and the pressures and rates during the foam generation are plotted in Fig. 17. Foam generation began in mid-July 1992 following injection of a three month adsorption slug of surfactant. As shown on Figs. 16 and 17, the injection pressure rose dramatically when CO_2 was injected indicating foam was being formed. The maximum allowable injection pressure for CO_2 was 1800 psi which was reached at the beginning of the third SAG period. From then on the rate was reduced to stay within the allowable pressure limit. Therefore the CO_2 rate at the beginning of the each cycle, starting with the third cycle, was reduced for the first few days of each cycle until the injectivity improved and the returned to the target rate of 1000 bbls/day. The injectivity continued to decrease during the first three SAG periods as foam propagated away from the wellbore and then reached a somewhat repeatable behavior for the fourth through sixth periods, even though a slight loss of injectivity was still occurring during the last 3 periods. The higher injection pressures during and after the rapid SAG infer that the reduced injectivities can be attributed to in-situ foam generation.

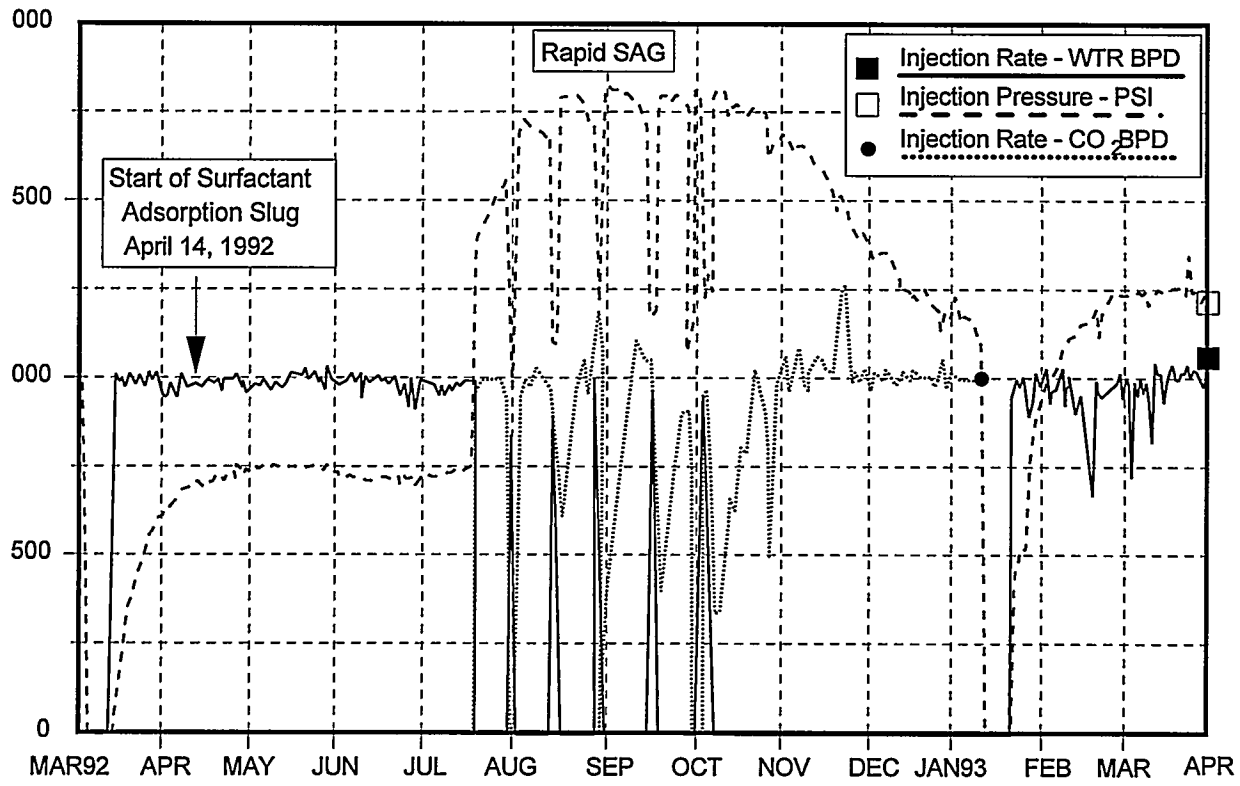

Fig. 17. 3332-001 Injection Pressure and Rate during Foam Generation

Fig. 18 shows a direct comparison of injection pressure from the rapid WAG to that of the rapid SAG normalized to the same start time. Note that the only apparent effect of the rapid WAG was that it elevated the baseline water injection pressure by 200 psi as shown by the difference between the two curves at the start (left side) of the plot. After compensating for this 200 psi, the net surface injection pressure decrease near the end of the SAG was about 700 psi.

Injectivity and In-Situ Mobility Reduction

The injection pressure and rate data indicate that injectivity during the rapid SAG foam generation period was significantly lower than that during the baseline rapid WAG period. Two independent techniques, Hall[28] plots and falloff testing, were used to estimate in situ fluid mobilities at various points during the baseline and foam generation periods. Daily injection pressure and rate data were analyzed using Hall plots. Flowing gradient surveys were run during CO_2 injection to ensure an accurate surface to bottom hole pressure correlation. Since the slope of the Hall plot is inversely proportional to the effective fluid mobility, stabilized Hall plot slopes (Fig. 19) can be used to estimate an effective in situ fluid mobility, provided that the thickness and completion efficiency of the injection interval do not change significantly.

Periodic falloff tests were also used to investigate the in situ fluid mobility reduction achieved as a result of foam generation. Theoretically, falloff tests are capable of detecting individual banks of different

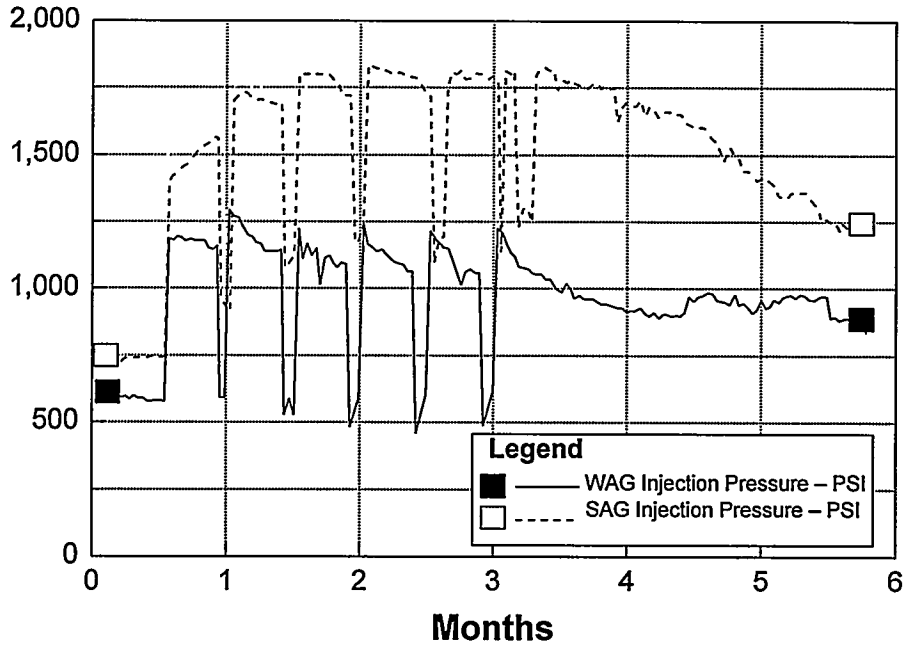

Fig. 18. 3332-001 Injection Pressure and Rate Comparison of WAG vs SAG

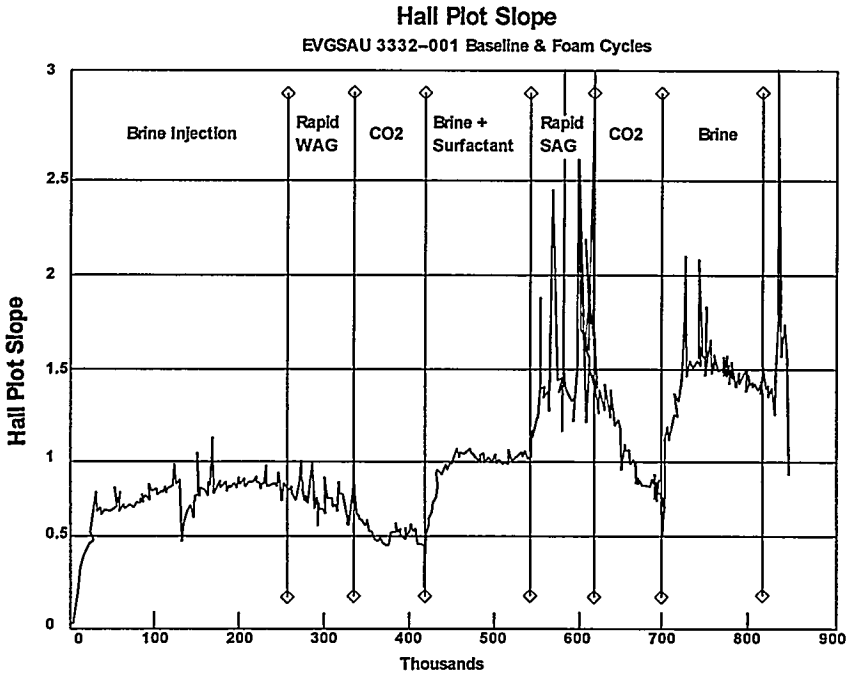

Fig. 19. Cumulative Fluid Injected (Res. Bbls.)

fluid mobility in a region of radial flow surrounding the foam injection well. However, the falloff tests in this well showed long periods of linear flow with only the beginning of a transition toward radial flow during the 7 to 10 day shut-in periods. Because of this, no direct measurements of flow properties in the radial flow region were possible and the tests were analyzed using type curve matching techniques. The type curve matches for all five falloff tests available from this well yielded similar effective fracture half-lengths (ranging from 365 to 390 feet). Accurate estimates of effective fluid compressibility are necessary for correct quantitative interpretation of falloff test data in a CO_2 flood.

Results of a falloff test run after the baseline rapid WAG CO_2 injection and a falloff test run after the rapid SAG foam generation period show significant periods of linear flow.[15] However, the test run after foam generation shows a different character in the late-time portion of the test that does not appear to be caused by any mechanical or measurement malfunction in the test. One possible explanation is to note that this character in the derivative response is qualitatively similar to that which would be expected for a "thick skin" region of reduced mobility around a fracture.[15]

Table 6 summarizes effective in-situ fluid mobility data estimated from stabilized Hall plot slopes and from falloff tests for the foam injection well 3332-001. The mobility values calculated using the two different techniques compare favorably. Three measurements of water mobility in a "normal" WAG half-cycle averaged 165 ± 20 md-ft/cp. The water mobility measured during the extended period of water injection prior to beginning the baseline period was somewhat higher. The mobility of CO_2 at the end of the half-cycle following baseline rapid WAG was approximately double the water mobility in a normal water half-cycle. The mobility of CO_2 following rapid SAG foam generation was reduced to about one-third of the CO_2 mobility measured at the same point in the baseline period. This measured mobility reduction is comparable to the difference seen in CO_2 injectivity following rapid SAG vs. rapid WAG (measured approximately one month into continuous CO_2 injection).

TABLE 6
ESTIMATED EFFECTIVE IN-SITU FLUID MOBILITIES FROM HALL PLOTS
AND FROM FALLOFF TESTS IN THE FOAM INJECTION WELL 3332-001

Foam Pattern Operations	Date of Falloff Test	FALLOFF (kh/μ) md-ft/cp	Hall Plot Slope	HALL PLOT (kh/μ) md-ft/cp
First Water Half Cycle	9/86	145	---	---
Second Water Half-Cycle	9/87	188	---	---
Extended Water Injection (Fifth Half-Cycle)	5/91	224	0.72	206
Baseline (Sixth) CO_2 Half-Cycle	3/92	308	0.475	313
Baseline Water Half-Cycle	---	---	0.90	164
Foam (post SAG) CO_2 Half-Cycle	1/93	116	1.3	114

TABLE 7
RESULTS FROM FALLOFF TESTS AND HALL PLOT SLOPES

	Apparent Viscosity, cp*
Rapid WAG	0.6
CO_2	0.3
Surfactant Solution	0.9
Rapid SAG	1.5

*Based on μ_w=0.72 cp @ bottomhole conditions and assuming P_e=1800 psi

Analysis of pressure falloff tests, injectivity indices, and modified Hall Plots provides the apparent viscosities shown in Table 7. Compared to water with a bottomhole viscosity of 0.72 cp, the foam generated during the rapid SAG had an "apparent" viscosity of 1.5 cp. Compared to the rapid WAG, a resistance factor of 2.5 was observed during foam generation near the end of the rapid SAG test. These data suggest that the foam treatment reduced mobility of CO_2 by about one-third to one-half of the prefoam value.

Injection Profiles

Periodic injection profiles had been run in the candidate foam injection well (3332-001) under normal CO_2 WAG operations. These profiles showed that almost two-thirds of the injected fluids (both CO_2 and water) were entering Subzone C2 and the lower portion of Subzone C3. These zones correlate directly with the highly leached, high permeability (200 md) interval in the observation well core located 150 feet away from the injector. In contrast, Zone E, which exhibits very high porosity (22.7% average) and moderate permeability (18 md arithmetic average in the observation well core), was indicated to be taking only 15-20 percent of the injected fluids in well 3332-001. A production log run in foam pattern producing well 3332-032 showed approximately 60 percent of the produced fluids were coming from these same two C2 and C3 Subzones. This "offending" production well had historically responded to CO_2 injection (started to flow) within 6 to 14 weeks after the beginning of the CO_2 injection half-cycle in WAG injector 3332-001. The well would then cease flowing before the end of the subsequent water injection half-cycle. It was concluded from these observations that a primary objective of the foam injection project must be to divert a larger percentage of the injected CO_2 away from the high permeability channel in Zone C, both areally into other portions of Zone C and vertically into lower permeability zones (such as Zone E) which were not being effectively swept under current WAG operations.

A total of 17 injection profiles were run during foam injection in order to better understand what is happening downhole as foam generation progressed. Profiles were run during the last of the 3 days of water and surfactant injection and one or two logs were run during the 12 to 15 day CO_2 injection period. Fig. 20 indicates the change that occurred before and after foam injection. A significant though not overly dramatic change occurred in the profile during foam generation where 12% of the fluid was diverted away from the C zone (thief zone) to other zones in the wellbore. Fig. 20 represents the average of multiple profiles as

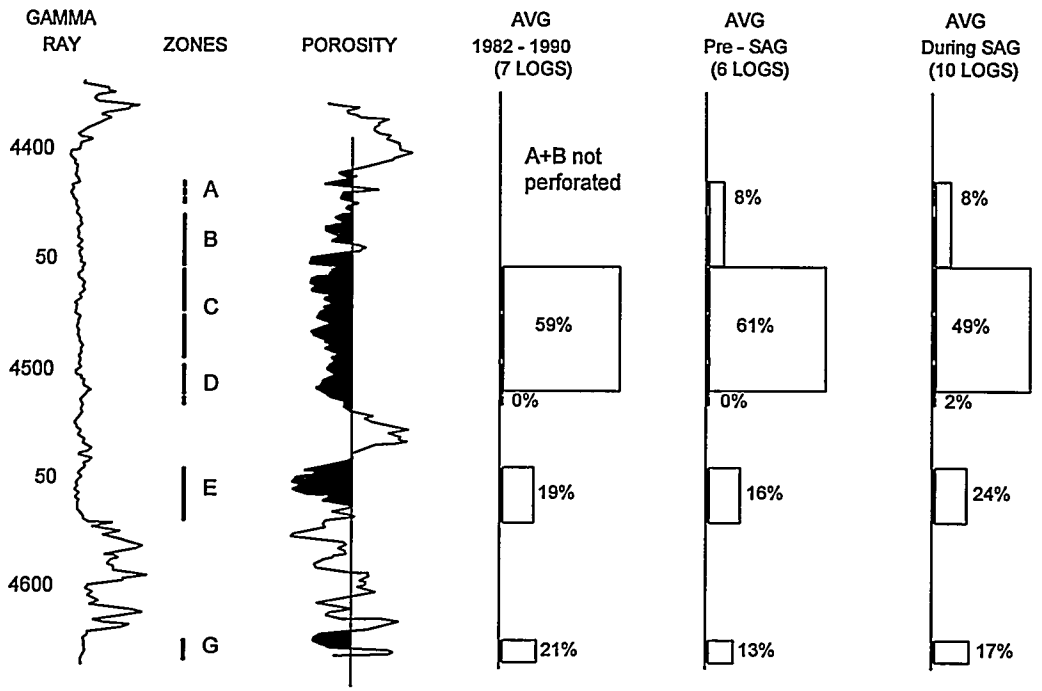

Fig. 20. Injection Profile for Well 3332-001

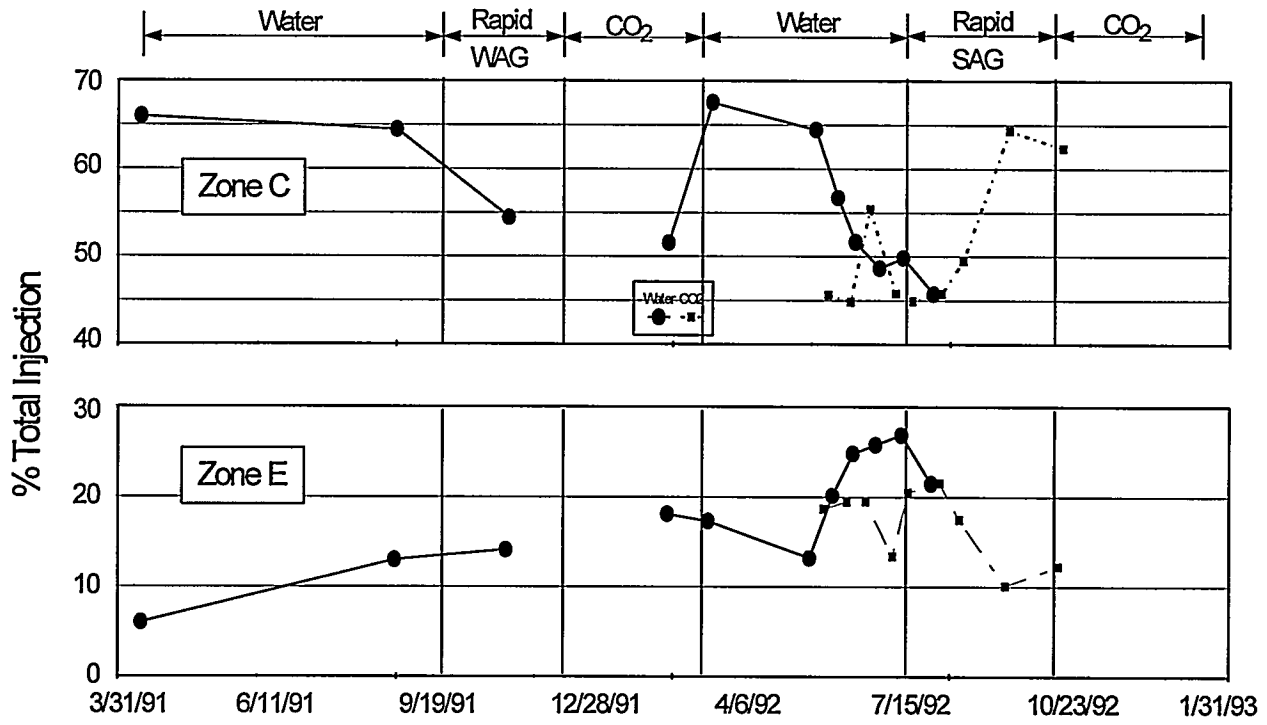

Fig. 21. Results of Injection Profile Surveys—Percent of Total Injection Entering Zones "C" & "E" in Foam Injection Well 3332-01

individual profiles may not be completely representative of the downhole conditions. The majority of the 12% reduction in the C zone occurred near the beginning of foam generation, and the profile varied only slightly until the end of foam generation. The profile then reverted back to its original profile during the water and CO_2 injection that followed the foam. This experience highlights the flexible nature of foam for profile improvement as the profile changed quite quickly in response to foam generation yet did not change the profile permanently. As a result, an operator could use foam as an intermediate solution to improve areal sweep before using a more permanent method for profile improvement.

Diversion of Injected Fluids

A series of radioactive tracer injection profile surveys were run in the foam injection well (3332-001) throughout the baseline and foam generation periods. These surveys were run during both water and CO_2 injection, including during individual rapid WAG and rapid SAG injection cycles, to monitor fluid entry profiles and to look for evidence of possible fluid diversion during and after foam generation. This series of injection profiles was examined to identify any evidence of changes in the vertical distribution of injected fluids during the project. Fig. 21 summarizes the results of twenty-six injection profile surveys, showing changes in the distribution of injected CO_2 and water into Zones C and E during the course of the project. It should be noted that two profiles were run during the 12-day CO_2 half-cycles of the rapid SAG foam generation period, and results of these pairs of injection profile surveys have been averaged for presentation.

There is evidence in the sequence of injection profile results to suggest that the maximum CO_2 injection profile change was achieved quickly (during the first rapid SAG cycle), and that the CO_2 injection distribution did not change significantly through the remainder of the five SAG cycles. Injection into Zone C at the start of rapid SAG foam generation showed an immediate drop from 65% to 45% of total fluid injection (Fig. 21). The CO_2 injection profile stayed at this level (45%) throughout the five rapid SAG foam generation cycles (with the exception of an anomalously high value of 55% injection into Zone C during the third SAG half-cycle). In contrast, surfactant injection into Zone C during the rapid SAG period showed a progressive diversion from its pre-foam level of approximately 65% of total injection until it approached the CO_2 profile of approximately 45% of total injection entering Zone C during the final foam generation SAG cycle. The injection profile results in Fig. 21 also provide evidence of a corresponding increase in the fraction of total injected fluids entering Zone E during the rapid SAG injection process. The fraction of total injection entering Zone E increased from a level of 10-15% during the pre-foam baseline to a level of 20-25% of total injection indicated to be entering Zone E during the SAG period. This evidence of diversion is somewhat subtle, and inferred changes in fluid distribution may be below the accuracy of any single survey; however, the frequency, consistency, and trends in the profile results lend some credence to the conclusion that beneficial fluid diversion into these zones did occur during the SAG period.

The profile results also show some evidence of injection profile changes during and immediately following the rapid WAG baseline period, with fluid being diverted away from Zone C. This indicated diversion appears to be about half the magnitude observed during the rapid SAG foam generation period. These observations are based on only a few profiles taken during the baseline and, given the small magnitude of the changes (5-10%), any conclusion about fluid diversion as a result of the rapid WAG must be considered speculative.

OBSERVATION WELL RESPONSE TO FOAM INJECTION

The observation well (3332-003), located 150 feet west of the foam injector, was completed with fiberglass casing across the reservoir interval to allow neutron and induction time lapse logging runs to be used to monitor saturation changes during the foam injection project. A total of 15 logging runs were made over the duration of the foam project. Each logging run consisted of three passes of neutron data and two passes of induction data. Open hole logs, core data, and baseline cased hole log responses from the observation well were combined to develop a petrophysical model for analyzing the subsequent time lapse logging runs. Using these data, changes in water, CO_2, and oil saturations were determined for each reservoir zone during the baseline and foam generation periods. A comprehensive description of the complete monitor logging program for the EVGSAU foam project has been presented.[9] Zone H, which was penetrated in the observation well but not completed in either the injection well or any of the foam pattern producing wells, was used as a "standard" for quality control and consistency checking during the time lapse logging runs. Quantitative calculations were made only for intervals with porosity greater than 10 percent to maximize reliability of the saturation calculations. The interpretation of saturation changes in a multi-layered reservoir undergoing rapid WAG operations and foam injection is very difficult, and there is significant uncertainty in the quantitative interpretation of the logging responses.

Water and CO_2 were the predominant flowing phases detected in Zone C2 (the suspected high permeability channel in this pattern). Changes in oil saturation in Zone C2 during the project were generally below the reliable resolution of the logging tools. These observations indicate that Zone C2 was dominantly a CO_2/water flow system at this location in the pattern. This is consistent with the sponge core oil saturation data from this interval which indicates that this zone was at or near the expected CO_2 miscible residual oil saturation at the time the observation well was drilled. During the baseline rapid WAG period, water and CO_2 saturation changes were detected in a monitor logging run made 31 days after a WAG cycle change in the injector 150 feet away. This indicates that the response time for fluid movement through Zone C2 was less than 31 days during the baseline rapid WAG period. During the foam generation period, saturation changes in Zone C2 were detected between monitor logging runs 8 and 9, made 41 days and 63 days, respectively, after the start of the rapid SAG foam injection period. Injection rates during rapid SAG were slightly less than during the rapid WAG baseline, however after correcting for this, the time lapse logging results still indicate fluid transit time in Zone C2 increased during the foam generation period. This is a good indication that fluid mobility was reduced in Zone C2 and/or injected fluid was being diverted away from the high permeability channel as a result of foam generation.

Monitor logging runs indicated a much slower response time in Zone E than in Zone C2. This is consistent with injection profile data and core permeability data. Significant saturation changes were observed for oil and CO_2 in Zone E. This may indicate that CO_2/oil displacement was continuing in Zone E at this location in the pattern. Water bulk volume in Zone E changed very little during the course of the project. The correlation of the timing of saturation changes in the monitor logging runs with specific WAG cycle injection changes is much less certain for Zone E due to the longer response times. Saturation changes were detected in Zone E in a logging run made 160 days after the start of the rapid WAG injection in the baseline period. This indicates that the response time for fluid movement through Zone E was less than 160 days prior to foam injection. During the foam generation period, saturation changes in Zone E were detected between monitor logging runs 13 and 14, made 111 days and 180 days, respectively, after the start of the rapid SAG foam injection. Thus, the response time in Zone E was not demonstrably different after foam injection than during the baseline period. However, CO_2 saturations in Zone E

following the foam generation period were five-fold higher than at the end of the baseline WAG injection cycle.[9] This may be an indication that a larger percentage of the injected CO_2 was being diverted into Zone E, as was shown in the injection profile surveys run in the foam injector.

These results indicate that most of the saturation changes as a result of the foam treatment are occurring primarily in the highest permeability C-2 Subzone and in the E Zone, with significant change also occurring in the C-3 Subzone.[5,9] During the CO_2 injection cycle at the end of 1992, an increase in CO_2 saturation in the high permeability C-2 zone presumably corresponds to a higher trapped CO_2 saturation. In January 1993, a change in profile was indicated, and the increase in CO_2 saturation and a decrease in oil saturation in Zone E suggest that mobile oil was being displaced as a result of the foam. These results are consistent with the results of the profile tests in the injector and provide additional details about fluid movement and diversion that are not available from the injection well tests.

INTERWELL TRACER AND SURFACTANT RESPONSE

It was observed that the proposed foam injection well showed significant linear flow behavior on falloff tests during both water and CO_2 injection half-cycles. This behavior is typical of most WAG injection wells in the Unit. There were concerns expressed within the JPAT that these observations could indicate the presence of a very long fracture in the candidate foam injection well. The primary concern was that foam might not be generated in situ if fluid flow between these wells was predominantly through a fracture system. Interwell tracers were injected to investigate the nature of the high permeability flow channels in this pattern. Both the water phase and CO_2 phase were tagged at the end of the rapid WAG portion of the baseline period. Tritiated water and Krypton-85 were the respective tracers selected. Four months later, when the time came to begin injection of the sacrificial surfactant slug, neither of these tracers had been detected in any producing wells in the pattern. At this time an additional tracer, Cobalt-60, was injected with the leading edge of the sacrificial surfactant slug. When the time came to begin the rapid SAG foam injection period, none of the tracers had been detected at any producing wells. This was taken as evidence that there was probably not direct fracture communication between the foam injector and the "offending" production well and that fluid flow was most likely occurring dominantly through high permeability channels in the rock matrix.

Samples from producing wells in the pattern area were analyzed for both gas-phase and water-phase tracers that were injected into Well 3332-001. In December 1991, Tritium was injected in the water phase at the end of the rapid WAG cycle, and Krypton 85 was injected at the beginning of the 3-month CO_2 injection cycle. Additionally, Cobalt 60 was injected in the water phase just prior to the start of the adsorption slug of surfactant in mid-April 1992. None of the injected gas-phase tracer has been detected in any of the pattern producing wells, and water-phase tracers have been observed only in Producing Well 3332-032. This producer is referred to as the offending well because it has experienced excessive CO_2 breakthrough. The results of the water-phase tracer analyses presented in Fig. 22 suggest the Cobalt appeared more quickly on the basis of time than did the Tritium. However, the Tritium was injected just prior to three months of CO_2 injection, whereas the Cobalt was injected after about one month of water injection and just prior to about three months of surfactant solution injection. On the basis of cumulative water injected, the arrival times of the two tracers are expected to be more similar. In any event, the tracer results indicate that there is not direct fracture communication between the injector and the producers in this pattern.

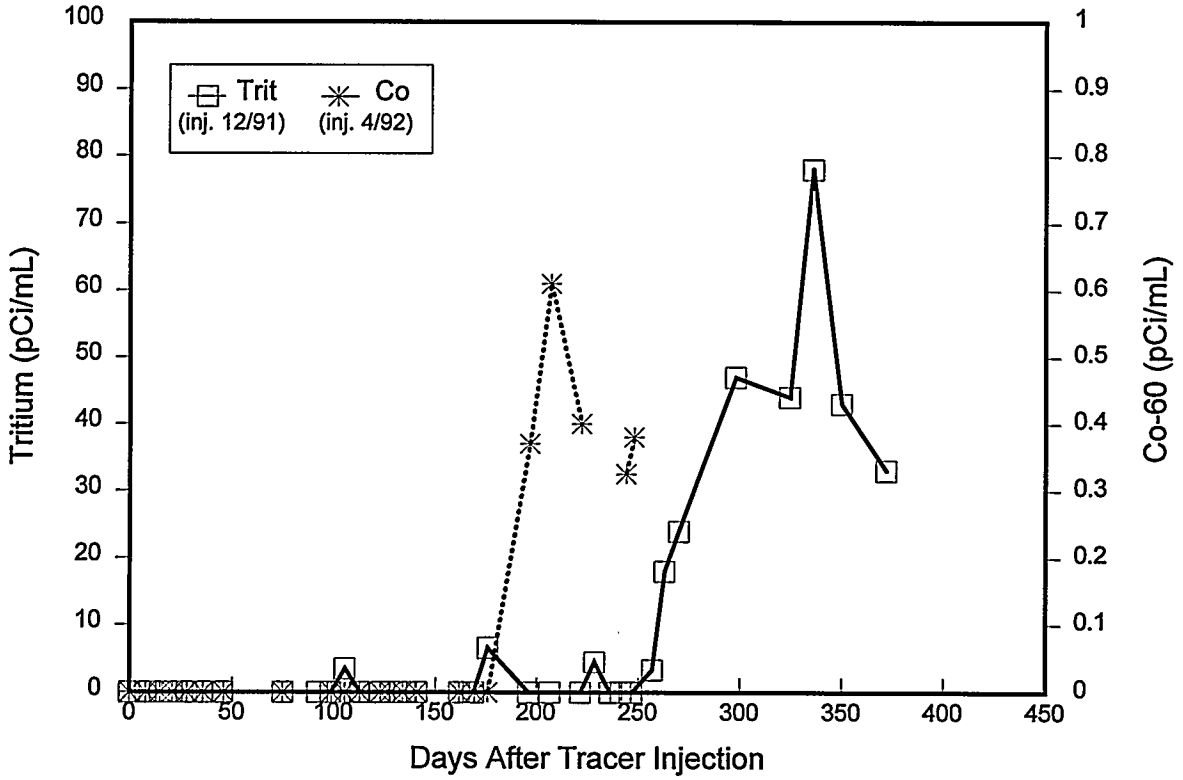

Fig. 22. Tracer Content in Brine Produced from Well 3332-032

Weekly water samples were taken at the offending well (3332-032) to detect the presence of the surfactant injected in Well 3332-001. As shown in Table 8, no surfactant has been found in the water produced from Well 3332-032 through the end of December 1992.

PRODUCTION WELL RESPONSE TO FOAM INJECTION

Offending Well Behavior

The most conclusive indication of the in-situ formation and technical effectiveness of CO_2-Foam in this application was seen in the changes in producing characteristics of the "offending" production well (3332-032) in the foam pattern. Prior to the foam project, the majority of the gas injected into well 3332-001 channeled, via a small high permeability layer, directly to the offending well. Therefore, shortly after CO_2 injection began, the offending well would start flowing large volumes of gas but relatively small amounts of liquid and only about 5 BOPD. This would result in a high bottomhole pressure, and apparently the other layers did not contribute to the production. A production log run during one of the flowing periods indicated that the high bottomhole pressure was causing fluids to crossflow and exit out the bottom of the borehole. This condition also presented a safety hazard to the field personnel from a workover standpoint, in combination to the obvious wasteful and inefficient CO_2 usage, therefore the well was left shut in. The well was allowed to produce during the pre-foam period to establish a baseline for comparison.

TABLE 8
ANALYSES OF PRODUCED FLUIDS FROM WELL 3332-032
FOR SURFACTANT CONTENT

Sample Date	Hyamine (mL)	CD1045 (ppm)
1-9-92	0.00	0
1-11-92	0.00	0
1-13-92	0.00	0
1-18-92	0.00	0
1-20-92	0.00	0
1-21-92	0.00	0
1-24-92	0.00	0
1-31-92	0.00	0
2-25-92	0.00	0
3-17-92	0.00	0
3-20-92	0.00	0
4-14-92	0.00	0
4-17-92	0.00	0
5-29-92	0.00	0
10-26-92	0.00	0
11-6-92	0.00	0
11-20-92	0.00	0
12-12-92	0.00	0
12-17-92	0.00	0
12.5 ppm standard soln.	0.02	12

The offending producer (3332-032) experienced a positive oil response and reduced CO_2 production as a result of the foam test. As expected, this well was the first to respond to foam injection. Production data for this well is shown in Fig. 23. The improvements in oil cut and gas-oil ratio (GOR) are shown in Fig. 24, where the oil cut is expressed as a percentage of the total reservoir barrels of produced fluids. Whereas it took 6 weeks after the rapid WAG before the offending well started flowing CO_2, after the rapid SAG it took 11 weeks before the well started flowing, and then the gas rate was much less than in previous tests. Because the production behavior was then controllable, a rod pump and packer were run, and a non-productive well was turned into a productive one.

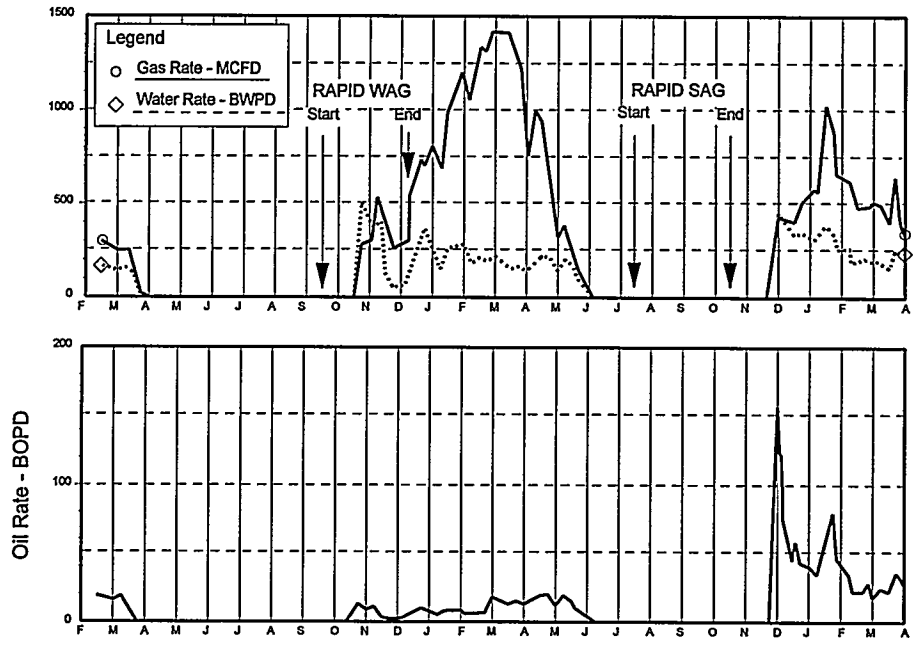

Fig. 23. Weekly Well Tests for EVGSAU Well 3332-032

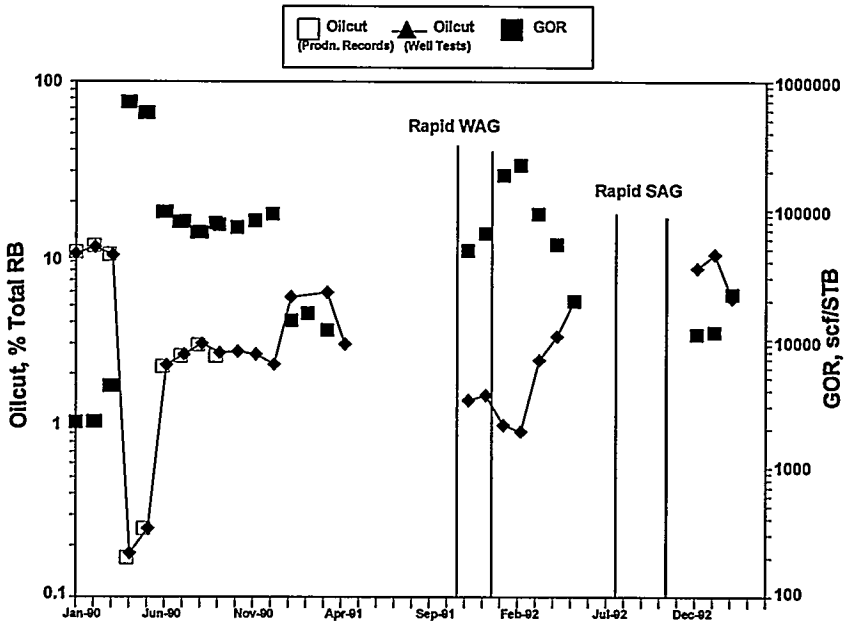

Fig. 24. EVGSAU Well 3332-032

The rapid onset of CO_2 production at well 3332-032 was lengthened from less than six weeks after the start of CO_2 injection in the baseline rapid WAG period to over 4 months after the start of CO_2 injection in the rapid SAG foam generation period. Cumulative CO_2 produced from this well in the ten months following the start of rapid SAG injection was less than half the produced CO_2 in the same period following the start of rapid WAG in the baseline period. Peak CO_2 production rates following rapid SAG were also less than half of the peak rates in the baseline period (with the exception of spikes in one or two of the weekly tests). Oil production rates were also somewhat higher in the period following foam generation, although no dramatic oil production rate increases were observed. Thus, it is apparent that the foam pilot project in this pattern had a significant impact on the problem producing conditions at well 3332-032.

Behavior of Other Producers

Well No. 2801-001, which is on the opposite side of the pattern from the offending well and thus in line with the same trend of directional permeability, also showed a response from the surfactant. The response was difficult to quantify due to the rapid nature of the oil spike and the fact that the total fluid production did not increase; only the oil cut increased. However a conservative estimate is that

East Grayburg-San Andres Unit Well No. 2801-001 Foam Pattern Testing
January 1, 1992–November 17, 1993

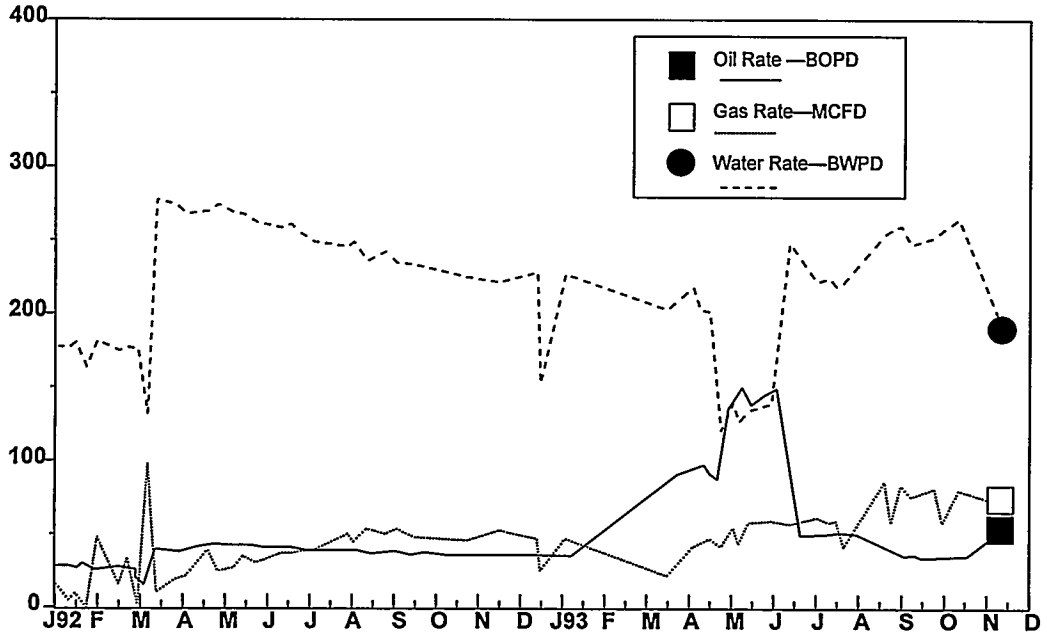

Production History for Well 2801-001

incremental oil amounted to 3700 bbls as shown in Fig. 25. A strong response was also noted in well 2801-004 (Fig. 26) as total liquid production increased as well as oil cut increased. Total incremental oil in this well was estimated at 6200 bbls. No other wells to date in the pattern have shown any response to foam injection. Total incremental oil was estimated at 14,700 bbls.

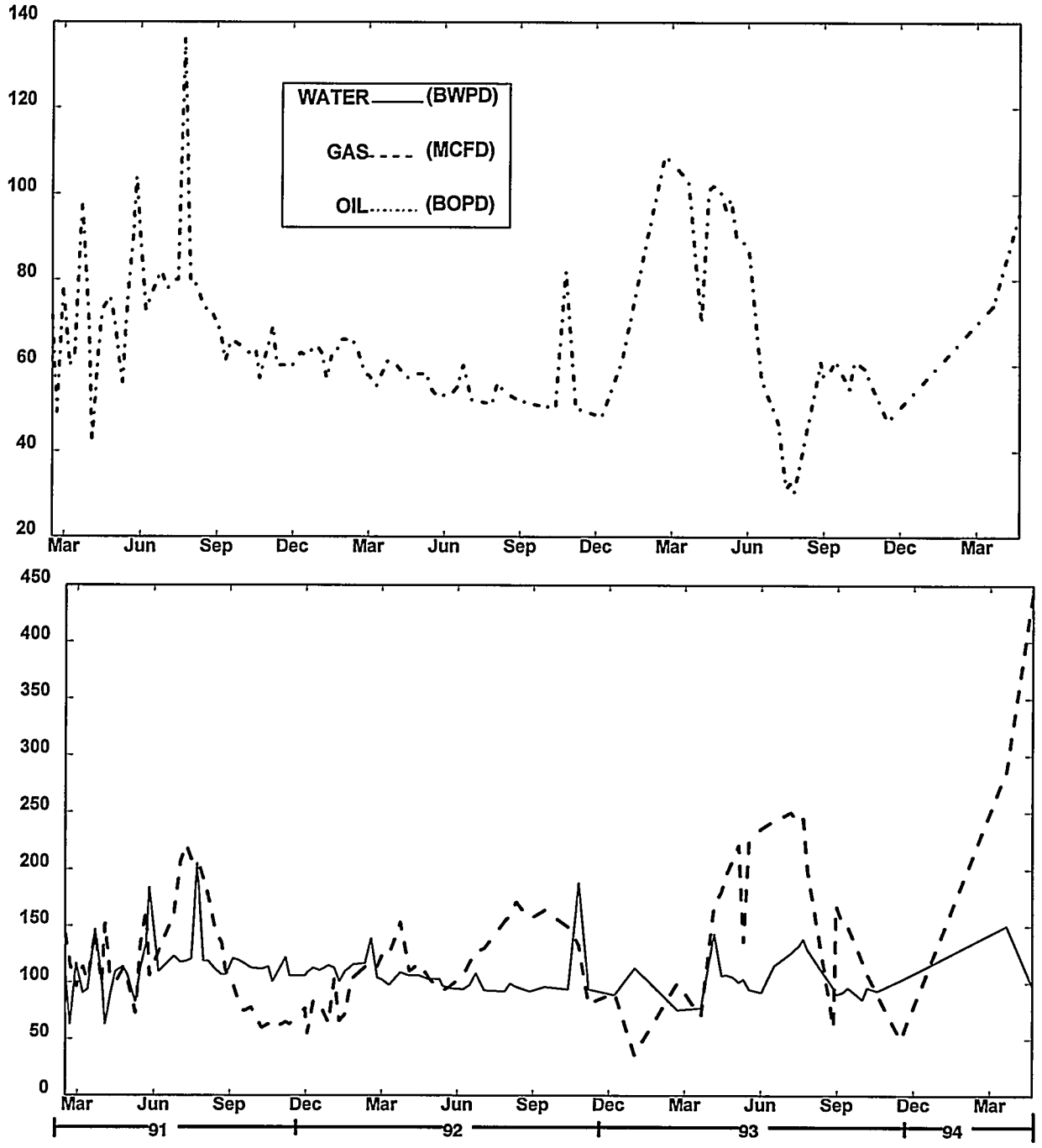

Fig. 26. Production History for Well 2801-004

RESPONSE FROM THE SECOND FOAM TEST

Based on the favorable response observed as a result of the first foam injection test, a second foam test was initiated in the same injection well used for the first foam test. Following the four months of water injection on May 21, 1993, CO_2 was injected for 12 days to establish a base gas injection rate. As is typical when switching from water to CO_2, the injection pressure increased about 600 psi because of the difference in hydrostatic pressure between water and CO_2. On June 2, 1993, the second foam test was started with the same conditions as in the first test. Early response indicated that foam was generated quickly and the wellhead pressure response during the second foam test at a surfactant concentration of 2500 ppm was similar to the first test at the same concentration. However, at some period after the initiation of the second foam test, a facilities problem was discovered that resulted in uncertainties in the injected gas composition and the resulting bottomhole pressures. Therefore, the second foam test was aborted, and plans were made to reimplement the second foam test after the water injectivity stabilized and pre-foam baseline injectivity was reestablished. The rates and pressures in the test well, before and after the aborted second foam test, are shown in Fig. 16.

However, the foam injection test planned for early 1994 was again delayed due to a waterline leak on the line directly connected to the foam injector. The foam injector was on a CO_2 cycle for about three months while the waterline was out of service. The repair was finished, and the well was switched back to water by mid-April. Rate and pressure data for the foam pattern injection well indicated that injectivity levels in the foam injection well were lower than injectivity levels prior to the foam test.[5] At the beginning of the field trial, the water injection pressure at 1000 BWPD was about 750 psi, and after the first foam test, it was 1300 psi (maximum pressure) at only a rate of 750 BWPD. Therefore, a small acid job was performed in mid-1994 to determine if the low rates were due to the normal type of skin damage that is usually easily fixed with acid or whether it was something further away from the wellbore that may be due to the surfactant. After the acid treatment, water injectivity improved but was still lower than the pre-foam level.

Although the second foam test was aborted, production response was observed at the offending well. A comparison of the production responses in the offending well for the first and second foam tests is shown in Figs. 27 and 28, respectively. The results demonstrate that CO_2 breakthrough had been reduced after the foam treatment, and oil production increased in the offending well. The foam did appear to be persisting because gas production did not increase substantially during or after the CO_2 injection that followed the foam test. Only two cycles of foam generation were injected during the second foam period with each cycle consisting of 3 days of surfactant and water followed by 12 days of CO_2. This was followed with 3 months of CO_2 injection. Normally this amount of CO_2 would have caused the offending well to flow vigorously yet it appears (see Fig. 23) that even this smaller slug of surfactant was enough to cause a positive response in the offending well.

ECONOMICS

It is important to note that the project goal was not to prove if foam was economic but was merely to prove that a foam could be generated and to assess how strong a foam could be generated. Due to a large variance in laboratory adsorption measurements, there was some uncertainty as to how much surfactant would be needed to satisfy adsorption. Therefore, in order to give the surfactant the best possibility of success, a large amount of surfactant was injected. The members of the JPAT realized that

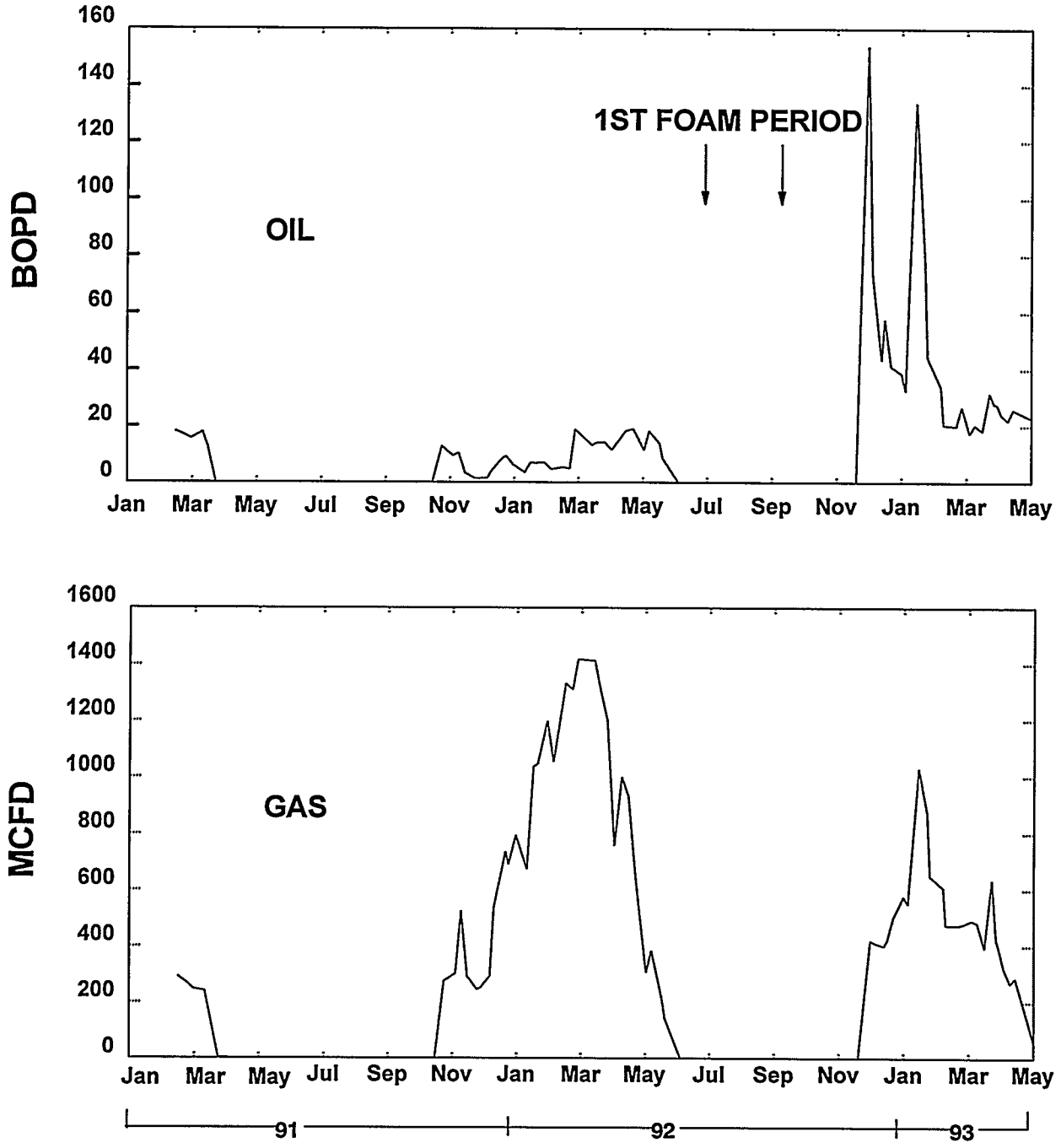

Fig. 27. Oil Response of Offending Well from First Foam Period

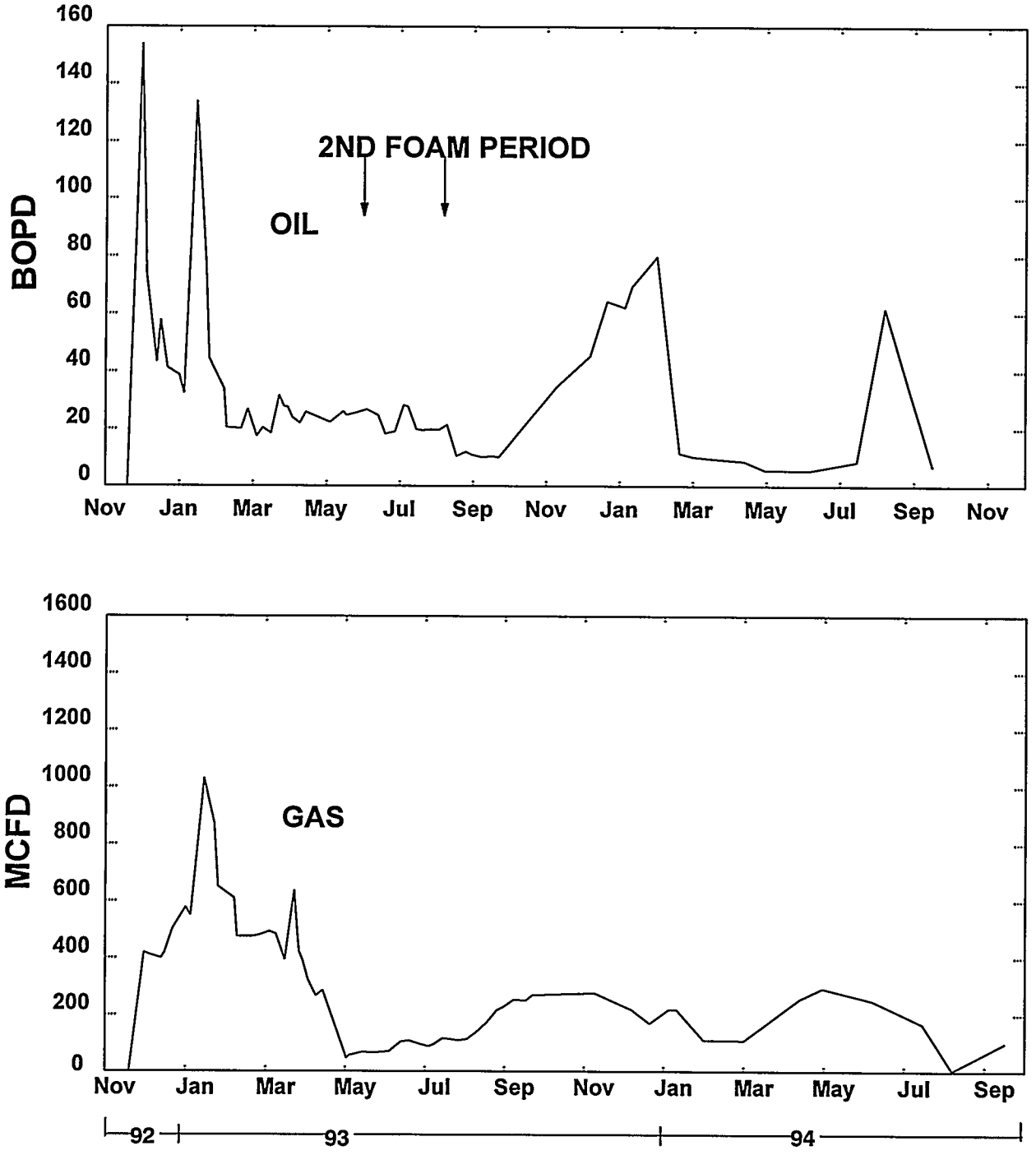

Fig. 28. Oil Response of Offending Well from Second Foam Period

the amount injected may have been more than was required from an economic view point. In light of the strong mobility reduction in the injection well and the noted production response, the success of the field trial can not be disputed. However it does make difficult a definitive statement about the economics of injecting surfactant because such a large amount was injected.

Revenue produced from the foam project came in two forms— 1) revenue from the incremented oil and 2) savings in compression costs. The compression savings below were determined by rationing the amount of gas produced during the WAG by the amount injected during WAG and using that ratio to adjust the produced gas volumes from each SAG period. This method compares numbers adjusted to the same volume injected for each period. Since less gas was injected during the SAG periods, it follows that less would be produced, and it would not be a fair comparison to compute simply the amount of gas produced before and after the foam injection. Thus, the method shown is a more conservative approach, and the actual savings could be somewhat higher.

	1st Foam	2nd Foam	Total
Incremental Oil, bbls	14,700	4,460	19,160
Less 1/8 Royalty	12,862.5	3,902.5	
Avg. Oil Price/bbl	$17.50	$15.45	
Gross Revenue	$225,094	$60,294	
Lifting Costs @ 5.50/bbl	-80,850	-24,530	
Net Revenue	$144,244	$35,764	$180,008

Compression Savings:

1993	82,000 MCF x .25/MCF	$20,000
1994	97,000 MCF x .25/MCF	$24,250
		$44,250

Surfactant Costs

Surface Facilities, Pump & Tank	$10,000
Surfactant Cost	166,000
	$176,000

Net from Incremental Oil	$180,008
Compression Savings	$ 44,250
	$224,258

Total Revenue and Savings:	$224,258
Less Surfactant Costs	$176,000
Net Yield of Project	**$ 48,258**

The foam resulted in the production of a considerable volume of incremental oil (19,160 bbls) that was more than enough to cover surfactant cost, but the revenue produced was not sufficient to provide an attractive rate of return. The present worth value of the project was adversely affected by the large upfront investment for the surfactant used and the one-year delay before recovery of the incremental oil. However, this leaves hope for developing foam into a useful reservoir management tool if a smaller adsorption slug or lower surfactant concentration could be used that would produce the same incremental oil. Additionally, these results suggest that in times of slightly higher oil prices (greater than $20/bbl), surfactant-generated foam could prove economic.

RESERVOIR SIMULATION STUDIES

University of Houston Studies

This section summarizes work done under the direction of J.B. Killough of the University of Houston.[29,30] Simulation of the East Vacuum/Grayburg San-Andres CO_2-Foam Field Pilot Verification was performed using a modified miscible flood simulator. Three phases of the simulation were performed: the field pilot history match, scaleup of the mechanistic foam model to field level, and simulation of five predictive cases. A fair history match of both the waterflood (1980-1985) and CO_2-WAG flood (1986-1992) portions of the field history were achieved. Historical data was compared with simulated data for all of the twenty-five wells in the field pilot area. Good matches of historical cumulative water and CO_2 production, and GOR and WOR behavior were achieved for most wells. Most matches were of good quality with a few of the producers showing only a fair match of historical production. The miscible flood simulator (VIP-MISC) was modified to account for the apparent increase in gas viscosity with the generation of foam. In a separate study it was verified that WAG injection can be modeled accurately with this simplified viscosity modification concept on the field level. Finally, five predictive cases were simulated. Unfortunately, although an increase in total oil production was noted for the maximum foam case, on a basis of oil recovered per barrel of CO_2 injected, the foam case had poor results and did not match the field results. All other cases showed approximately the same recovery per barrel of CO_2 injected.

Field Pilot History Match

The field plot history match model was constructed based on data provided by Phillips and Masera Corporation. The pilot location was taken as the twenty-five wells including and surrounding well 3332-001 (see Fig. 1). The model consists of a 31x31 grid with the twenty-five wells placed on the grid. The model consisted of seven separate layers for a total of 6727 grid blocks. Layer net thickness, porosity thickness, and structure were based on zonation (A, B, C1, C2, C3, D, E, G, H) of the Type Log (see Fig. 2). The F intervals were assumed to be non-productive. Derived porosity values were used to calculate permeabilities from permeability-porosity correlations provided by Phillips. Zones A and B of the original model nine-layer description were eliminated since little or no production occurred from these layers.

The first thirty years of the simulation consisted of a history match of primary depletion. The twelve year period of waterflood (1980-1986) and CO_2-WAG flood (1986-1992) was simulated in two phases. Initial simulations of the waterflood showed that in general water production was low compared to historical data. The process to achieve an acceptable match consisted of manipulations of completion KH's until no further gain was possible, then interwell injector-producer permeabilities were modified to achieve

better cumulative water production behavior. Fig. 29 compares historical and simulated cumulative water production for the eight producing wells of the center nine-spot of the pilot area. The match was good for the first nine years, but starting in 1989, the predicted water-oil ratio deviated significantly. Fig. 30 is an example comparison of the original simulation, the matched simulation and historical cumulative water production for Well 3333-004. The improved match was achieved by increasing the permeability between the central injector and Well 3333-004.

The first simulations of CO_2 production for the WAG injection period from 1986-1992 showed poor match of field performance with some wells producing little or no CO_2 and others producing ten times the historical level. To match this behavior, modifications were made to the interwell permeabilities. It was found that the CO_2 production was dominated by permeabilities in layers C3 and C2 while the water production was dominated by layer C1. With only one exception, changes to permeabilities in layers C3 and C2 had little effect on the water production history for the pattern. Fig. 31 compares historical and simulated data for the total cumulative solvent production for the central eight producers. The match is good until about 1990 when the field GOR and cumulative solvent production becomes greater than the simulated values.

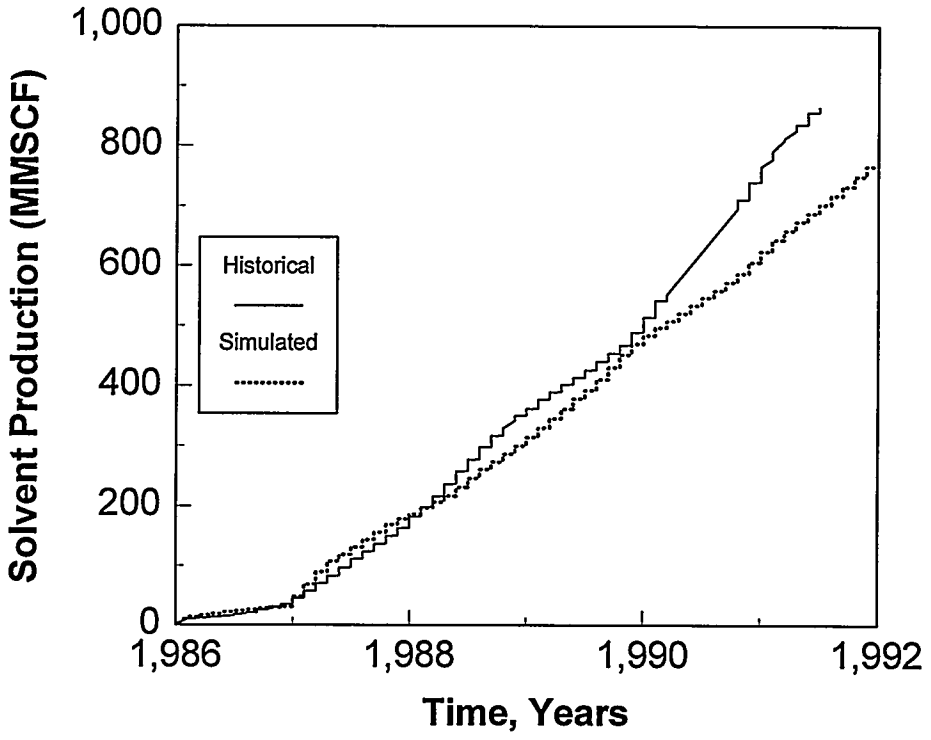

Fig. 29. Comparison of Simulated and Historical Cumulative Water Production for the Pilot Pattern (Killough 1994)

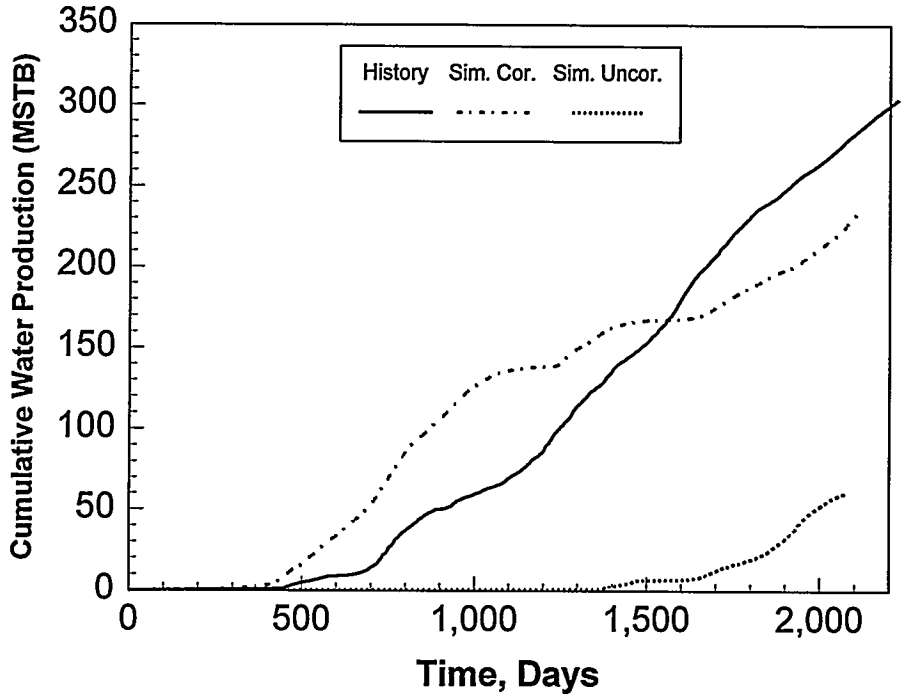

Fig. 30. Water Production, Well 3333-004. Comparison of Historical, Uncorrected Simulation, and Corrected Simulation (Killough 1994)

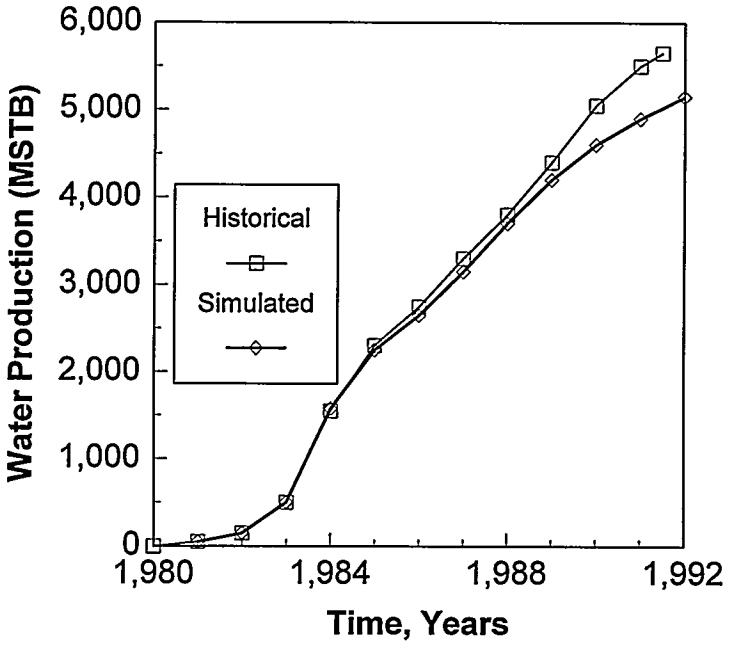

Fig. 31. Comparison of Historical and Simulated Cumulative Solvent Production (Killough 1994)

Development and Validation of a Simplified Foam Model

To better understand the simulation of the CO_2-foam process, use was made of a mechanistic foam simulator (MFS) that used the mechanistic model described by Chang et al.[31] In particular, the effect of radial, near-well, flow on foam generation was investigated. Chang's mechanistic model was modified to include radial geometry instead of the original Cartesian geometry. Coefficients and finite difference cell volumes were modified to include radial (R-Z) effects.

MFS provides a robust model for foam flow simulation in porous media but it is too expensive for a field scale simulation. The bubble population balance magnifies the problem dimension and retards the simulation time. Thus, there was a need to find a simpler model of representing foam behavior in porous media.

The simplified foam mode use in the large scale simulator MVIP (Miscible Vectorized Implicit Program—from Western Atlas Integrated Technologies) assumed the apparent viscosity of foam to be a function of gas velocity and surfactant concentration only. The surfactant equation was solved implicitly, and the foam viscosity was obtained by interpolation. To obtain agreement with observed bottomhole pressure, the apparent viscosities used were about an order of magnitude lower compared to the laboratory observed foam viscosity (see experimental section and reference 11). Below is a model description of a simplified three-dimensional case to demonstrate the ability of the simplified foam treatments.

Grid:

- 11 x 11 x 15
- Grid block dimensions in the x and y direction: 10',20',40',80' ,160',313',160',80',40',20',10'
- Constant DZ: 10'
- Depth to the center of the upper layer: 8400 ft
- Well radii = 0.5 ft (production well)

Rock Properties:

- Permeability in the first six layers and bottom six layer: Kx=Ky=500md
- Permeability in the seventh, eighth, and ninth layer: Kx=Ky=3000md
- Vertical permeability: Kz=0.5*Kx
- Porosity : 0.30

Operating Conditions:

- Injection well is perforated in all of the layers and maintained at constant injection rate
- Production well is perforated in layers seven, eight, and nine and subject to the following constraints:
  1. Limiting bottom-hole pressure of 3000 psia at the center of top layer
  2. Maximum production rate of 2000 RB/D of oil.

Simulation Parameters:

- Solvent (CO_2)-oil mixing parameter = 0.7 (0.0=immiscible, 1.0=complete mixing)
- Cutoff solvent saturation = 0.05 (below which solvent displacement of oil is immiscible)
- SORM = 0.05 (minimum oil saturation because of water blockage)

Five simulations were conducted to investigate the effect of foam on oil recovery:

1. Straight solvent injection for four years (2000 RB/D),
2. Surfactant injection (1 lb/bbl) for one year (2000 RB/D), followed by solvent injection for three years (2000 RB/D),
3. Surfactant injection (1 lb/bbl) for one year (2000 RB/D) followed by simultaneous injection of surfactant (1000 RB/D) and solvent (1000 RB/D),
4. Water injection for one year (2000 RB/D), followed by simultaneous injection of water (1000 RB/D) and solvent (1000 RB/D),
5. Surfactant injection (10 lb/bbl) for one year (2000 RB/D), followed by simultaneous injection of surfactant (1000 RB/D) and solvent (1000 RB/D).

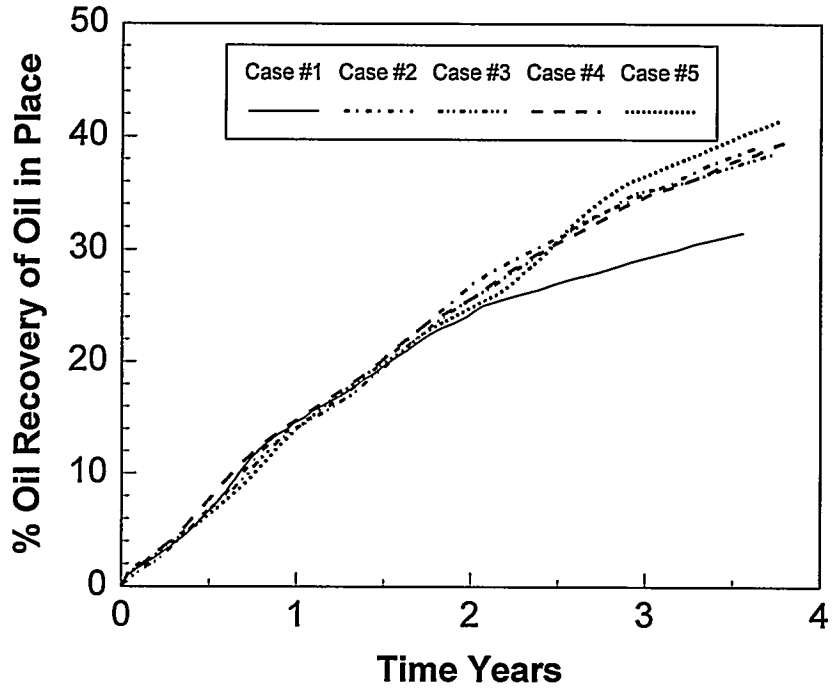

Fig. 32. Comparison of Five Predictive Cases of Oil Recovery During Foam Tests (Killough 1994)

Fig. 32 shows the oil recovery for each case. In case 1, most of the oil recovered is from the top part of the reservoir. In cases 2 and 3, where foam is formed, the foam effect is significant only at the well vicinity. In case 5, higher surfactant concentration, the calculated oil recovery was not affected very much even with better CO_2 mobility control. A surprising result comes from case 4 (straight WAG injection), where the oil recovery is comparable with the foam case although the CO_2 does not exhibit a good sweep efficiency. Thus, the simulation did not show significant improvement between WAG and SAG.

Field-Scale Simulation of the Foam Process

During the simulations, the bottomhole pressure of the injection well was about 400-600 psi higher during the water cycle of the WAG process. On the other hand, the bottomhole pressure of the CO_2 portion of the SAG cycle was about 400 psi greater than during the water injection. The greater bottomhole pressure for the CO_2 injection during the SAG cycle was measured in the field. Unfortunately, unlike the field results, the simulation had little response from the foam cycles.

Field Pilot Predictive Cases

Five field pilot predictive cases were simulated to determine if the model would predict recovery from the foam injection. These cases are summarized as follows:

1. Continued operations of 4 months CO_2, 8 months water (assumes no SAG flood in 3332-001)
2. Same as 1 but WAG cycles of 1 month CO_2 and 2 months water.
3. Rapid WAG and First Foam Cycle followed by 3 months CO_2, 4 months water, and then continued 4 months CO_2, 8 months water.
4. Rapid WAG, First Foam Cycle followed by continued Foam Cycles of 3 Months SAG (18 days water, 72 days CO_2), 3 Months CO_2, 4 Months water.
5. Same as 4 but adjust WAG cycles to average 4 months total CO_2 injection and 8 months water-water/surfactant injection.

Case 5 was a modification of original specifications by Phillips to maintain the same basic WAG ratio of 4 months CO_2 followed by 8 months of water.

Each of these cases was simulated for 5-6 years. Results are shown in Fig. 33. Basically, all cases at the same WAG ratio yield similar results (within about 5%) for oil recovery per MCF of CO_2 injected. About 5% additional oil was recovered in Case 4 over the same time period due to the increased rate of CO_2 injection. However, on a barrel of oil per MCF of CO_2 injected this case was the worst. Maximum surfactant penetration was about eight hundred feet from the central injection well for cases 4 and 5. This lack of effect for recovery due to WAG ratio, with or without foam was in contrast to the field results, thus further study in this area was indicated.

PRRC Studies

History Matching

At the PRRC, the simulated annealing method (SAM) for inverse reservoir modeling has been applied to the EVGSAU.[10, 12] SAM is a nongradient, global optimization technique that can incorporate hundreds of variables yet jump over local minima to converge on the optimum solution. This history matching method characterizes the individual grid blocks in terms of permeability, saturations, and pressure. Additionally, an estimate of the average oil-water relative permeability and capillary pressure functions is produced. SAM is a nonsubjective means of automatically matching reservoir pressure and production/injection history, and the resulting grid block description is a useful reservoir management tool.

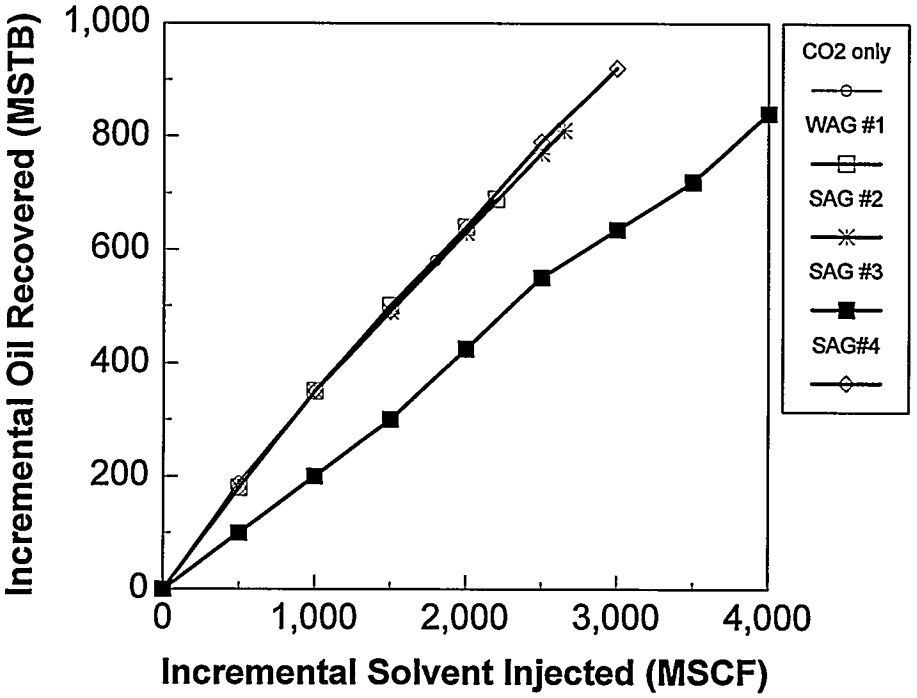

Fig. 33. Summary of Predictive Cases: Incremental Oil vs Solvent Injected

In the EVGSAU project, SAM was used to match six years of water injection and the oil, water, and solution gas history of 15 wells surrounding the CO_2-foam injection well. SAM was used with DOE's black oil simulator, BOAST, to solve the inverse problem. A good match was obtained for oil, water, and solution gas production for all the wells in the pilot pattern. The reservoir and engineering parameters automatically estimated were the permeability distribution of the pilot pattern area, average relative permeability and capillary pressure curves, the productivity index of each producer, the injectivity index of each injector, and the effective injection rates in the pilot area. All parameters were estimated at reservoir scale with this new approach. Hence, there is no upscaling problem, which is usually encountered in geostatistical techniques.

The resulting reservoir description was then used to match the six years of CO_2 injection performance using the UTCOMP compositional simulator, graciously provided by Gary Pope of the University of Texas. A very good match for all phases of production was obtained with only a slight modification of the gas-oil relative permeability curves. Results obtained with SAM as applied to the new integrated reservoir description are described in a recent technical paper.[12] Plans for further development include an adaption of SAM and a black oil simulator to full parallelization for use on fast, parallel-processor computers.

Laboratory Determination of Reservoir Simulator Foam Parameters

Laboratory foam tests were performed that were used to determine foam parameters. Foam tests were performed at average reservoir conditions of 101°F and 2100 psig with EVGSAU cores. Foam was generated in situ by simultaneous injection of surfactant solution and CO_2 into a brine-saturated core. In this study, the gas-liquid volumetric injection ratios of 2, 4, and 6 (with foam qualities of 66.7%, 80.0%,

and 85.7%, respectively) were examined. The flow rate in terms of total interstitial velocity varied from 0.36 to 34.38 ft/day. The surfactant was tested at concentrations of 1000 and 2500 ppm active.

The resistance factor has been found to be the most useful measure of mobility change due to foam, see the next section for more detailed description of this factor. The resistance factor of each test ranged from 3 to 63, indicating that foam was generated at all the testing conditions. Brine permeability, which changed after each foam test, had a significant effect on the calculation of foam apparent viscosity. Because of varying brine permeability, the resistance factor data is more suitable for simulator input than apparent viscosity data.

For full details refer to the previously published work by Chang and Grigg[11]. Tables 2 and 9-12 summarize the test parameters and experimental data. Fig. 34 summarizes the gas mobility without surfactant in the brine versus interstitial velocity at different gas qualities and using two different core samples.

TABLE 9
PROPERTIES OF SURFACTANT SOLUTION

Concentration (ppm active)	1000	2500
Weight Fraction	0.00214	0.00535
Density (g/cm^3)	1.017	1.023

TABLE 10
EVGSAU CORE PROPERTIES

Property	Core #1	Core #2	Core #3	Core #4
Length (cm)	7.44	8.13	5.01	4.83
Diameter (cm)	1.35	1.35	3.81	3.81
Porosity	0.12	0.12	0.12	0.12
Pore Volume (cm^3)	1.28	1.40	6.84	6.61
Initial Brine Permeability (md)	19.78	17.01	16.75	75.25

TABLE 11
SUMMARY OF EVGSAU CORE FOAM TESTS

Core #	Exp. #	Brine Perm. (md)	App. Visc. (cp)	Press. Drop (psid/ft)	Mobility (md/cp)	Inverse Mobility (cp/md)	WAG Mobility (md/cp)	Resist. Factor	Foam Qual. (%)	Tot. Flow Rate (cc/hr)	Interstitial Velocity (ft/day)	Surf. Conc. (ppm act.)	PVI	Surf. Inj. (g)
1	2	50.2	23	302	2.16	0.46	7.1	3.3	66.7	7.50	34.38	1000	170	0.16
	3	34.1	28	270	1.21	0.83	7.1	5.9	66.7	3.75	17.19	1000	67	0.06
	5	35.7	18	334	1.95	0.51	10.6	5.4	80.0	7.50	34.38	1000	164	0.09
	6	28.6	15	170	1.91	0.52	10.6	5.5	80.0	3.75	17.19	1000	135	0.08
	8	98.0	44	295	2.21	0.45	10.6	4.8	80.0	7.50	34.38	2500	135	0.19
	9	98.6	64	197	1.55	0.65	10.6	6.9	80.0	3.50	16.04	2500	115	0.16
	11	88.5	41	303	2.15	0.47	7.1	3.3	66.7	7.50	34.38	2500	293	0.68
	12	64.6	39	197	1.66	0.60	7.1	4.3	66.7	3.75	17.19	2500	94	0.22
2	15	42.9	50	153	0.85	1.17	39.6	46.5	66.7	1.50	6.88	2500	45	0.12
	16	86.5	64	96	1.36	0.74	51.3	37.8	80.0	1.50	6.88	2500	48	0.07
	17	98.5	57	75	1.74	0.58	51.3	29.5	80.0	1.50	6.88	1000	49	0.03
	18	106.3	76	94	1.39	0.72	39.6	28.5	66.7	1.50	6.88	1000	97	0.10
	19	105.4	65	81	1.62	0.62	62.1	38.4	85.7	1.50	6.88	2500	126	0.14
	20	105.0	42	53	2.48	0.40	62.1	25.0	85.7	1.50	6.88	1000	130	0.06
	24	182.2	195	98	0.94	1.07	39.6	42.3	66.7	1.05	4.81	2500	68	0.17
	25	107.0	84	71	1.28	0.78	51.3	40.1	80.0	1.05	4.81	2500	90	0.14
	26	50.2	79	86	0.63	1.57	39.6	62.4	66.7	0.63	2.89	2500	45	0.12
	27	45.9	72	86	0.63	1.57	39.6	62.4	66.7	0.63	2.89	1000	119	0.12
	28	45.4	45	90	1.01	0.99	39.6	39.0	66.7	1.05	4.81	1000	92	0.09
	29	39.8	23	53	1.74	0.58	51.3	29.5	80.0	1.05	4.81	1000	181	0.11
	30	53.9	27	45	2.03	0.49	62.1	30.6	85.7	1.05	4.81	1000	265	0.12
	31	46.3	46	90	1.01	0.99	62.1	61.2	85.7	1.05	4.81	2500	106	0.12
	32	47.5	51	98	0.94	1.07	39.6	42.3	66.7	1.05	4.81	1000	191	0.19
3	33	21.4		1945					66.7	5.01	2.89	1000	190	0.94
	35	9.6		2317					66.7	5.01	2.89	1000	24	0.12
4	36	79.8	293	25	0.27	3.67	6.8	24.8	66.7	0.63	0.36	1000	36	0.17
			132	19	0.61	1.65	25.1	41.4	80.0	1.05	0.60	1000	44	0.20
			88	25	0.91	1.10	25.1	27.6	80.0	2.10	1.21	1000	51	0.22
	39	61.4	85	76	0.72	1.38	6.8	9.3	66.7	5.02	2.89	1000	129	0.62
			64	95	0.96	1.04	6.8	7.0	66.7	8.36	4.81	1000	276	1.32
			53	114	1.15	0.87	6.8	5.9	66.7	11.95	6.88	1000	357	1.71
	40		68	101	0.90	1.11	6.8	7.5	66.7	8.37	4.82	1000	65	0.31
			65	139	0.94	1.06	6.8	7.2	66.7	11.95	6.88	1000	201	0.96
			113	101	0.54	1.84	6.8	12.4	66.7	5.02	2.89	1000	250	1.20
			282	32	0.22	4.59	6.8	31.0	66.7	0.63	0.36	1000	261	1.25
			296	66	0.21	4.82	6.8	32.5	66.7	1.26	0.73	1000	266	1.27
			67	142	0.92	1.09	6.8	7.3	66.7	11.95	6.88	1000	275	1.32

TABLE 12
SUMMARY OF BASELINE EXPERIMENTS

Core #	Exp. #	Brine Perm. (md)	Pressure Drop (psid/ft)	Mobility (md/cp)	Interstitial Velocity (ft/day)	CO_2 Fraction (%)	Total Flow Rate (cc/hr)
1	1W	19.8	368.7	7.1	137.52	66.7	30.00
2	21W	101.6	6.0	21.7	6.88	66.7	1.50
			4.5	29.0	6.88	80.0	1.50
			4.1	31.6	6.88	85.7	1.50
	22W	154.8	8.6	37.8	17.19	66.7	3.75
			6.8	48.3	17.19	80.0	3.75
			5.3	62.1	17.19	85.7	3.75
			15.8	41.4	34.38	66.7	7.50
			12.0	54.3	34.38	80.0	7.50
			10.5	62.1	34.38	85.7	7.50
	23W	165.1	3.8	34.8	6.88	80.0	1.50
			4.5	29.0	6.88	66.7	1.50
			2.6	49.7	6.88	85.7	1.50
			2.6	20.9	2.89	66.7	0.63
			3.8	24.3	4.81	66.7	1.05
			2.6	34.8	4.81	80.0	1.05
3	33W	16.8	23.1	2.4	2.89	66.7	5.01
	34W	4.0	103.3	0.5	2.89	66.7	5.01
	35W	2.5	60.8	0.9	2.89	66.7	5.01
4	36W	75.3	3.0	2.3	0.36	66.7	0.63
	37W	51.0	2.5	2.8	0.36	66.7	0.63
			2.5	4.7	0.60	80.0	1.05
			2.4	9.6	1.21	80.0	2.10
			2.9	15.8	2.42	80.0	4.20
	38W	67.6	3.0	3.8	0.60	80.0	1.05
			3.2	7.3	1.21	80.0	2.10
			3.2	14.5	2.42	80.0	4.20
			4.8	19.1	4.83	80.0	8.40
			7.1	25.9	9.67	80.0	16.80
			15.1	24.2	19.34	80.0	33.60
			5.7	16.1	4.83	80.0	8.40
	41W	36.2	8.2	6.7	2.89	66.7	5.02
			17.7	7.4	6.88	66.7	11.95
			21.5	6.6	7.49	66.7	13.02
			10.7	5.1	2.89	66.7	5.02
			16.4	5.6	4.81	66.7	8.35
			4.4	2.6	0.60	80.0	1.05
			4.4	1.6	0.36	66.7	0.63
			18.9	4.8	4.81	66.7	8.35
			58.1	6.3	19.34	66.7	33.60

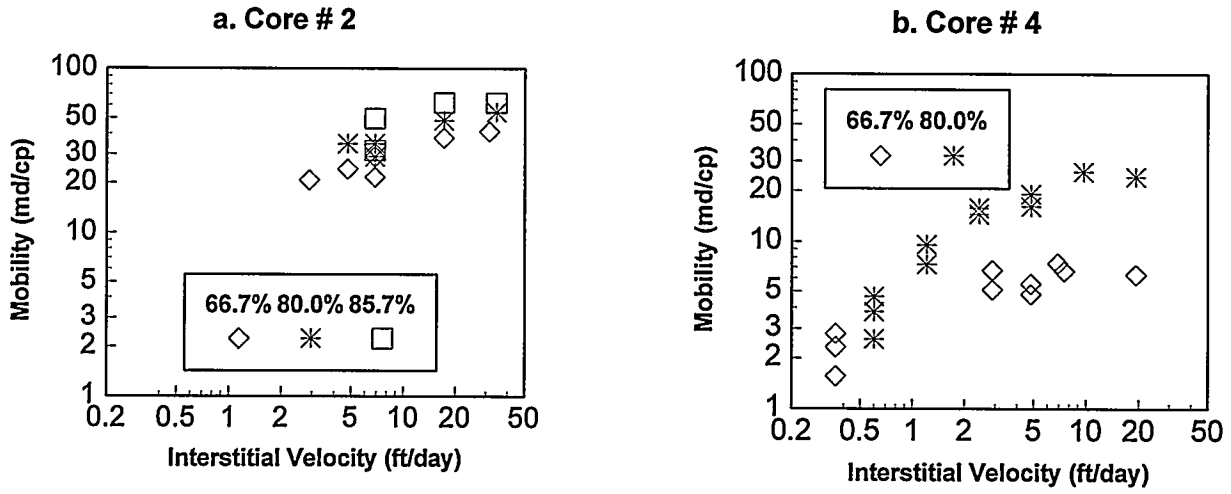

Fig. 34. Mobility vs Interstitial Velocity for WAG Core Systems at Different CO_2 Qualities

The mobility of CO_2 and brine was found to increase with interstitial velocity until it reached a plateau at higher interstitial velocities. Fig. 35 is a comparison of all tests performed using three different EVGSAU cores. Note that all the resistance factors were found to be above 1, ranging from 3 to 63, indicating that foam was generated at all the conditions tested with interstitial velocity ranges from 0.36 to 34.38 ft/day. The resistance factor decreases and mobility increases with increasing interstitial velocity. In general, higher concentrations of surfactant have higher resistance factors (lower mobility), but the effect of concentration between 1000 to 2500 ppm is not significant. The effect of foam quality on resistance factor is not significant over the studied range. Brine permeability, which changed after each foam test, has a significant effect on the calculation of foam apparent viscosity. The pressure drop reached steady state with less injected surfactant at higher flow rates and lower surfactant concentrations.

Incorporating CO_2-foam Features into Reservoir Simulations

Work at the PRRC has been conducted on incorporating CO_2-foam features into reservoir simulators. The reservoir simulators used in this work include a multi-component pseudo-miscible reservoir simulator, MASTER (Miscible Applied Simulation Techniques for Energy Recovery), obtained from the Department of Energy and a compositional reservoir simulator, UTCOMP.

By utilizing the tracer features in UTCOMP, a foam model was developed. The surfactant solution movement is tracked by treating the surfactant solution as an aqueous tracer without the addition of a surfactant-solution conservation equation into UTCOMP. [The tracer adsorption model has been modified to account for the adsorption isotherm.] Instead of using a mechanistic, bubble-population-balance approach to calculate the mobility of the gas-foam phase, the foam model reads, as input, the foam-resistance-factor data described in the last section as lookup tables. The resistance factor is treated as a function of interstitial velocity, gas-liquid volumetric ratio, and surfactant concentration based on laboratory test results. In order for foam to exist, the following conditions must be satisfied:

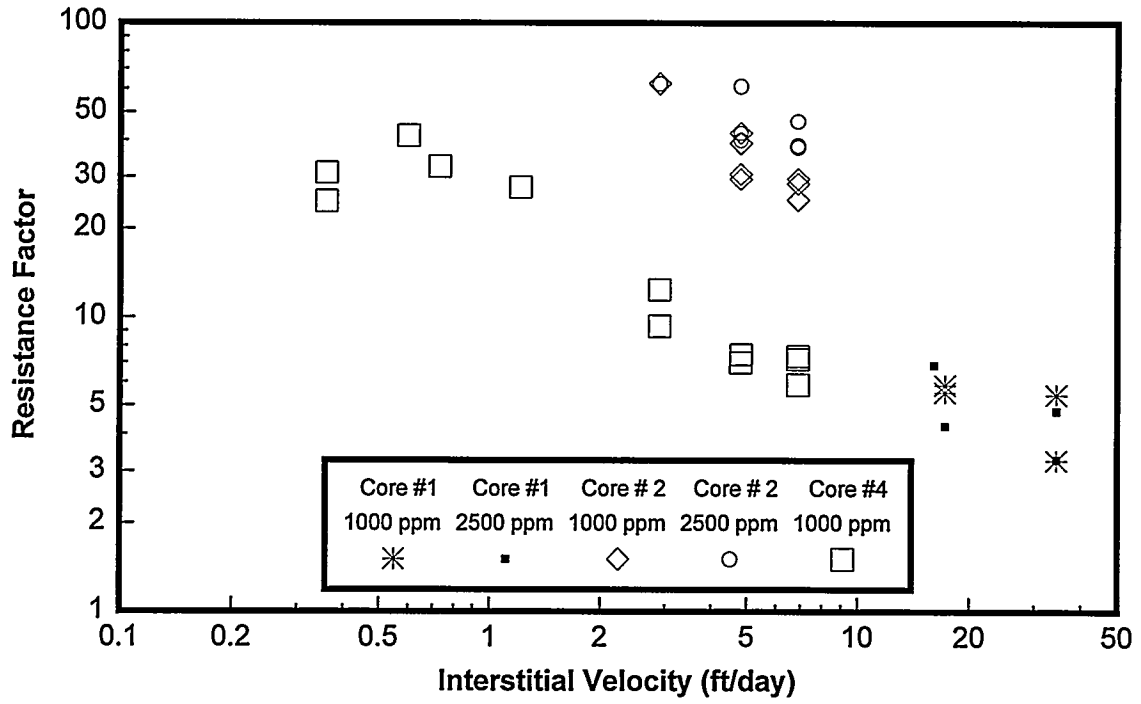

Fig. 35. Comparison of the Resistance Factor of Tests from Cores #1, #2, and #4

$$S_g > S_g^{\lim},\ S_o < S_o^{\lim}$$

$$C_s > C_s^{\lim},\ S_w > S_w^{\lim}$$

where S_g, S_o, and S_w are the gas-, oil-, and water-phase saturations, respectively, and C_s is the surfactant concentration. The variable with superscript *lim* corresponds to the limiting value of each variable. If any of these conditions are not met, foam does not exist and the gas-phase mobility is not modified. By assuming foam has no effect on the water phase, the mobility of the gas-foam phase is calculated according to

$$M_g^{\text{foam}} = \frac{1}{R_f}\left(M_w + M_g\right) - M_w$$

where M_w is the water-phase mobility, M_g is the foam-free gas-phase mobility, and R_f is the resistance factor which is defined as

$$R_f = \frac{M_{CO2+BR}}{M_{CO2+SS}}$$

Here, M_{CO2+BR} is the mobility obtained from the experiment of simultaneous injection of CO_2 and brine, M_{CO2+SS} is the mobility obtained from the experiment of simultaneous injection of CO_2 and surfactant solution, and both measurements are conducted at the same gas-liquid volumetric ratio. The resistance factor represents the pressure drop attributed to the presence of foam. If foam is not formed, the resistance factor would be unity. The mobility of the gas-foam phase is calculated after the foam resistance factor is determined from lookup tables.

The major modifications that were made to MASTER include (1) the addition of two conservation equations to permit simulation of surfactant solution and foam bubble, (2) the addition of an algorithm to calculate the mobility of gas-foam phase, and (3) the addition of a foam-resistance-factor table-lookup option similar to the one that has been incorporated into UTCOMP. In this new foam-flood simulator, the mobility of gas-foam phase can be calculated by two approaches. The first approach involves the using of the foam-bubble population balance equation and the second approach is the foam-resistance-factor table-lookup option. The foam features can be easily bypassed, giving essentially the MASTER model, which can be used to simulate a wide range of immiscible-to-miscible gas-injection recovery processes. In addition, the simulator can be used to simulate most of the common primary and secondary recovery mechanisms by bypassing both the foam and miscible features in the model.

Simulation tests on a three-dimensional quarter of a five-spot pattern have been performed to assess the sensitivity and adequacy of the included foam features in UTCOMP. The reservoir is divided into five layers and the reservoir model description is as follow:

Grid:
- Reservoir size: 660 ft x 660 ft x 160 ft (20-acre well spacing)
- Mesh dimension: 8 x 8 x 5
- Grid block size in the x and y directions (constant size): 82.5 ft
- Grid block size in the z direction: 27, 40, 35, 18, 40 ft
- Well radii: 0.33 ft

Rock Properties:
- Porosity of each layer: 0.1, 0.06, 0.08, 0.15, 0.07
- X-direction permeability of each layer: 150, 70, 112, 1000, 70 md
- Y-direction permeability of each layer: 150, 70, 112, 1000, 70 md
- Z-direction permeability of each layer: 15, 7, 11.2, 100, 7 md

Operation Condition:
- Injection well is perforated at the whole layers and maintained at constant molar injection rate: 2500 lb-moles/day water during water injection
  800 lb-mole/day CO_2 during CO_2 injection

Production well is perforated at the whole layers and limited at bottom-hole pressure of 1500 psia at the first layer.

The initial conditions for foam tests was established by simulating a 10-year water flooding and a

5-year CO_2 flooding from an initial pressure of 1500 psia and an initial water saturation of 25%. The foam test is performed using the following injection schedule:

(1) Surfactant (2500 ppm active) injection for 122 days.

(2) Rapid SAG injection of 6 SAG cycles during a 90-day period. A SAG cycle consists of 3-days of surfactant solution and 12-days of CO_2.

(3) CO_2 injection for 153 days.

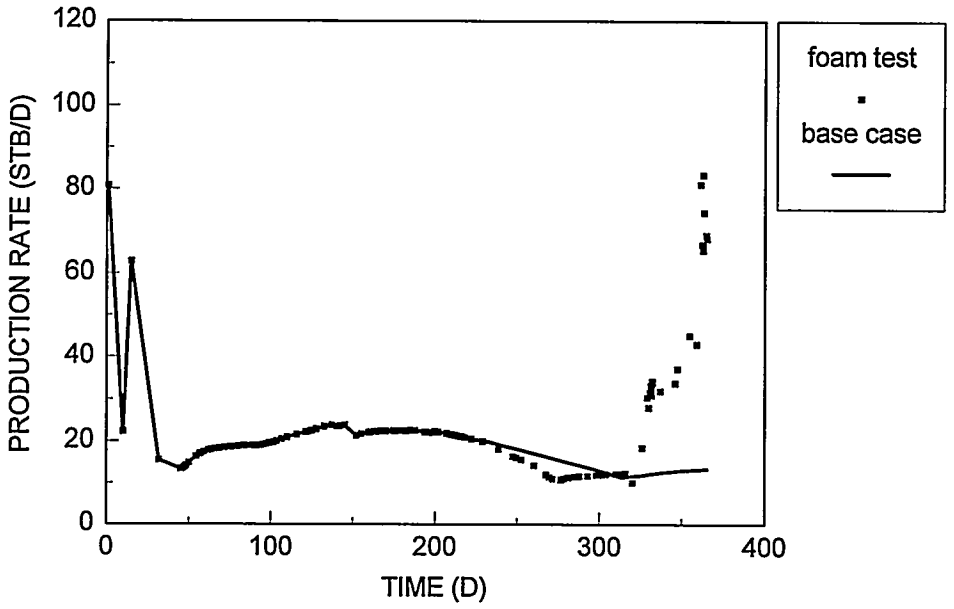

Fig. 36. Two Case Studies of Oil Production History Using UTCOMP with the New Foam Option

In order to evaluate the foam test, a base case simulation was performed. In this base case, the injection schedule is identical with that of the foam test except surfactant solution is replaced with surfactant-free brine. Fig. 36 shows the oil rate history for the foam test and the base case. Observe the significant increase in the oil rate from about 10 STB/D to about 85 STB/D, commencing from about 320 days for the foam test compared to the base case. To understand the results better, the injection profile for the two cases at 236 days of simulation are shown in Fig. 37. Note that layer 4 is the most permeable layer with a permeability of 1000 md, while layers 2 and 5 are the least permeable layers at 70 md. Fig. 37 shows that, at the base case, most of the injected CO_2 would be injected through the highest permeability layer, while the least amount of CO_2 would be injected through the least permeable layers. Consequently, the sweep is poor and the oil rate is low. However, for the foam test, there were significant increases in the amount of CO_2 injected through layers 2 and 5. At the same time, the amount of CO_2 injected through layer 4 was reduced by half. Therefore, the profile modification due to the presence of the foam significantly improved the sweep and thus resulted in the higher oil rate.

The effect of the magnitude of the foam-resistance factor on the oil rate was examined by using a scaling parameter F. As shown in Fig. 38, the response to the foam for the oil rate to increase was delayed when the magnitude of the foam-resistance-factor data was scaled down by the parameter F. Sensitivity study of one of the parameters that determine the existence of foam, S_g^{lim}, has also been performed. When

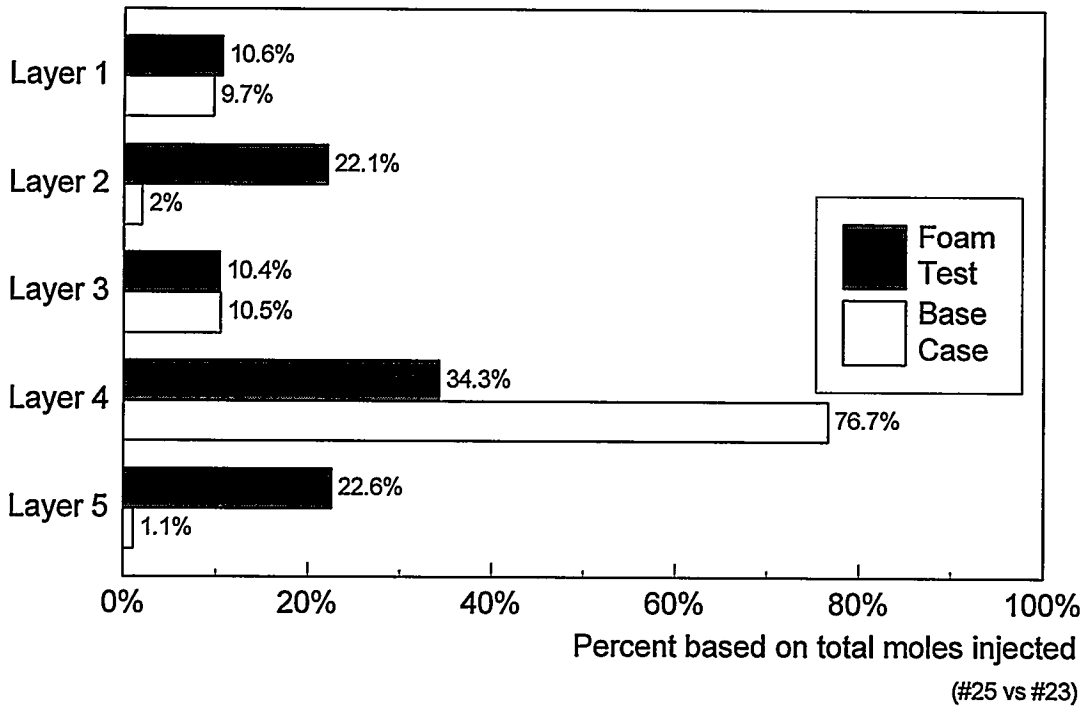

Fig. 37. CO_2 Injection Profile at 263 Days Using UTCOMP with the New Foam Option

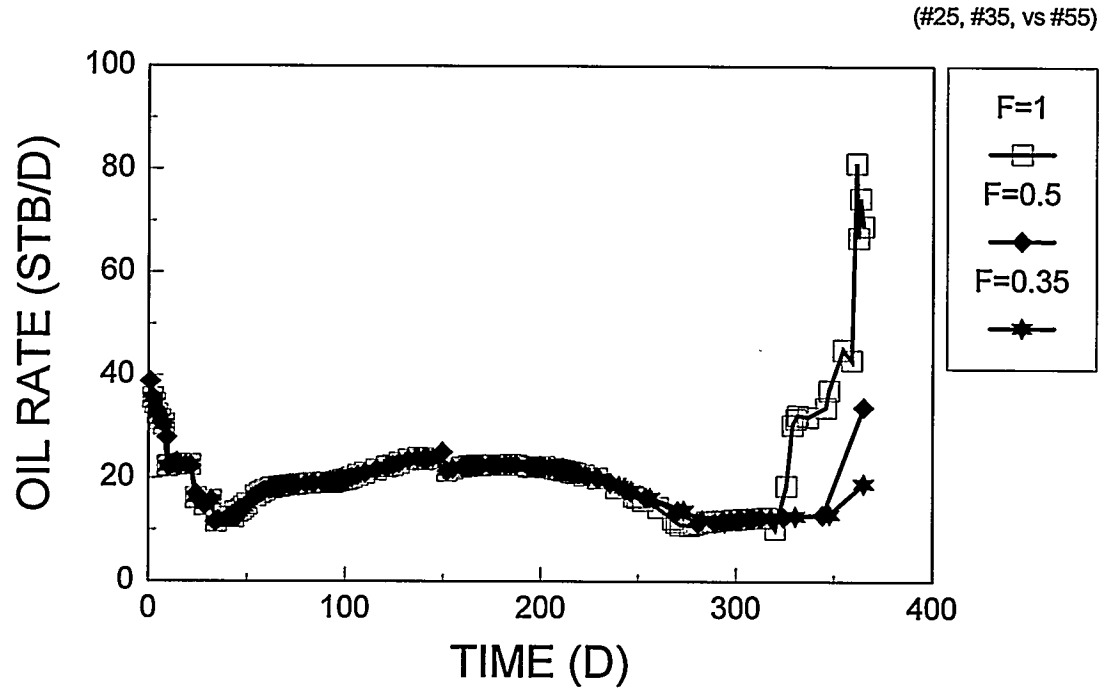

Fig. 38. Effect of Scaling Factor on Oil Response Magnitude Using UTCOMP with the New Foam Option

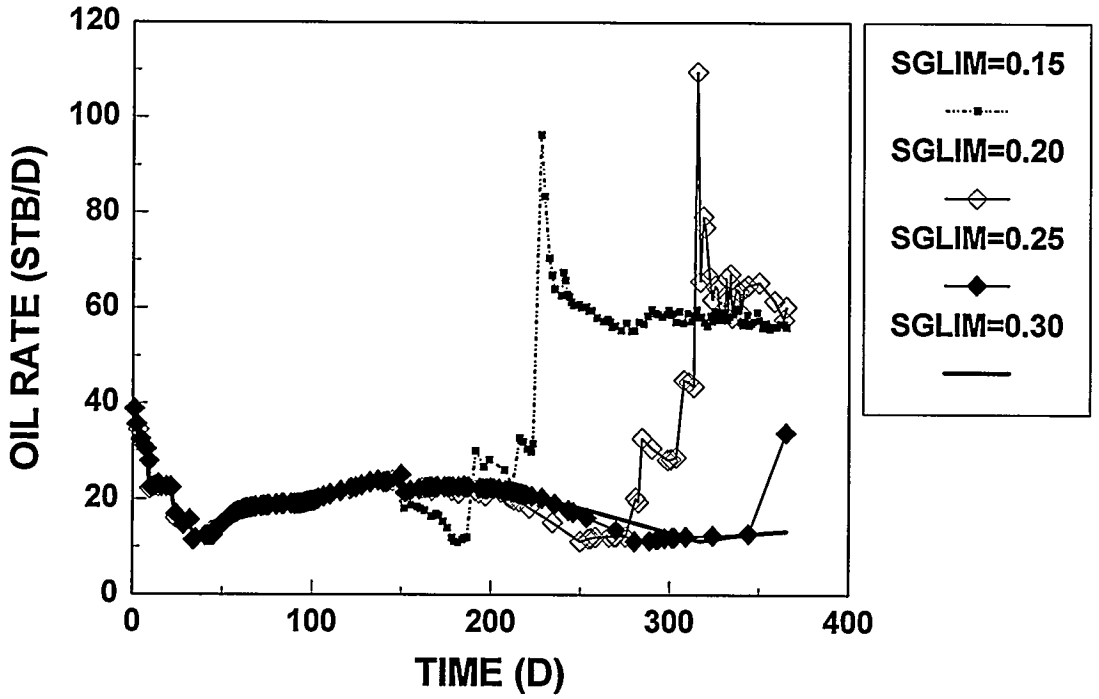

Fig. 39. Effect of Limiting CO_2 Saturation on Time of Oil Response

gas saturation is less than S_g^{lim}, foam cannot exist. Fig. 39 shows the simulation results when S_g^{lim}(SGLIM) is equal to 0.15, 0.2, 0.25, and 0.3, respectively. When S_g^{lim} decreases, the response to the foam occurred earlier. The oil production rate for the case when S_g^{lim} is equal to 0.15 increased to a peak and the dropped and leveled off at a higher oil rate. This kind of response is similar to that observed in the field, as shown in Fig. 40. When S_g^{lim} increases from 0.25 to 0.3, the response to the foam was not observed by the end of CO_2 injection . The results plotted in Fig. 39 were identical to that of the base case.

Our results to date have shown that the effects of foam that have been seen in the field can be simulated using the resistance factor lookup option. The timing and magnitude of the resulting oil response can be controlled by adjusting the limiting gas saturation and scaling up factor, both of which are presently under further investigations.

TECHNOLOGY TRANSFER ACTIVITIES

During the course of the project, annual reports [1-5] and technical papers [6-15] related to the EVGSAU project were prepared. Several of the technical papers [11-15] which were prepared in the latter stages of the project and presented at conferences, document the results that were obtained .

A paper[11], entitled "Laboratory Flow Tests Used to Determine Reservoir Simulator Foam Parameters for EVGSAU CO_2-Foam Pilot," presented the results of laboratory foam tests that were used to determine foam parameters for use in foam-flood reservoir simulators. Foam was generated in situ by simultaneous injection of surfactant solution and CO_2 into a brine-saturated EVGSAU core at a variety of test conditions.

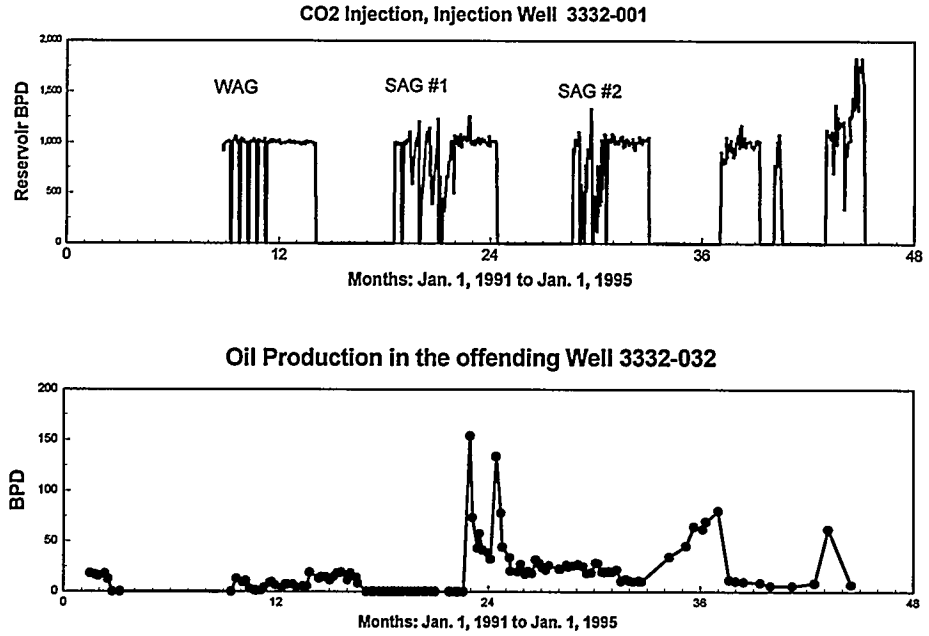

Comparison of Oil Rate to the CO2 injection cycles in Well 32032.

Fig. 40. Comparison of Oil Production Rate in Well 3332-032 to the CO_2 Injection Cycles in Well 3332-001

The resistance factor of each test ranged from 3 to 63, indicating that foam was generated at all test conditions. Brine permeability, which changed after each foam test, had a significant effect on the calculation of foam apparent viscosity. Because of varying brine permeability, the resistance factor data is more suitable for simulator input than the apparent viscosity data.

A paper [12], entitled "Automatic History Matching for an Integrated Reservoir Description and Improving Oil Recovery," static (geologic) and dynamic (production history) field data from the EVGSAU were used to obtain a reservoir description by an automatic history matching algorithm using the SAM. The EVGSAU reservoir was characterized by using an automatic history matching algorithm that solves an inverse problem using the SAM. The major advantages of this approach are: 1) it can estimate a large number of reservoir parameters and 2) it is able to integrate various disciplines, such as geology, petrophysics, and reservoir engineering. The reservoir description was used in a numerical "what if" experiment to examine the outcome of continued waterflooding (no CO_2 flood) at EVGSAU coupled with targeted infill drilling in the foam pilot area.

A paper[13], entitled "CO_2-Foam Field Verification Pilot Test at EVGSAU: Phase IIIA - Surfactant Performance Characterization and Quality Assurance," provided a summary of laboratory work done in support of the CO_2-foam application at the EVGSAU. Results concentrated on work with the surfactant (CHASER® CD1045) selected for use in this field pilot, and tests were performed over wide ranges of surfactant concentration and core permeability.

CD1045 is an effective CO_2-foaming agent that provides foam mobility with a slightly favorable, but not prominent, dependence on rock permeability. Surfactant CHASER® CD1045 showed great effectiveness as a CO_2 mobility reduction agent at concentrations as low as 1000 ppm, and showed a significant effect even at 500 ppm. The mobility of foam was affected by changes in the rock condition; because of relative permeability effects, the mobility was higher under conditions when less residual oil was present in the rock sample. Adsorption of surfactant increased as water salinity increased, and the adsorption values varied considerably, even for cores from the same reservoir.

Experiments in which additional EVGSAU crude oil was added prior to the mobility tests showed that the CO_2-foam was a more efficient displacing agent than had been apparent from "preserved core" tests alone. Effective demulsifiers and foam breakers were selected in the laboratory for contingency use in the field operation in case of the appearance of foam or emulsion in production facilities; however, these chemicals were not needed at the EVGSAU field pilot test.

A paper[14], entitled "CO_2-Foam Field Verification Pilot Test at EVGSAU: Phase IIIB: Project Operations and Performance Review;" summarized the injection well and production well responses from foam injection at the EVGSAU. The CO_2-foam field trial performed at EVGSAU proved that a strong foam could be formed in situ and that the foam reduced the mobility of CO_2 by one-third. Incremental oil was produced in three of the eight producers in the pattern, and gas cycling was dramatically reduced in the offending well as a direct result of surfactant injection. In light of the fact that a large amount of surfactant was injected, the revenue and savings produced from the foam injection shows promise of being an economical method for conformance control. Control of gas breakthrough in the offending well during a second CO_2 injection period was achieved with a much smaller amount of surfactant.

A paper[15], entitled "CO_2-Foam Field Verification Pilot Test at EVGSAU: Phase IIIC - Reservoir Characterization and Response to Foam Injection," summarized the comprehensive reservoir characterization effort for the foam pilot area and discussed the response to foam injection at the EVGSAU. Results from the detailed study of the pilot pattern geology were shown to provide an understanding of the major controls on fluid flow in the foam pattern. Pattern performance data, falloff testing, profile surveys, and interwell tracer results were integrated into the geologic model to guide project design work and provide a framework for interpretation of foam performance.

Localized regions of high permeability resulting from solution enhancement of the matrix pore system appear to be the primary cause of the early CO_2 breakthrough and channeling of injection CO_2 toward production well 3332-032, (referred to as the "offending" well) in the foam pilot pattern. Because the high permeability channels are depositionally and diagenetically controlled, these features may be expected to occur in other areas of the field with similar conditions. No evidence of direct fracture communication was found between the foam injector (3332-001) and the "offending" producing well 3332-032. Interwell tracer results indicate that the interwell fluid transit time between these wells is about six months. One explanation for the rapid CO_2 production response observed in the "offending" production well prior to foam treatment (the well started flowing six weeks after the start of rapid WAG CO_2 injection) is that remobilization of a significant trapped CO_2 saturation occurred in the high permeability channel between this well and the injector.

SUMMARY

The San Andres reservoir section at EVGSAU is comprised of a series of repeated, anhydritic, dolomitized, fining-upward, carbonate sequences composed of grain-rich dolostiones which grade upward into mud-rich dolostones. The best reservoir-quality rock is associated with subtidal grain-rich lithofacies. Skeletal/pelletoidal grain-rich rocks are dominated by intercrystalline and intergranular pore types and show a consistent relationship between porosity and permeability. Oolitic grain-rich rocks contain significant moldic porosity and show no consistent relationship between porosity and permeability. Dissolution within the reservoir, resulting from both natural geologic processes and waterflood-induced dissolution, plays a major role in determining reservoir rock quality and fluid flow patterns. Dead oil, not genetically related to the currently producing oil, may plug as much as twenty percent of the available pore space in the lowermost portion of the grain-rich facies in many depositional cycles. The presence of this dead oil may have a significant impact on log interpretation, wettability, and displacement characteristics.

No evidence of direct fracture communication was found between the foam injector (3332-001) and the "offending" producing well 3332-032. Interwell tracer results indicate that the interwell fluid transit time between these wells is about six months. One explanation for the rapid CO_2 production response observed in the "offending" production well prior to foam treatment (the well started flowing 6 weeks after the start of rapid WAG CO_2 injection) is that remobilization of a significant trapped CO_2 saturation occurred in the high permeability channel between this well and the injector.

A CO_2-foam field test was successfully designed and implemented in a New Mexico CO_2 flood, and an extensive data gathering program was implemented to monitor results from the field test.

Reduced injectivity, as evidenced by surface injection pressure and rate data, provided an immediate indication that in situ foam generation and mobility reduction had been achieved. This reduced injectivity persisted for over three months.

As evidenced by the pressure increase observed in the injection well, foam was generated in the reservoir. Because the observed injection pressure increase remained high for several months, it appears that the foam persisted or was continuing to be formed in the reservoir. The favorable production response (increased oil rate and lower GOR) that was observed at an offset producing well is an indication of the technical success of the foam injection test. Based on the favorable results obtained, a second foam injection test was conducted.

CONCLUSIONS

1. The detailed geologic model developed for the foam pilot pattern area provided a necessary framework for understanding controls on fluid flow and for subsequent design work and interpretation of foam project performance.

2. Localized regions of high permeability resulting from solution enhancement of the matrix pore system within reservoir Zone C appear to be the primary cause of the early CO_2 breakthrough and channeling

of injected CO_2 toward production well 3332-032 in the foam pilot pattern.

3. Based on laboratory results and EVGSAU rock and fluid characteristics, Chevron CD1045 was selected to generate CO_2-foam in this field test.

4. The CO_2-foam field trial performed at EVGSAU proved that a strong foam could be formed insitu and that the apparent in-situ mobility of CO_2 after foam generation was approximately one-third of that observed during the baseline CO_2 injection. In-situ mobilities calculated using Hall plots were comparable to falloff test results.

5. Injection profile surveys indicate that the foam did achieve some diversion of injected fluid away from the high permeability zone and into lower permeability zones which had not been taking desired quantities of CO_2 prior to the foam treatment.

6. Time lapse monitor logging in the observation well indicates that foam generation was effective in slowing the rapid movement of CO_2 through the high permeability interval in Subzone C2, but more frequent logging during the project would have helped reduce the uncertainties in interpreting the monitor logging results.

7. Incremental oil was produced in three of the eight producers in the pattern and gas cycling was dramatically reduced in the offending well as a direct result of surfactant injection.

8. In light of the fact that a large amount of surfactant was injected, the revenue and savings produced from the foam injection shows promise of being an economical method for conformance control.

9. Control of the offending well during a second CO_2 injection period was achieved with a much smaller amount of surfactant.

ACKNOWLEDGEMENTS

Several individuals at PPCo have made valuable contributions to this project. The author is particularly grateful for the numerous efforts of Jim Stevens, Laura Sugg, Ken Harpole, Ahmad Moradi-Araghi, and David Zornes. A special thanks goes to Don Thorp and Joe Brown for their devotion in supervising the collection of the field data, and to Matt Gerard, Larry Hallenbeck, Don Weir, Terry Siemers, Scott Balke, Don Kuehne, and J.E. Kim for their technical contributions. The project would not have run as smoothly as it has without the participation and input from the various JPAT representatives listed below:

Arco -	Erwin Sutanto, Sophany Thach
Chevron -	Doug Jasek
DOE -	Royal Watts
Exxon -	Todd Reppert, Gary Teletzke
Marathon -	Gwen Ginley
Mobil -	Ed Shaw
Texaco -	Jim Ware, John Prieditis

Funding for this joint government-industry project, provided by the U.S. Department of Energy, the State of New Mexico, and the Working Interest Owners of the EVGSAU, is greatly appreciated. We also thank Abu Dhabi National Reservoir Research Foundation, Amoco Production Company, and JAPEX for their contributions to this project.

REFERENCES

1. Martin, F.D., Heller, J.P., and Weiss, W.W.: "Field Verfication of CO_2-Foam," Annual Report to U.S. Department of Energy, No. DOE/MC/26031-4 (May 1991).

2. Martin, F.D., Heller, J.P., and Weiss, W.W.: "Field Verification of CO_2-Foam," 2nd Annual Report to U.S. Department of Energy, No. DOE/MC/26031-6 (May 1992).

3. Martin, F.D., Heller, J.P., and Weiss, W.W.: "Field Verification of CO_2-Foam," 3rd Annual Report to U.S. Department of Energy, DOE/MC/26031 (Dec. 1992).

4. Martin, F.D., Heller, J.P., and Weiss, W.W.: "Field Verification of CO_2-Foam," 4th Annual Report to U.S. Department of Energy, DOE/MC/26031 (Dec. 1993).

5. Martin, F.D., Heller, J.P., and Weiss, W.W.: "Field Verification of CO_2-Foam," 5th Annual Report to U.S. Department of Energy, DOE/MC/26031 (Dec. 1994).

6. Martin, F.D., *et al.*: "CO_2-Foam Field Verification Pilot Test at EVGSAU Injection Project Phase I: Project Planning and Initial Results," SPE/DOE 24176, *Proc.* SPE/DOE Eighth Symposium on Enhanced Oil Recovery, Tulsa, OK (April 22-24,1992) 201-213.

7. Tsau, J.S. and Heller, J.P.: "Evaluation of Surfactants for CO_2-Foam Mobility Control," paper SPE 24013 presented at the 1992 Permian Basin Oil and Gas Recovery Conference, Midland, March 18-20.

8. Stevens, J.E., *et al.*: "CO_2-Foam Field Verification Pilot Test at EVGSAU: Phase II—Foam Injection Design and Operating Plan," SPE 24642 *Proc.* 67th Annual Technical Conference and Exhibition of SPE, Washington, D.C. (Oct. 4-7, 1992) 115-128.

9. Butler, R., Gerard, M., and Stevens, J.: "The Use of Monitor Logging to Evaluate CO_2-Foam Flooding in the East Vacuum Grayburg San Andres Unit," presented at the SPWLA 34th Annual Logging Symposium, June 13-16, 1993.

10. Sultan, J., Ouenes, A., and Weiss, W.: "Reservoir Description by Inverse Modeling: Application EVGSAU Field," paper SPE 26478 presented at the 1993 SPE Annual Technical Conference and Exhibition, Houston, Oct. 3-6.

11. Chang, S-H. and Grigg, R.B.: "Laboratory Flow Tests Used to Determine Reservoir Simulator Foam Parameters for EVGSAU CO_2-Foam Pilot," paper SPE 27675 presented at the 1994 SPE Permian Basin Conference, Midland, TX, March 16-18.

12. Sultan, A.J., Ouenes, A., and Weiss, W.W.: "Automatic History Matching for an Integrated Reservoir Description and Improving Oil Recovery," paper SPE 27712 presented at the 1994 SPE Permian Basin Conference, Midland, TX, March 16-18.

13. Tsau, J.S., Heller, J.P., Moradi-Araghi, A., Zornes, D.R., and Kuehne, D.L.: "CO_2-Foam Field Verification Pilot Test at EVGSAU: Phase IIIA - Surfactant Performance Characterization and Quality Assurance," paper SPE 27785 presented at the Ninth Symposium on Improved Oil Recovery, Tulsa, OK, April 17-20, 1994.

14. Stevens, J.E. and Martin, F.D.: "CO_2-Foam Field Verification Pilot Test at EVGSAU: Phase IIIB: Project Operations and Performance Review," paper SPE 27786 presented at the Ninth Symposium on Improved Oil Recovery, Tulsa, OK, April 17-20, 1994.

15. Harpole, K.J., Siemers, W.T., Gerard, M.G.: "CO_2-Foam Field Verification Pilot Test at EVGSAU: Phase IIIC - Reservoir Characterization and Response to Foam Injection," paper SPE 27798 presented at the Ninth Symposium on Improved Oil Recovery, Tulsa, OK, April 17-20, 1994.

16. Brownlee, M.H. and Sugg, L.A.: "East Vacuum Grayburg-San Andres Unit CO_2 Injection Project: Development and Results to Date," *Proc.* 62nd Annual Technical Conference and Exhibition, Dallas (1987) 241-254.

17. Siemers, W.T. and Balke, S.C.: "Geological Character and Controls on San Andres Reservoirs, East Vacuum Grayburg-San Andres Field, Lea County, New Mexico, An Integrated, Interactive, Multidisciplinary Study," Research and Services Report 14627, Phillips Petroleum Company (Sept. 1993).

18. Yang, S.H. and Reed, R.L.: "Mobility Control Using CO_2-Foams," paper 19689 presented at the 64th Annual Technical Conference of the SPE, San Antonio, Oct. 8-11, 1989.

19. Lee, H.O., Heller, J.P., and Hoefer, A.M.W.: "Change in Apparent Viscosity of CO_2-Foam with Rock Permeability," paper SPE 20194 presented at the 1990 SPE/DOE Seventh Symposium on Enhanced Oil Recovery, Tulsa, April 22-25; SPE Reservoir Engineering, November 1991, pp 421-428.

20. Ransohoff, T.C and Radke, C.J.: "Mechanisms of Foam Generation in Glass Bead Packs," *SPERE* (May 1988) 573-85.

21. Duyvis, E.M. and Smits, L.J.M.:"A Test for the Wettability of Carbonate Rocks", SPEJ (March 1970), p. 3-4.

22. Campbell, B.T. and Orr, F.M., Jr.: "Flow Visualization for CO_2/Crude-Oil Displacements," *SPEJ* (Oct. 1985) 665-678; paper SPE 11958 presented at 58th Annual Technical Conference, San Francisco, Oct. 5-8, 1983.

23. Shelton, J.L. and Yarborough, L.: "Multiple Phase Behavior in Porous Media During CO_2 or Rich Gas Flooding," *JPT* (Sept. 1977) **29**, 1171-78.

24. Ehrlich, R., Tracht, J.H. and Slack, W.W.: "Laboratory and Field Study of the Effect of Mobile Water on CO_2 Flood Residual Oil Saturation,",JPT (Oct. 1984) p. 1797-1809.

25. Kuehne,D.L.,Frazier,R.H.,Cantor,J.,and Horn,W.:"Evaluation of Surfactants for CO_2 Mobility Control in Dolomite Reservoirs", paper SPE 24177 presented at the 1992 SPE/DOE Enhanced Oil Recovery Symposium, Tulsa, April 22-24.

26. Mannhardt, K., Schramm, L.L., and Novosad, J.J.: "Effect of Rack Type and Brine Composiont on Adsorption of Two Foam-Forming Surfactants," paper SPE 20463 presented at the 65th Annnual Technical Conference and Exhibition, New Orleans, Sept. 23-26, 1990.

27. Prieditis, J. and Paulett, G.S.:"CO_2-Foam Mobility Tests at Reservoir Conditions in San Andres Cores", paper SPE 24178 presented at the 1992 SPE/DOE Enhanced Oil Recovery Symposium, Tulsa, April 22-24.

28. Hall, H.N.: "How to Analyze Waterflood Injection Well Performance," *World Oil* (Oct. 1963) 128-130.

29. Killough, J.E., aand Hidajat, I.: "Reservoir Simulation of the East Vacuum Grayburg San Andres CO_2-Foam Field Verification," report prepared for the EVGSAU Foam Project JPAT,March 1, 1994.

30. Hidajat, I.: "Numerical Simulation of Foamflow in Porous Media," MS Thesis, University of Houston, Houston, TX (1992).

31. Chang, S.-H, Owusu, L.A., French, S.B., and Kovarik, F.S.: "The Effect of Microscopic Heterogeneity on CO_2-Foam Mobility: Part II— Mechanistic Foam Simulation," paper SPE/DOE 20191 presented at the 1990 SPE/DOE Enhanced Oil Recovery Symposium, Tulsa, April 22-25.